UNIVERSITY OF OKLAHOMA

GRADUATE COLLEGE

DEVELOPING ELECTROOSMOTIC-PUMP-BASED MINIATURIZED DEVICES: TOWARD A LIQUID CHROMATOGRAPHY CARTRIDGE COUPLED WITH MASS SPECTROMETER AND A SUB-PICOLITER PIPETTOR FOR SINGLE CELL SURGERY

A DISSERTATION

SUBMITTED TO THE GRADUATE FACULTY

in partial fulfillment of the requirements for the

Degree of

DOCTOR OF PHILOSOPHY

By

APENG CHEN
Norman, Oklahoma
2017

DEVELOPING ELECTROOSMOTIC-PUMP-BASED MINIATURIZED DEVICES: TOWARD A LIQUID CHROMATOGRAPHY CARTRIDGE COUPLED WITH MASS SPECTROMETER AND A SUB-PICOLITER PIPETTOR FOR SINGLE CELL SURGERY

A DISSERTATION APPROVED FOR THE
DEPARTMENT OF CHEMISTRY AND BIOCHEMISTRY

BY

_____
Dr. Shaorong Liu, Chair

_____
Dr. David W.McCauley

_____
Dr. Robert Thomson

_____
Dr. Yihan Shao

_____
Dr. Zhibo Yang

This doctoral thesis is dedicated to my wife Yi, my parents Min and Caiping, and my sister Yu.

Acknowledgements

Without the advice of my mentor Dr. Shaorong Liu, a doctoral thesis such as this would not have been possible. Thus, I would like to gratefully and sincerely acknowledge Prof. Shaorong Liu, as well as his wife, Joann Lu, for their constant support and encouragement in the past five years. Dr. Shaorong Liu's supervision made my research work more productive; and Joann Lu's help made my work more efficient.

I would like to thank my committee members, Dr. David McCauley, Dr. Yihan Shao, Dr. Robert Thomson, and Dr. Zhibo Yang. Their kind guidance and help are very much appreciated.

I would like to thank all the lab members in the past and present. They are Dr. Congying Gu, Dr. Qiangshen Pu, Dr. Wei Wang, Dr, Ruibo Li, Dr. Lei Zhou, Dr. Haiqing Yu, Dr, Xiaochun Wang, Dr. Min Zhang, Dr. Jiangtao Ren, Dr. Zaifang Zhu, Kyle Lynch, Huang Chen, Mitchell Weaver, Yu Yang, Piliang Xiang, and Matthew A. Beckner. Their help and suggestions contributed a lot to the completion of my doctoral thesis.

I also would like to thank Dr. David McCauley's Ph.D. student, Tian Yuan, for her suggestions and kindly help on setting up and maintaining zebrafish system, Dr. Sam E.V. Linsen for his suggestions on the manipulation of zebrafish embryos, Dr. Paul A. Sims for his kind permission of letting me use his facility, Dr. Anthony W. Burgett, and Dr. Naga Rama Kothapalli for their kind donation of cell lines.

Finally, I would like to thank the publisher ELSEVIER, including journals Analytica Chimica Acta and Journal of Chromatography A, for publishing my work and

permitting me to reuse it in this doctoral thesis. Thanks to all other the publishers for giving me the permission to reuse some figures in this dissertation.

Table of Contents

List of Figures

Abstract

There has been increasing interest on miniaturizing high performance liquid chromatography (HPLC), since it can reduce the costs of instrument manufacturing and perform onsite analysis. The electroosmotic pump (EOP) is one of the most promising micropumps that can be used for HPLC due to its compact size, and low fabrication cost. We have recently reported an electroosmotic pump (EOP), consisting of monolithic columns, capable of producing more than 1200 bar output pressure. However, when it pumps organic solutions, the flow rate becomes unstable. Hence, we here report two ways to address the issue.

In the second chapter, we describe the first method. A ten-port valve was used to create a gradient profile by inserting it between an EOP and an injection valve (Figure 2-1). In the position as shown in Figure 2-1, an eluent in loop 1 was delivered to the separation column, while a higher concentration eluent was loaded into loop 2. Once the valve was switched, loop 2 was connected to the separation column, while the next gradient eluent was loaded into loop 1. Repeating these steps formed a gradient profile that was close to linear.

In the second method (Chapter 3), we added a mixing chamber after the EOP (Figure 3-1). When a high voltage was applied, the EOP withdrew a series of gradient eluents having different elution strengths via a selection valve. The eluents went through the mixing chamber and towards to EOP. Once an opposite high voltage was applied, the EOP pushed the eluents out, through the mixing chamber again, and towards to the separation column. During the movements of these eluents (i.e., back and forth in the mixing chamber, as well as inside of capillary assembly), a smooth gradient

profile was formed. Since it is possible to change the size of mixing chamber, the number of eluents, as well as the volume, concentration, and the movement pattern (i.e., duration, velocity, and movement style), any desired gradient profile can be generated. Finally, we incorporated either approach with HPLC and a mass spectrometer for the separation and analysis of peptides and proteins.

In the fourth chapter, we described the application of EOP on single cell analysis. There has been increasing interest and requirement of single cell analysis with the development of bioanalytical and biochemical methods, since average data from population eliminate the heterogeneity of single cells. However, there are few methods currently available that can transfer mass into, and especially out of single cells under precise control. In this study, we developed a monolith-based EOP-driven pipettor (EDP), which was able to inject solutions into and withdraw cellular contents out of single cells down to ~250 fL. We subsequently demonstrated an application of the EDP in real-world samples by quantitative analysis of cholesterol from zebrafish embryos, and 89.3%-91.7% of the embryos survived after surgery that was performed at different developmental stages. Since the compatibility of the pump solution, an EDP has potential to be directly coupled with mass spectrometry. Taken together, our results showed an EDP can be used for living-single-cell analysis.

Chapter 1 Introduction

1.1 Background

Small volume transport for separation has become increasingly important recently from biological research to clinical medicine. The electroosmotic pump (EOP) is one of the most promising micropumps that can be used due to its small size and low cost. Our lab has developed a new type of EOP based on a monolithic column, which is able to produce over 17,000 psi of output pressure. The advantages of the monolithic EOP would benefit separation that require high back pressure (e.g., over 6,000 psi) as well as low flow rate (e.g., ~ 200 nL/min). However, the gradient profiles of organic solutions, which are often needed for HPLC separation, will cause the flow rate of EOP to be unstable. In this dissertation, we incorporated a selection valve into the EOP to separate the pump solution and gradient solution, which generated a promising stable flow rate and separation of peptides and proteins. We also developed an EOP-based pipettor, which is able to transport volume down to femto-liter scale for single cell analysis.

1.2 Electroosmotic pumps (EOPs)

The principle of EOPs are based on eletroosmotic flow (EOF), which is produced by the movement of bulk solution close to charged surface of a capillary under an electric field. As shown in Figure 1-1, the inner wall of a capillary is modified to form negative groups. For example, the inner surface silanol (Si-OH) of a fused silica capillary can be ionized to negatively charged silanolate ($Si\text{-}O^-$) groups when pH is

above three. The negatively charged silanolate groups attract counter-ions from the bulk liquid to shield the surface charge. The counter-ions form a so-called electrical double layer (EDL), one of which is a fixed layer, while the other one is a mobile layer. The mobile layer will drag the liquid phase in the direction of the electric force. That is, the motion of mobile layer is from left to the right when a positive high voltage is applied (Figure 1-1), and *vice versa*.

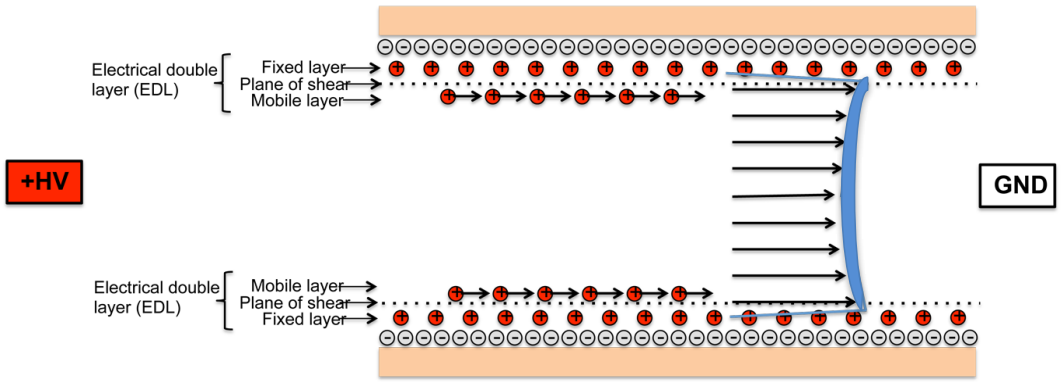

Figure 1-1 Principle of the EOP.

+HV - + high voltage; GND - Ground.

When two capillaries are modified with negative and positive charge, respectively, they can be put together in series and work like batteries to produce higher out-put pressure than a single capillary does (Figure 1-2). When an open capillary is filled with monolith, which can be modified either as negative charge or positive charge (Figure 1-3), it will produce higher out-put pressure than an open capillary. Putting these monolithic EOPs in series (Figure 1-4) and applying a high voltage can produce high out-put pressure. Since there are many published reports describing EOP,[1-8] details of EOP are not introduced in this dissertation.

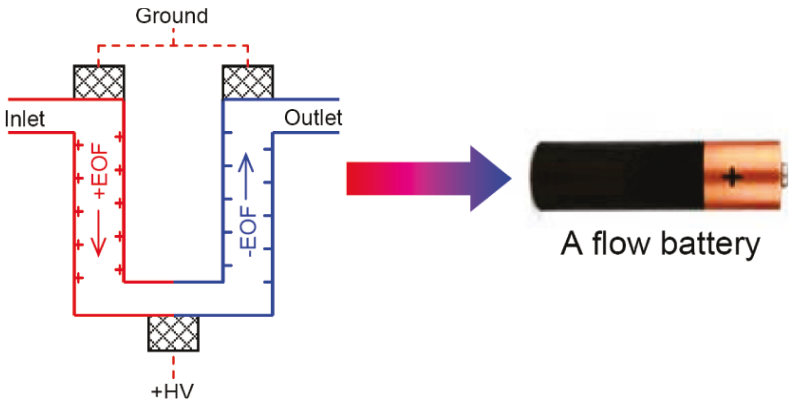

Figure 1-2 Schematic Configuration of EOP assembly.

+HV - + high voltage.

[Reprinted with permission from He et al., Analytical Chemistry (2011). 83(7):2430-2433. Copyright (2011) American Chemical Society]

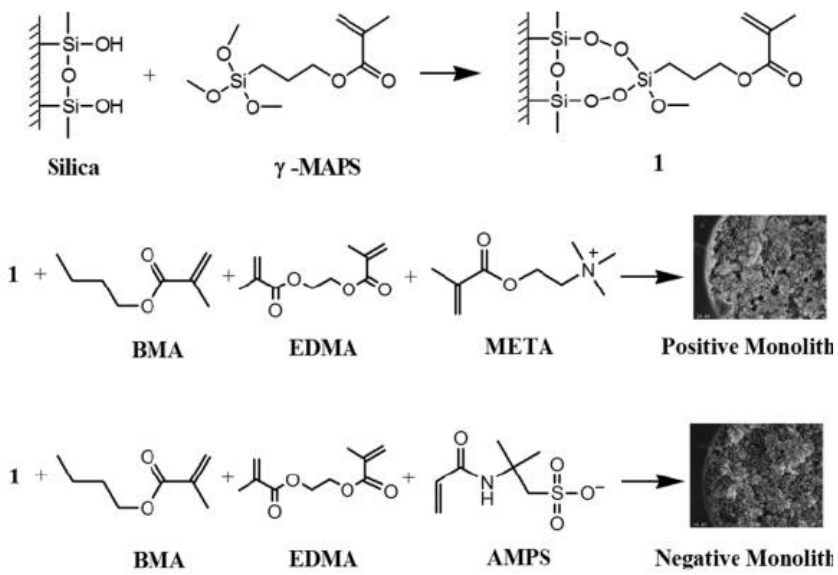

Figure 1-3 Preparation of Monolithic columns.

γ-MAPS-Methacryloyloxypropyl-trimethoxysilane;

BMA-butyl methacrylate;

EDMA-Ethylene glycol dimethacrylate;

META-2-(methacryloyloxy)-ethyl]- trimethylammonium chloride;

AMPS-2-Acrylamido-2-methylpropane sulfonic acid.

[Reprinted with permission from Gu et al., Analytical Chemistry (2012). 84(21):9609-9614. Copyright (2012) American Chemical Society]

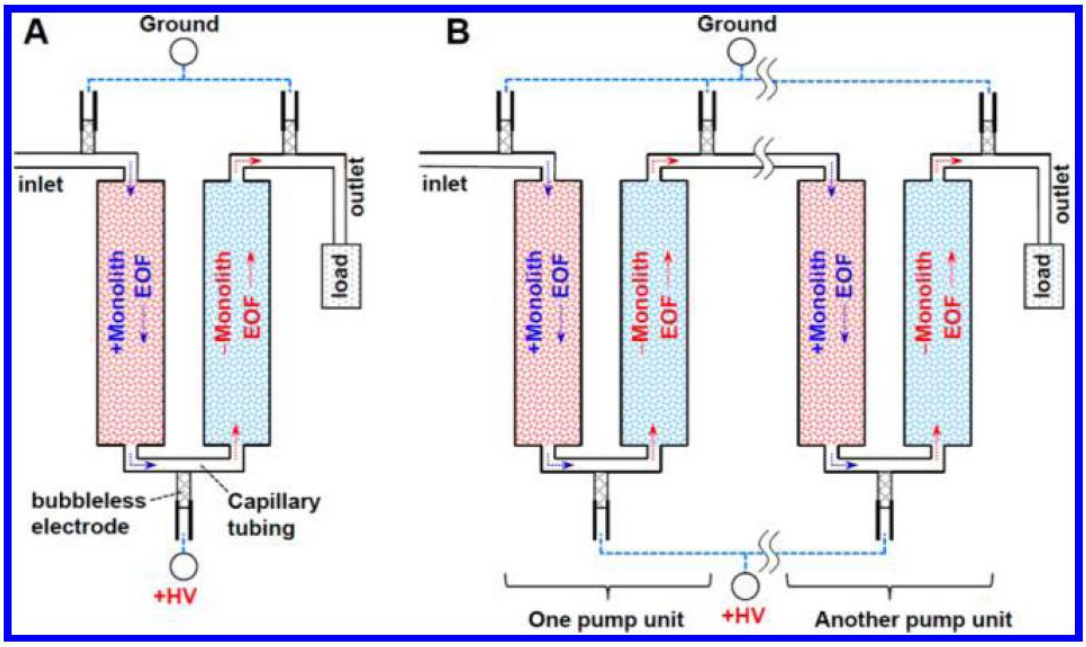

Figure 1-4 Schematic configuration of pump assembly.

(A) A fundamental pump unit. (B). A pump assembly.

[Reprinted with permission from Gu et al., Analytical Chemistry (2012). 84(21):9609-9614. Copyright (2012) American Chemical Society].

1.3 Techniques and instrumental development for single cell analysis

Systemic analysis of "-omics", including genomics, transcripts, proteomics, metabolomics, and localizomics, with single cell resolution is one of the most important aspects to understanding biochemical processes, since data from population cells are averaged and subsequently undermine the cellular specificity and heterogeneity. There are many methods that can be used for single cell analysis, including fluorescence labeling and detection by microscopy, transmission electron microscopy (TEM), enzymatic assays, and PCR-based methods. Since there have been many reviews and research articles about those methods and approaches,[9-21] we here only address the advance of methods for mass transfer by using a micropipette to deliver foreign reagents into or pick up mass from a living cell for analysis.

1.3.1 Pipettor tips for microinjection

One of the most common pipettor tips used for microinjection or suction from single cells is based on a glass capillary. A glass capillary can be pulled by a puller to a very thin tip (less than 1 μm of outer diameter). Shen et al. have successfully used a micropipette around 1 μm to perform single cell manipulation in budding yeast W303 cells [22,23.] Besides, commercial pipette tips for microinjection can reach 1.0 μm o.d., 0.5 μm i.d. (e.g., Catalog No. E5242952008, Fisher Scientific Inc.). Although the diameter of glass tips can reach the sub-micron level, there are several disadvantages, including fragility, easily causing damage to the cell membrane, relatively large size compared to cells, and easy to be blocked by cellular contents [24-27.]

The pipettor tip may also be coated and directly coupled with mass spectrometry. Masujima's group has used a micropipette to transfer cytosol contents from single cells for MS [28]. They used a micromanipulator to pull a gold-coated glass capillary (1.2 mm outer diameter) to a slim tip, the caliber size of which at the top was adjusted to 1~2 μm, based on the size of the target cells [29]. The fabricated tip was used as a micropipette to suck the content of cytoplasm or specific organelles, and the tip which also functions as a nano-electrospray emitter, was then coupled to a mass spectrometer for subcellular molecule detection. Since the diameter of a typical mammalian cell is ~10 μm (e.g., a HeLa cell with the volume around one picoliter), the diameter of the micropipette on the top should smaller than 10 μm as much as possible to reduce injury to the cells. For smaller eukaryotic cells such as budding yeast *Saccharomyces cerevisiae*, with diameter less than 5 μm, a micropipette smaller than 1 μm is required. Yang's group utilized a probe, which has two channels, coupled with mass spectrometry to analyze single cells (Figure 1-5).[30] The probe can be directly inserted into a Hela cell to perform on-line analysis via an Obitrap mass spectrometer.[30-32]

Recently, it has been reported that carbon-based nanoprobes or carbon nanopipettes (CNPs) can be used for cell biology [24,25,33,34]. CNPs were made based on depositing carbon on the inner wall and then removing the outer wall (Figure 1-6).[24] First, iron III nitrate in isopropanol as catalyst solution is filled into capillaries (360 μm o.d. × 20 μm i.d. × 15 cm in length) and deposited on the inner surfaces of the quartz by drying them with helium gas. Second, a 1~2 cm window will be opened to expose the glass part of the capillaries and further fabricated by pulling the window using a micropipette puller. After which, the fabricated capillaries will be placed in a chemical vapor deposition furnace, in which a mixture of methane and argon at about 900 °C will

go through, and carbon will be deposited on the inner surface of the capillaries. Finally, the glass of the tips will be removed by dipping the capillaries into hydrofluoric acid (5:1 diluted by deionized water) and the carbon tips will expose.

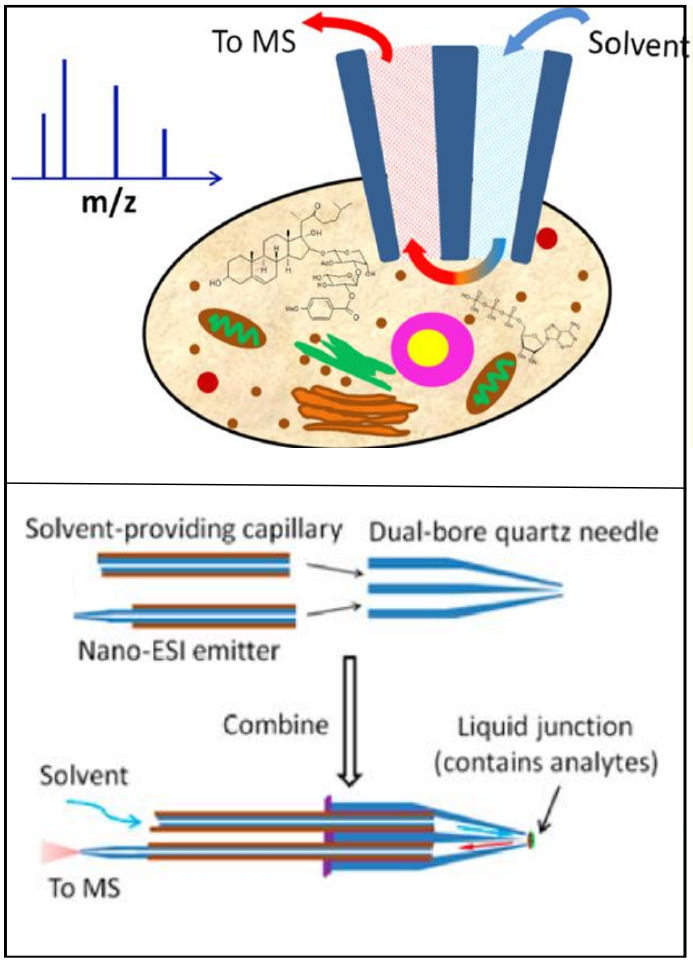

Figure 1-5 Single-probe mass spectrometry system.

Top panel: Schematic diagram of Single-probe mass spectrometry system;

Bottom panel: Fabrication steps of the Single-probe.

[Adapted with permission from Pan et al., Analytical Chemistry (2014). 86: 9376-9380. Copyright (2014) American Chemical Society].

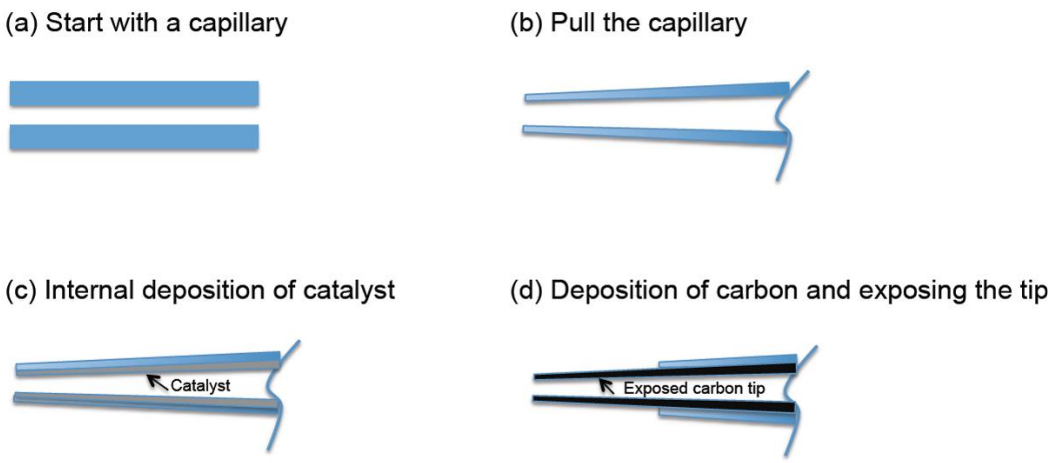

Figure 1-6 A schematic description of the fabrication of CNPs.

[Modified from Schrian and Bau with permission, Microfluid Nanofluid (2009). 7:439-450. Copyright (2009) Springer-Verlag; License number: 4090421173807].

CNPs exhibit several advantages over glass pipettes. First, CNPs can be made with a relatively small size (usually range from 10~200 nm i.d., 200~500 nm o.d.) based on different approaches, providing more sensitivity, accuracy, and reliability than glass pipettes. Second, CNPs have remarkable mechanical properties, [24,33] and are flexible and rigid enough to perturb a cell, while glass pipettes are quite fragile, which is not suitable for delivery of drugs into some organisms such as *C. elegans.* [35] Third, CNPs are inert, and conductive heat transfer allows heat to be dissipated into its surroundings efficiently. These properties allow us to heat the CNPs when they are blocked by cellular contents especially complexes from nucleus. Heating to around 100-200 °C will allow CNPs to be unblocked without any melting or configuration changes, while the glass pipette usually can be used to inject 20~30 cells before either the tips become stuck or blocked completely, [36] and heating can easily melt the glass tips. Additionally, CNPs, like glass pipettes, are transparent to light, which makes the mass transfer easily detectable under microscope. Besides, there are several other properties of CNPs including conductivity, which has potential as electrode probes for neurons, but we will not discuss these properties in detail. Last, but not least, CNPs are compatible with biological laboratory equipment, such as injection systems in conjunction with light microscopes.[24] However, CNPs may also have some downside, including the repeatability of the tip shape, which is dependent upon the pulling tip. Another potential issue is that it may cause leakage from the side due to its small thickness.

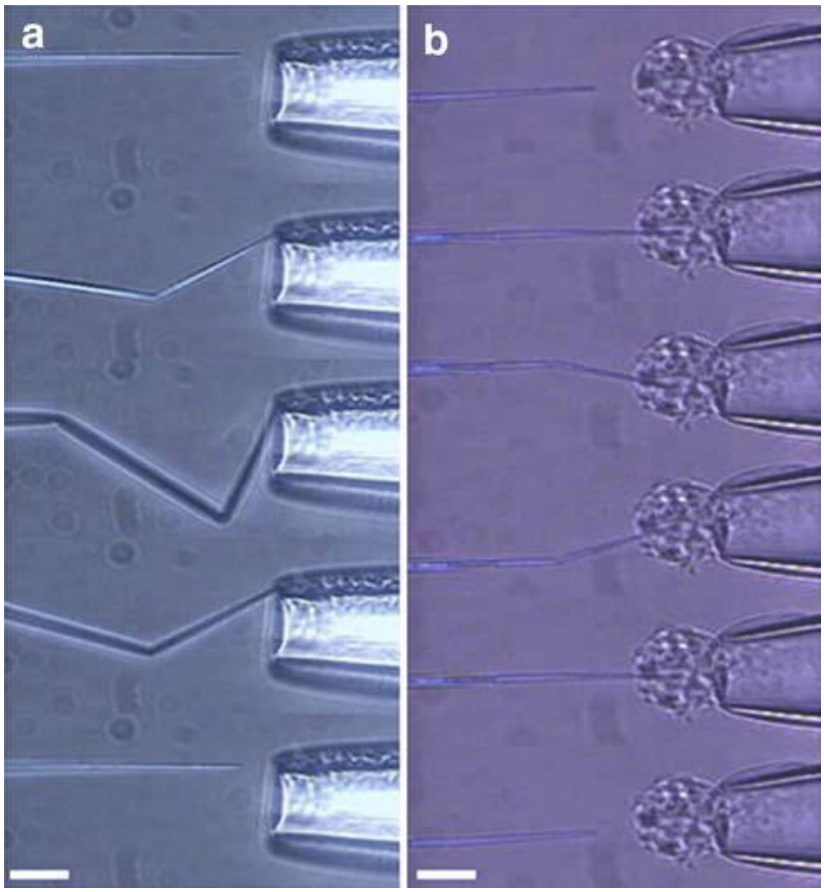

Figure 1-7 mechanical properties of CNPs.

(A) From top to bottom: the carbon pipe tip of the CNP buckles when pushed against the wall of a glass pipette and recovers its initial shape once the force is removed. Scale bar 15 µm. (B) From top to bottom: a CNP penetrates through the membrane of an smooth muscle cell. The cell is held in place by glass micropipette aspiration. Scale bar 15 µm.

[Reprinted with permission from Schrian and Bau with permission, Microfluid Nanofluid (2009). 7:439-450. Copyright (2009) Springer-Verlag; License number: 4090421173807].

Microfabrication is another way to make a pipettor tip for single cell analysis. It has been reported that nanofluidics systems have good accuracy and repeatability to deliver liquid into single cells, and can be precisely controlled to insert into single cells when combined with atomic force microscopy.[37-40] As shown in Figure 1-8, the fabricated pipettor tip has a small outer and inner diameter, which minimizes the injury to the cell when inserting the tip in. Additionally, since microfabrication has good reproducibility, unlike making the glass pipettor tip, fluidFM tip is uniform, which increases the stability of the whole system. Guillaume-Gentil et al. has used fluidFM to extract molecules from Hela cells for analysis, which has shown great reliability.[41]

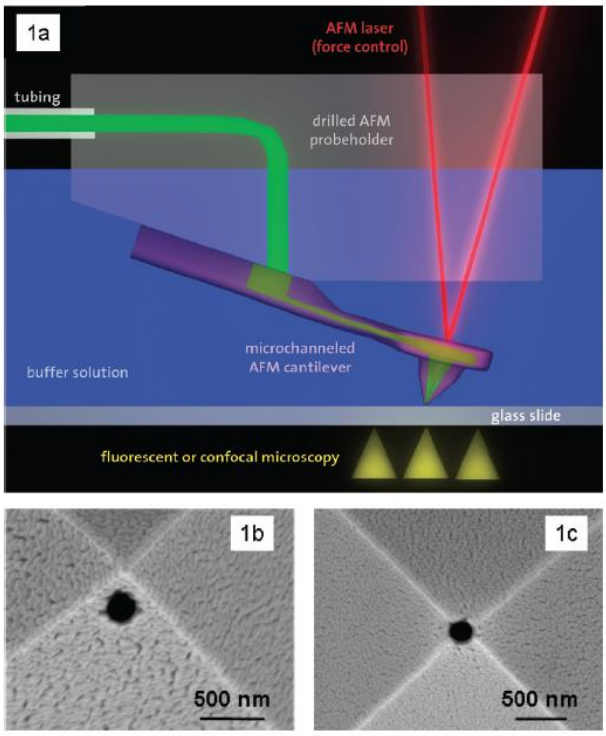

Figure 1-8 Schematic illustration of the fluidFM.

(a) figure showing a micro-channeled cantilever chip fixed to a drilled AFM probe holder. The position of the probe can be detected and finely controlled by AFM. (b) SEM imaging of the aperture beside the apex of the pyramidal AFM tip. The tip is made of silicon nitride (Si_3N_4) with a wall thickness of 100 nm. (c) SEM imaging of the aperture at the apex of the pyramidal AFM tip.

[Reprinted with permission from Meister et al., Nano Letters (2009). 9(6):2501-2507. Copyright (2009) American Chemical Society].

1.3.2 Driving force of microinjection or micro-suction

The most commonly used driving force to deliver a solution into single cells from a tip is based on air pressure. This method is often used on microinjection in biological research. However, the current microinjection methods based on pressure injection are challenged by the precise amount of foreign molecules delivered into a single cell. [42] Microinjection is controlled by injection pressure and time. For example, suggested injection pressure and time are usually 60~200 hPa and ~0.1 s, respectively, for human neuronal cells. [43] The amount of a solution injected into a cell is dependent upon a burst of injection pressure and the time it lasts. Since the pressure of this type of microinjection is discrete, the success of injecting quite consistent volumes into each cell is highly dependent upon the skill and experience of operators. [36] Guillaume-Gentil et al. recently have developed a tunable single-cell extraction method for molecular analysis.[41] Although they used a fabricated tip for single cell extraction and can precisely control the volume, the suction of cellular content was still driven by air force, which could potentially undermine the precision of solution suction.

An alternative way to drive a solution in a pipettor tip is based on an EOP. EOP-based pipettors can transfer solutions with high accuracy and precision. [1] Unlike the most common commercial microinjection systems based on pressure ejection or iontophoresis, this technique can function as a routine pipettor to pick up and dispense solutions. Recently, we have proved EOPs can drive HPLC separation [7] and also can be implemented on microfluidic devices. [44] In addition, we have developed flow batteries based on EOPs to generate high pressures of more than 1200 bar (c.a. 17,400 psi). [5,6] Besides, we have already successfully developed an electroosmosis-driven nanopipettor

with accuracy down to ~150 pL.[1] Since electroosmotic flow (EOF, no-load flow) is determined by the length and diameter of the pump capillary, and the voltage applied across the pump capillaries, one can achieve any flow rate, in theory, by adjusting the applied voltage when other parameters keep constant, which is impossible to achieved by current pressure injection methods.

1.3.3 Detecting methods of cellular content from single cells

One of the most powerful techniques for single cell analysis is microscopy. It can offer spatiotemporal information in living cells. Detecting fluorescence-labeling targets with optical microscopy is a common method for single cell analysis. Confocal microscopy is one of the microscopic techniques that allow one to detect the location of the targets with high resolution (down to ~200 nm) in single cells. Other techniques developed in recent years, including two- or three- photon, light-sheet, and especially super-resolution microscopy dramatically improved image resolution (e.g., down to ~ 10 nm on x- and y- axis).[45-50] Several groups further developed super-resolution to be suitable for 3D imaging analysis.[51-55] Although microscopy is powerful for imaging analysis, the disadvantages are also obvious, including that it can only be applied to a limit number of targets, [56-58] it is not easy to tracking targets in living cells, and bleaching of fluorescence when long time video-imaging is performed.

Mass spectrometry is an ideal method to analyze molecules in living single cells, due to its high sensitivity, high resolution, and its ability to detect many molecules simultaneously. That no labeling is needed for the detection of targets is another advantage of mass spectrometry, although it is still necessary for quantification of the targets in single cells. However, mass spectrometry does require lysed samples, which

is destructive and not suitable for timeline detection of the same cells. Additionally, the preparation of lysed sample is not only time-consuming, but more importantly, it may also change the natural states of the targets, such as the loss of post translational modification (PTM) [59] and change of metabolites. [60] Recently, Masujima's group insert nanospray tip into single cells, including yeast and plant cells, to collect cellular content based on capillary force; the nanospray tip was then directly coupled with mass spectrometry for the analysis of the targets (Figure 1-9). [28,29,61-66] Over 1,000 peaks of metabolites from yeast was detected by the method, although over 10,000 cells were needed for one measurement.[28] Yang's group used an Orbitrap mass spectrometer to analyze drugs in mammalian cells.[30-32] Mass spectrometry provides information on thousands of proteins and metabolites at a time, [64,67,68] however, it is currently limited to analyze abundant molecules in single cells, due to none of the current mass spectrometry methods having high enough sensitivity to reach the average concentration of macromolecules, including most inherent proteins, some metabolites, and lipids. [11,16] We are looking forward to the development of mass spectrometry with the sensitivity that can down to concentration of important macromolecules.

There are many other methods that can be used for the analysis of single cells, including PCR, single-cell sequencing, and enzyme-based measurement. Since there are several review papers that have described these methods,[9,10,13,18,20,69-71] details will not be discussed here.

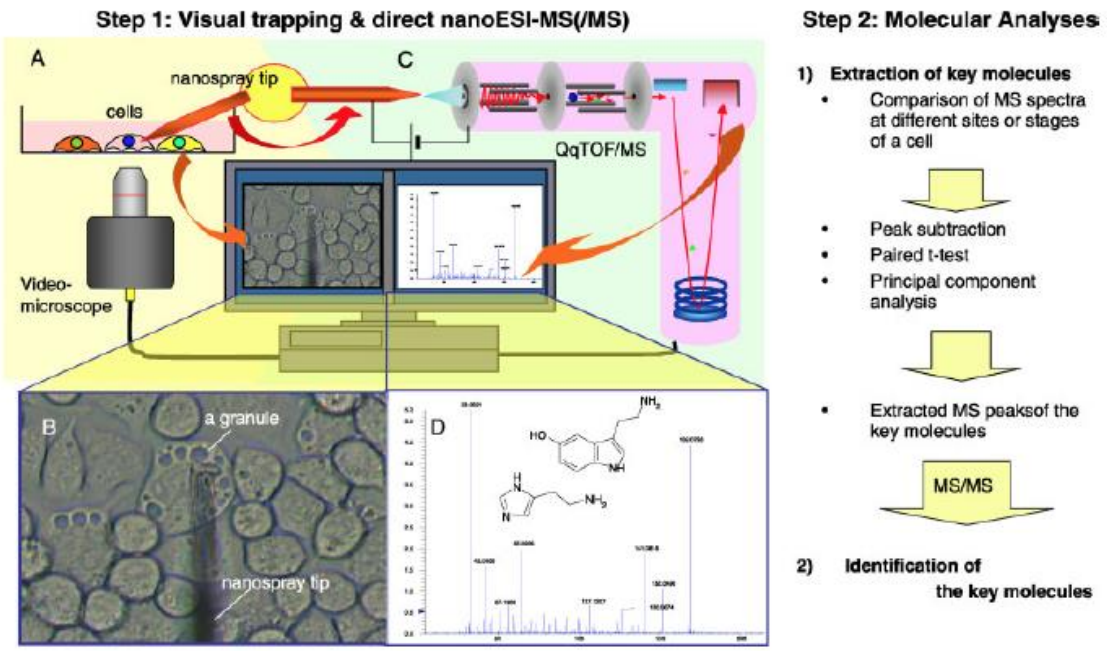

Figure 1-9 Scheme of live single-cell video mass spectrometry.

The analysis consists of two steps. In the first step, the cell behavior is observed by video-microscope. When the cell showed the response and/or has designated micro-areas to be analyzed, the contents of the cell or its organelle were sucked out directly into a nano-spray ionization tip. The tip (with addition of 1 μl ionization solvent) was then set in the nano-ESI probe to ionize the sample contents in a mass spectrometer (MS). In the second step, a set of MS spectra of the samples are compared with each other using the paired *t*-test and/or the principal component analysis to extract key molecules or classify the samples. Some extracted MS peaks were subjected to MS/MS analysis for identification of the molecules.

[Reprinted with permission from Mizuno et al., Journal of Mass Spectrometry (2008). 43:1692-1700. Copyright (2008) John Wiley and Sons; License number: 4098440102786].

Chapter 2 Incorporating A High-Pressure Electroosmotic Pump And A Nano-Flow Gradient Generator Into A Miniaturized Liquid Chromatographic System For Peptide Analysis

2.1 Abstract

We integrate a high-pressure electroosmotic pump (EOP), a nanoflow gradient generator, and a capillary column into a miniaturized liquid chromatographic system that can be directly coupled with a mass spectrometer for proteomic analysis. We have recently developed a low-cost high-pressure EOP capable of generating pressure of tens of thousands of psi, ideal for uses in miniaturized HPLC. The pump worked smoothly when it was used for isocratic elutions. When it was used for gradient elutions, generating reproducible gradient profiles was challenging; because the pump rate fluctuated when the pump was used to pump high-content organic solvents. This presents an issue for separating proteins/peptides since high-content organic solvents are often utilized. In this work, we solve this problem by incorporating our high-pressure EOP with a nano-flow gradient generator so that the EOP needs only to pump an aqueous solution. With this combination, we develop a capillary-based nano-HPLC system capable of performing nano-flow gradient elution; the pump rate is stable, and the gradient profiles are reproducible and can be conveniently tuned. To demonstrate its utility, we couple it with either a UV absorbance detector or a mass spectrometer for peptide separations.

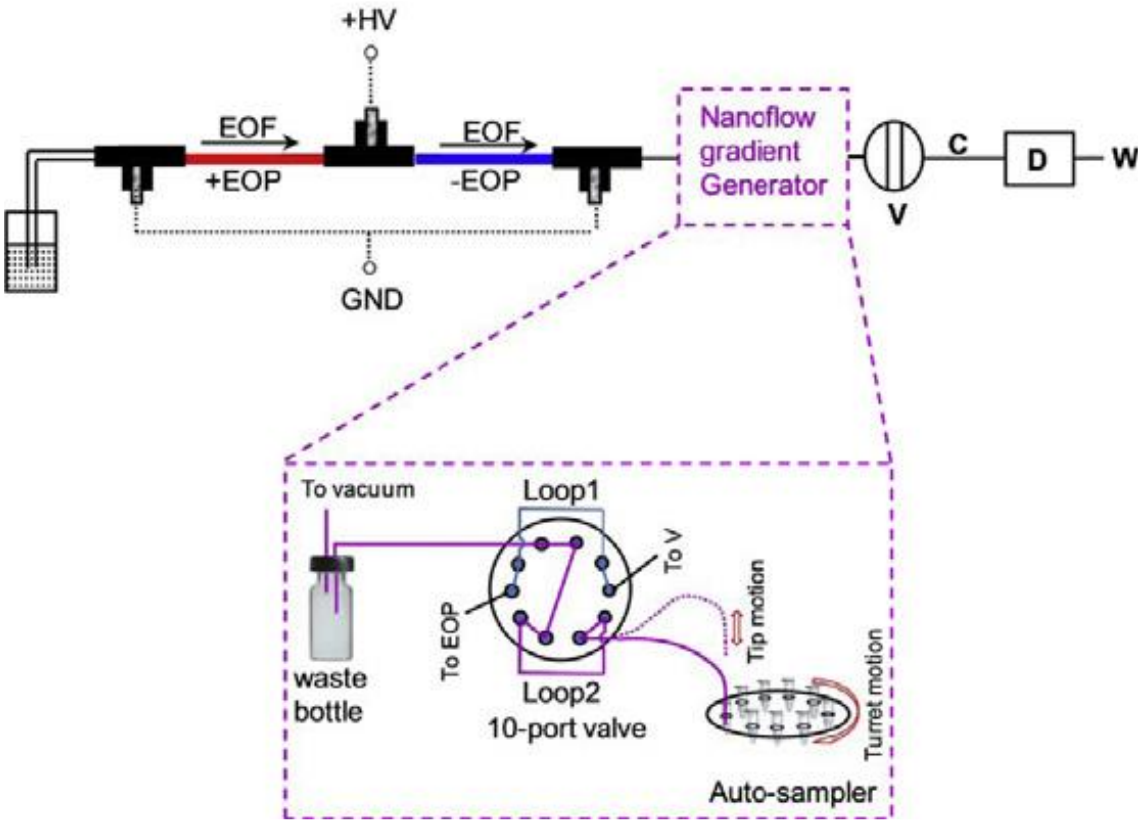

Figure 2-1 Graphical abstract.

2.2 Introduction

Since the introduction of microcolumn liquid chromatography (or micro-LC) by Horváth et al. [72,73] various aspects (e.g., basic theory, packing technology, instrumentation, detection, sample injection, etc.) of this technique have been extensively investigated .[74,75] It is generally agreed that separation efficiencies per unit time increase with the decreasing sizes of packing particles.[76] As particle sizes scale down and column diameters shrink, higher pumping pressures (more than 6000 psi) and lower flow rates (less than 1 mL min^{-1}) are required. These systems are now often called nano-flow HPLC (or nano-HPLC).[77] Nano-HPLC is particularly advantageous (with respect to conventional LC) when it is used in conjunction with a mass spectrometer (MS), because all of its effluent can be effectively transferred into the MS source.

Nano-HPLC–MS offers excellent detection sensitivity and is widely applicable in the field of proteomic research and biomarker discovery.[78,79] Ideally, nano-HPLC separations should be driven by reliable micropumps capable of generating low flow rates (a few to a few hundred nanoliters per minute) at high pressures (6000–10,000 psi), but such pumps are lacking. To address this issue, we have recently introduced a battery-like electroosmotic pump (EOP),[1,5-7] called a pressure power supply (PPS). A PPS consists of a +EOP (produced using a positively charged pumping element) and a –EOP (produced using a negatively charged pumping element), and the +EOP and –EOP are joined via a bubbleless electrode. The bubbleless electrode facilitates application of an external potential to the internal pump solution while preventing the internal solution from leaking out to the electrode and forming bubbles inside the pumping elements.[1,5] A single PPS may generate only a limited pump rate and a moderate pump pressure. When

a number of PPSs are connected in series and/or in parallel, desired pump pressures and/or pump rates can be achieved, just as a number of batteries can be stacked in series and/or in parallel to achieve a desired voltage and/or current.

The pump could be made at a cost of less than $1K (compared to $20–30K for a commercial high-pressure nanopump), and it worked smoothly when it was used to pump aqueous solutions, but its flow rate became unstable if it was used to directly pump an organic solvent. It was likely due to the incompatibility between the organic solvent and polyacrylamide gel inside the bubbleless electrode. This presents a significant issue if the pump is used to drive nano-HPLC for protein/peptide separations, because high concentrations of acetonitrile are often used to elute these analytes.

In our previous report, we managed to use the above EOP to generate a gradient eluent.[5] We first preloaded two eluent segments consecutively into a capillary (with the weaker eluent in front), and this capillary was then connected to the outlet of the EOP. As the EOP pumped an aqueous solution into the capillary, driving the eluent segments forward, the two eluents were mixed, forming a gradient eluent at the interfacial region. This gradient eluent was used successfully to elute some peptide samples,[5] but the operations were inconvenient, and it was challenging to precisely tune the gradient profile.

In general, it is not trivial to produce a stable mobile-phase gradient at a rate of nano liters per minute for nano-HPLC, although various nano-flow gradient generators have been developed. The most common means is to utilize a conventional HPLC pump combined with a flow splitter.[80,81] This approach has been used successfully for many applications, but it has several drawbacks, including waste of the majority of the

eluent, unstable or distorted gradient profile (due to changes in column backpressure), and gradient delay (due to the low flow rate). In addition, when a splitting ratio is high (e.g., more than 1000), the nano-flow becomes unstable. Another approach is to employ a switching valve holding a set of injection loops prefilled with a series of eluents with increasing elution-power.[77,82] The valve is operated in such a manner that weakest eluent is delivered to the column first, and then the next stronger eluent, and so on. Because only a limited number of injection loops can be incorporated in one valve, the choices of gradient profiles are limited. To solve this problem, Deguchi et al.[83] utilized a 10-port switching valve with two injection loops, combined with a conventional gradient delivery system, for delivering an unlimited number of (gradient) eluent segments. The basic idea is to use the conventional gradient delivery system to form a gradient eluent and deliver it to the switching valve, loading one of the two loops. As the valve switches, the eluent loaded in the first loop is delivered to the column, while the second loop is being loaded with a slightly stronger eluent. As the valve switches back, the eluent loaded in the second loop is delivered to the column, while the first loop is being loaded with the next stronger eluent. Since these operations can go continuously, a smooth gradient can be obtained. Brennen et al. [84] have experimented with a microchip gradient generator for reducing the delay volume between the gradient front and the HPLC column. The chip uses a few microliters of two mobile phases to passively form a gradient, and the delay volume is reduced to a few nanoliters. Other nanoflow gradient generators include a preformed gradient in which the desired slope, previously stored in a capillary, is then forwarded to the column by a syringe pump [85] and the exponential dilution method.[86,87] In this work, we incorporate our high-pressure

EOP, a nano-flow gradient generator, nanoliter injection valve, and a packed capillary column into a capillary-based nano-HPLC system. The nanoflow gradient generator is similar to Deguchi et al.'s design[88],[89] but the normal gradient delivery system was replaced with a mini auto- sampler. The assembled system has no flow splitters and generates only a few microliter of waste per run. Importantly, the EOP needs only to pump an aqueous solution so that the flow is stable. In addition, we can tune the gradient profile conveniently. To demonstrate the utility of the nano-HPLC, we optimize the experimental conditions for separation of peptides first using a UV absorbance detector, and then we couple the nano-HPLC with an electrospray ionization–mass spectrometer (ESI–MS) for analysis trypsin digests of proteins.

2.3 Experimental section

2.3.1 Chemicals and materials

Ethylene glycol dimethacrylate (EDMA, 98% w/w, hereinafter all % indicate % w/w unless otherwise stated) and butyl methacrylate(BMA) were purchased from Alfa Aesar (Ward Hill, MA). 2-Acrylamido-2-methylpropane sulfonic acid (AMPS, 99%) and [2-(methacryloyloxy)ethyl]-trimethylammonium chloride (META, 75% in water) were obtained from Sigma–Aldrich (St. Louis, MO). 1-propanol and 2,2-azobisiso-butyronitrile (AIBN, 98%) were obtained from Aldrich (Steinheim, Germany). Methacryloyloxy- propyl-trimethoxysilane (g-MAPS, 98%) was purchased from Acros (Fairlawn, NJ). Acrylamide, N, N-methylene bisacrylamide (bis), N,N,N,N-tetramethylethylenediamine (TEMED), and ammonium persulfate (APS) were obtained

from Bio-Rad Laboratories (Hercules, CA). 1,4-Butanediol (99%) was supplied by Emerald BioSystems (Bainbridge Island, WA). Cytochrome C and bovine serum albumin (BSA) were obtained from Sigma (St. Louis, MO). Sequencing grade modified trypsin was purchased from Promega (Madison, WI). HPLC grade Water and LC–MS grade acetonitrile (ACN) were purchased from Fisher Scientific (Fair Lawn, NJ). Fused silica capillaries were purchased from Polymicro Technologies Inc. (Phoenix, AZ). All solutions were prepared with ultra-pure water purified by a NANO pure infinity ultrapure water system (Barnstead, Newton, WA).

2.3.2 Preparation of EOP monolithic columns

The EOP monoliths (15 cm length ×75 μm i.d. × 360 μm o.d.) were prepared following the procedure from our group's publication described previously with modification.[5] In detail, a capillary of 100 - 150 cm (100 μm i.d. × 360 μm o.d.) was first vinlyized using the following procedure. Briefly, the capillary was first flushed with acetone and 1.0 M NaOH, each for 10 min. After the capillary was filled with 1.0 M NaOH and its ends were sealed by rubber septa, it was placed in an oven at 100 ºC for 2 h. The capillary was then taken out from the oven, and it was flushed with water, 0.1 M HCl, and acetone; each for 20 min. After the capillary was dried with N_2 at 60 psi for 1 h, the capillary was filled with 30% (v/v) g-MAPS in acetone, and its ends were sealed with septa, and then the capillary was put back in the oven at 50 ºC for 14 h. The capillary was vinylized and ready for the monolith preparation after being rinsed with acetone and dried with N_2 at 60 psi for 2 h.

The vinylized capillary was then cut to 16-cm-long segments. After degassing by purging with helium for ~5 min, a solution containing 10.0 mg AMPS, 230.0 mg BMA, 160.0 mg EDMA, 4.0 mg AIBN, 424.0 mg 1-propanol, 116.0 mg 1,4-butanediol and 60.0 uL water was loaded into a capillary segment. The capillary was placed in a water bath at 60 °C for polymerization for 20 h. +EOP is quaternary ammonium-based monolith, and –EOP is sulfonate-based monolith. The monoliths need to be equilibrated with a pump solution (3 mM sodium acetate, pH 5.0) right before a pump was assembled.

2.3.3 Preparation of bubbleless electrode

To prepare the bubbleless electrode, a 150-µm-i.d. (360 µm o.d.) and 20-cm-long capillary was cut, and its inner wall was cleaned by flushing the capillary with NaOH (1.0 M) for 45 min, DI water for 15 min, and acetonitrile for 15 min. After the capillary was dried with nitrogen gas, the inner wall was reacted with a solution containing 30% (v/v) g-MAPS in acetone at 50 ºC for 14 h. Then, the capillary was flushed with acetonitrile and dried with nitrogen gas. A degassed solution containing 9%T (%T stands for the total weight concentration of acrylamide and bis in the solution), 3%C (% C represents bis concentration relative to acrylamide), 0.2% (v/v) TEMED, and 0.1% APS was pressurized into the capillary and remained inside the capillary at 0 ºC overnight and then 4 ºC for another 24 h. After 1 cm of the capillaries at both ends were trimmed off, 50 mM sodium tetraborate was electrophoretically driven through the polyacrylamide inside the capillary until a stable current was

obtained. The above capillary was cut into 2-cm pieces, and each piece was used as a bubbleless electrode.

2.3.4 Preparation of monolithic polystyrene-divinylbenzene (PS-DVB) column

We followed the procedure by Premstaller et al. to prepare the PS-DVB column. Briefly, a 90.0-cm-long vinlylized fused silica capillary (360 μm o.d. × 150 μm i.d.) was filled with a helium-purged solution containing 45.31 mg styrene, 45.70 mg divinylbenzene, 107.77 mg decanol,17.78 mg tetrahydrofuran (THF), and 2.50 mg of AIBN. After both ends of the capillary were blocked, the capillary was placed into a water bath at 60 ºC for 24 h to allow the monolith formation. The capillary was then cut into two halves (two columns), and the columns were washed with acetonitrile for 5 h at 1000 psi to remove the unreacted monomers.

2.3.5 Preparation of samples: peptide and protein

Peptides were prepared by tryptic digesting cytochrome c and BSA (individually or as a mixture). Cytochrome c, BSA, or a mixture of the two was first dissolved in 50 mM ammonium bicarbonate with 30% ACN (v/v) to a concentration of 1 mg mL^{-1} for each protein. Trypsin was added at a substrate-to-enzyme ratio of 100:1 to digest the proteins for 4 h at 37 ºC. 1% (v/v) formic acid was added to the solution to terminate the digestion. The digest was vacuum-dried and stored at 20 ºC. It was re-dissolved in 2% ACN without any additional cleanup for analysis.

The intact proteins were used to evaluate the performance of the nano-HPLC system. The wild-type (wt) and mutant horse heart myoglobin (hh Mb) samples were kindly provided by Dr. Richter-Addo's group.[88] Briefly, a horse heart myoglobin gene

with a single base mutation (hhMb, H64V) was engineered and expressed in E. coli. The lysed proteins from E. coli were concentrated by ammonium sulfate precipitation and the mutant myoglobin was purified by a DEAE-Sepharose column. The wild type and mutant myoglobins were then mixed and diluted to a concentration of 10 mg/mL as a stock solution and stored at -20 °C.

2.3.6 Set-up of nano-HPLC system

Figure 2-2A presents a schematic diagram of the nano-HPLC system. It consisted of a high-pressure EOP, a nanoflow gradient generator (see Figure 2-2B), a nanoliter injection valve (Valco Instruments, Houston, TX), a packed capillary column (Waters, Atlantis dc18 NanoEase Column, 100Å, 3 mm, 75 mm 100 mm), and a UV absorbance detector (Linear UVIS 200, Spectra-Physics, Fremont, CA). To construct the high-pressure EOP, we trimmed positive monoliths to a length of 15 cm and the negative monoliths to a length of 11.9 cm; this ensured that both monoliths provided similar electroosmotic flows. Micro tees from Valco Instruments were used for component (bubbleless electrode, positive monolith, negative monolith, etc.) connections. The EOP outlet was connected to the gradient generator via a 250 mm i.d. 365 mm o. d. 20 cm length capillary. The detailed construction of the gradient generator is depicted in Figure 2-2B; it consisted of primarily a 10-port valve (VICI Valco Instruments, Houston, TX), an autosampler, and a vacuum line. The gradient generator was connected to a nanoliter injector (VICI Valco Instruments Co., Inc.) through C1, and then a packed capillary column from Waters. The Linear UVIS 200 absorbance detector was set at 210 nm for absorbance detection. The absorbance signal was acquired using a NI multifunctional card DAQ Card (6062E, National Instruments,

Austin, TX), and the data was processed with an in-house written LabView program. Alternatively, the nano-HPLC was coupled with an ESI–MS (LCQ Deca XP plus mass spectrometer, Thermo Fisher Scientific Inc., Waltham, MA) via a nano-spray emitter.

When the MS was used, the separation column was carefully butt-to-butt connected to a metal-film-coated nanospray-ionization (NSI) emitter (a 5-cm-long, 360-mm-o.d., and 20-mm-i.d. fused silica capillary with a 5-mm-i.d. spray tip, New Objective, Woburn, MA) with a zero-dead-volume PTFE coupler (Waters). The voltage was applied directly to the metal film on the spray tip. Xcalibur was used for instrumental control and data processing. Nano ESI–MS was performed at a full scan mode with an m/z range of 300–1800. Agilent 1200 HPLC pump with a flow-rate range of 0.01–20 mL/min was used for comparison to evaluate the performances of the EOP and the gradient generator.

(A)

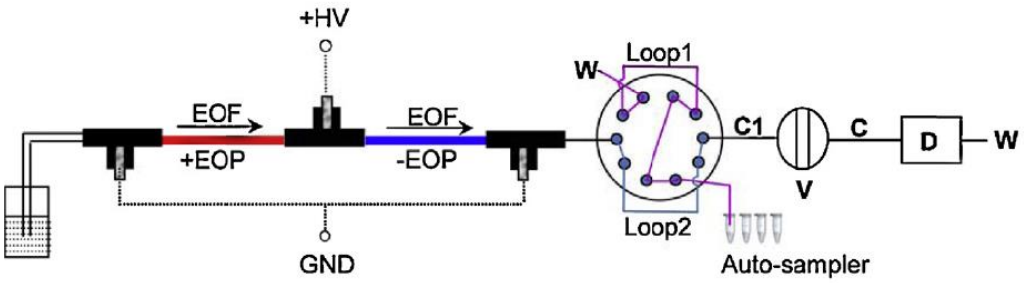

(B)

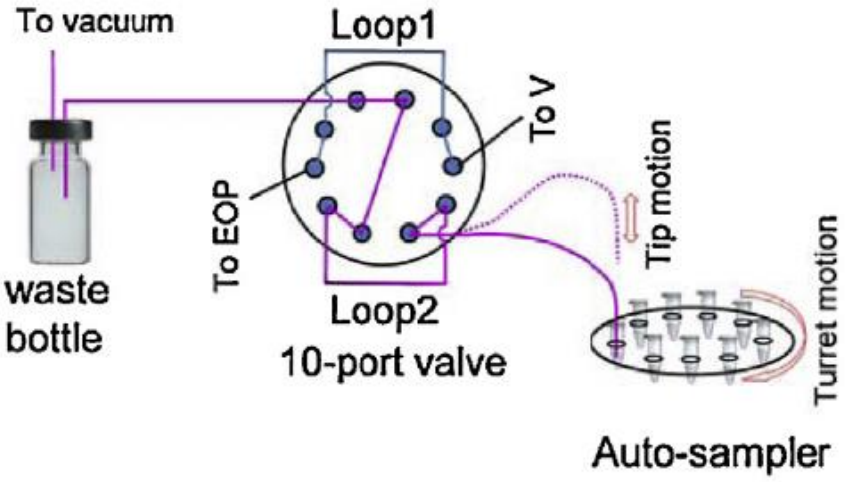

Figure 2-2 Schematic diagram of capillary-based nano-HPLC.

(A) An overall diagram of nano-HPLC. Both +EOP and EOP are capillary-based. The dashed lines indicate electric wires, and arrows indicate liquid flow directions. HV - high voltage, GND - ground, W - waste, C1 - connection capillary, V - 4-nL (or 60-nL) injection valve, C - packed capillary column, and D - UV absorbance detector (210 nm). (B) Detailed construction of our nano-flow gradient generator. The dashed line indicates the capillary position when it is raised.

2.4 Results and discussion

2.4.1 EOP Characterization

It is highly recommended that every EOP be characterized after it is built. Figure 2-3 presents the characterization of the EOP used in this work; the maximum output pressures of both +EOP and –EOP under different field strengths were measured (see Figure 2-3A), and the relationships between output pressure and flow rate were determined (see Figure 2-3B). This information was used for selecting proper lengths of "+" and "–" pumping elements to avoid negative pressure building up inside an EOP; the pump solution should always be pushed rather than being pulled to prevent bubble formation. Since the packed capillary column does not require a high pump pressure, only one PPS was employed in this experiment. The characterization of the one-PPS EOP was also presented in Figure 2-3. In general, the pressure output of the assembled EOP should be close to the sum of the pressure outputs of its individual pumping elements. Otherwise, the EOP may not have been assembled properly.

(A)

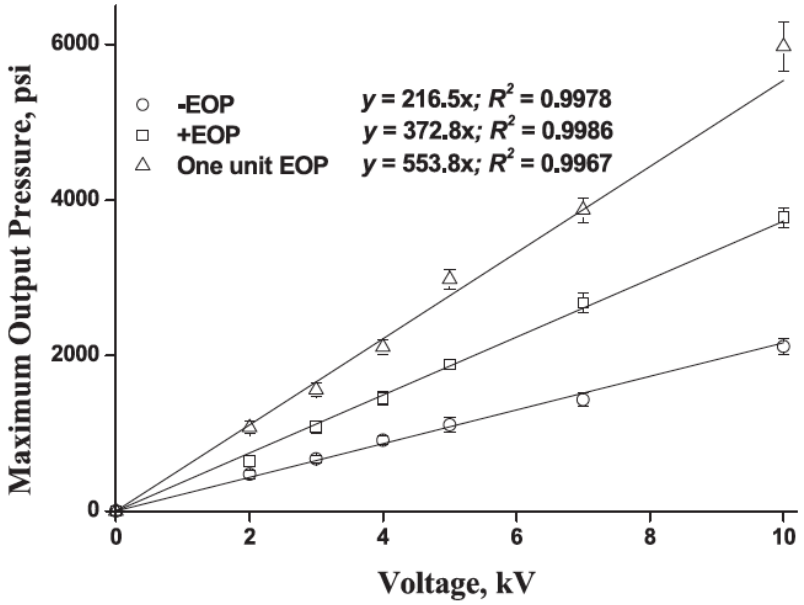

(B)

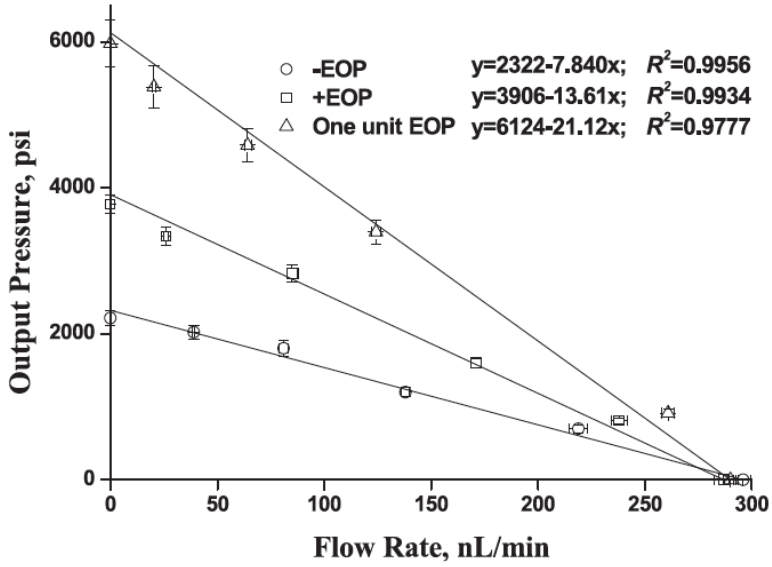

Figure 2-3 Characterization of EOP.

(A) Maximum pressure output vs applied voltage. +EOP – 75 µm i.d.×11.9 cm length, EOP – 75 µm i.d. ×15 cm, and pump solution – 3 mM sodium acetate at pH 5.0.

(B) Relationship between pressure output and flow rate output. Voltage applied – 10 kV.

2.4.2 Nano-flow gradient generation

Referring to Figure 2-2B, as vacuum was applied to W, the weakest eluent was first aspirated into Loop1 on the ten-port valve. After the injection valve (V) was activated to inject a sample to the separation column (C), the ten-port valve was switched to the position as shown in Figure 2-2B; the weakest eluent was delivered, via a connection capillary (C1) and V to C. At the same time, the eluent-inlet capillary was transferred to the next and slightly stronger eluent to load this eluent to Loop2. After a preset period of time depending on the separation needed, the ten-port valve was switched back (to the position as shown in Figure 2-2A) to deliver the eluent in Loop2 to C, while Loop1 was loaded with the next stronger eluent. As a train of eluent segments with increasing elution power was delivered to C consecutively, analytes were eluted out sequentially. The gradient profile could be adjusted by changing the compositions of the eluents in the vials on the auto- sampler, and/or the lengths of the eluent segments.

2.4.3 Performance of the gradient generator

In the study, we used a similar design to Takeda's group [16]; however, the normal flow gradient delivery system in the setup of Takeda's group was replaced with a mini auto-sampler (see Figure 2-2B), since our long-term goal was to develop a

capillary- or microchip-based HPLC system. Generally, a good gradient generator should be capable of generating smooth gradients and producing short delay times.

In order to generate a smooth gradient, we attempted to promote mixing by increasing the length of C1; however, we noticed that this method was not effective. One of the most efficient ways to generate a smooth gradient profile was through reducing the "step" size of the eluents and increasing the "step" frequency. The gradient delay time was, however, directly proportional to the volume of C1. In this experiment, C1 had a length of 7-10 cm and a diameter of 75 μm. This length was chosen because it was close to the shortest we could use to properly connect the 10-port switching valve to the injection valve. Using this capillary, the delay time was <2 min. The delay time could be effectively reduced by narrowing C1 (e.g., a delay time of 5 s could be obtained if C1 had a length of 10 cm and an i.d. of 10 μm), but special attention had to be paid to preventing the capillary from clogging when such narrow capillaries were used.

Based on the setup mentioned above, we create a gradient profile, as shown in Figure 2-4. We compared the performance of the nano-flow generator with an Agilent 1200 HPLC system. Figure 2-5A and B presents the chromatograms for the separation of cytochrome c and BSA digests using Agilent HPLC system and the proposed nano-flow gradient generator, respectively. It is clear that two systems show a similar separation profile. The gradient provided by the nano-flow gradient generator is comparable to the linear gradient generated from the commercial HPLC pump. It is also noticeable that the nano-flow gradient generator has less gradient delay compared to the Agilent HPLC pumps, which was mostly attributed to the smaller dwell volume of the

former system. (e.g., the connecting tubing between the pump and the separation column for the Agilent pump system was a 30 cm × 75 μm ID capillary. In the EOP system, a 10 cm × 75 μm ID capillary was used).

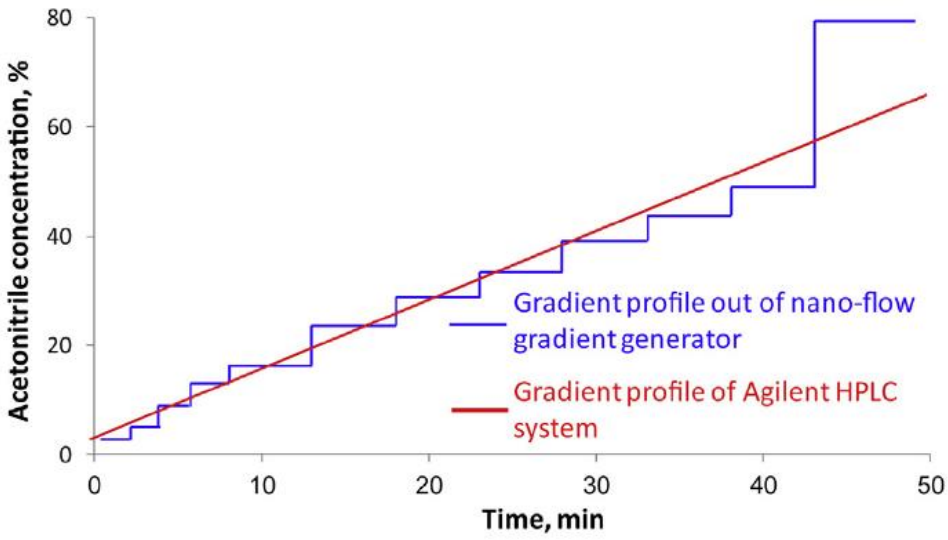

Figure 2-4 Gradient profile generated by nano HPLC system.

Gradient profile used for the separations shown in Figure 2-5. Blue line-gradient steps for the nano-flow generator: 2–6–10–14–18–25–30–35–40–45–50–80% ACN; all ACN solutions were prepared in water containing 0.1% TFA. Red line–Agilent HPLC gradient profile: 2–60% ACN in 50 min.

(A)

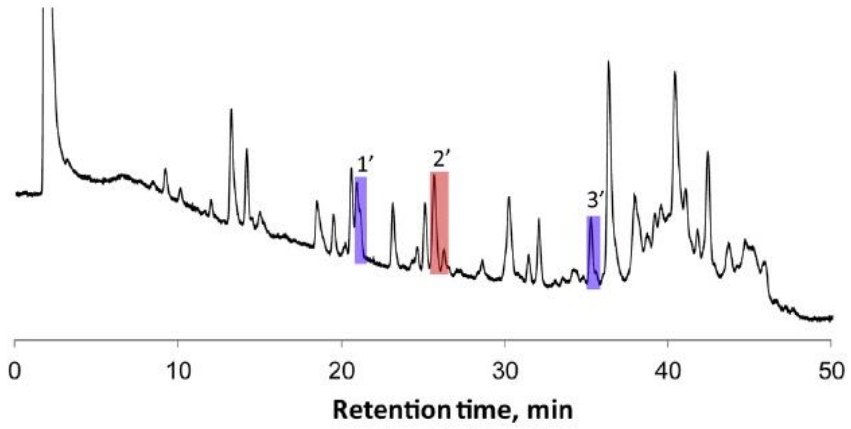

(B)

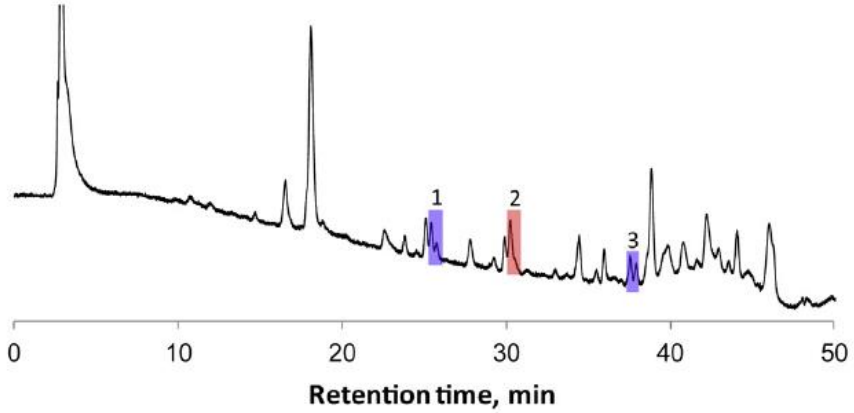

Figure 2-5 Comparison of peptide separation using the proposed nano-flow gradient generator and an Agilent HPLC system

Sample – digests of cytochrome c and BSA (10 mg/mL each) mixture, C1 – 10-cm-long and 75-µm-i.d. capillary, separation column – Waters Atlantis dC18, 3.0 µm, 75 µm i.d.×10 cm, injection volume – 15 nL, and detection wavelength – 210 nm. (A) Separation chromatogram using Agilent HPLC system; flow rate was set as 200 nL/min; (B) separation chromatogram using the nano-flow generator; backpressure drop of the separation column was around 1500 psi and the pump rate was around 200 nL /min.

2.4.4 Integrating nano-HPLC system into mass spectrometry for peptide and protein analysis

To demonstrate the utility of our nano-HPLC for peptide separation, we optimized the gradient for separations of trypsin digests. As shown in Figure 2-6, a gradient profile was generated by twelve steps from 2% to 80% ACN. We used nano-HPLC to separate tryptic digest of cytochrome c (Figure 2-7A) and BSA (Figure 2-7B). Both chromatograms in Figure 2-7A and B were obtained using the same gradient as exhibited in Figure 2-6. As can be seen in the chromatograms, most of the peptides were well resolved. When the digests of a mixture of cytochrome c and BSA were separated under the same conditions; however, a large base-line hump showed up between 38 and 47 min (see Figure 2-8A), an indication that the peptides under this hump were not resolved well. To improve the resolution, we shortened the gradient step-size and increased the step-frequency. With these modifications, the hump disappeared, i.e., the peptides under the hump were nicely resolved (see Figure 2-8B). We then coupled the above nano-HPLC with an ESI–MS (a Thermo Finnegan LCQ DECA XP Plus Mass Spectrometer) via a conventional metal-film-coated capillary emitter. Figure 2-9A presents a base-peak-intensity (BPI) chromatogram for the digests of cytochrome C and BSA mixture. Most of the peaks contained a single compound; Figure 2-9B and C displays two typical mass spectrum examples.

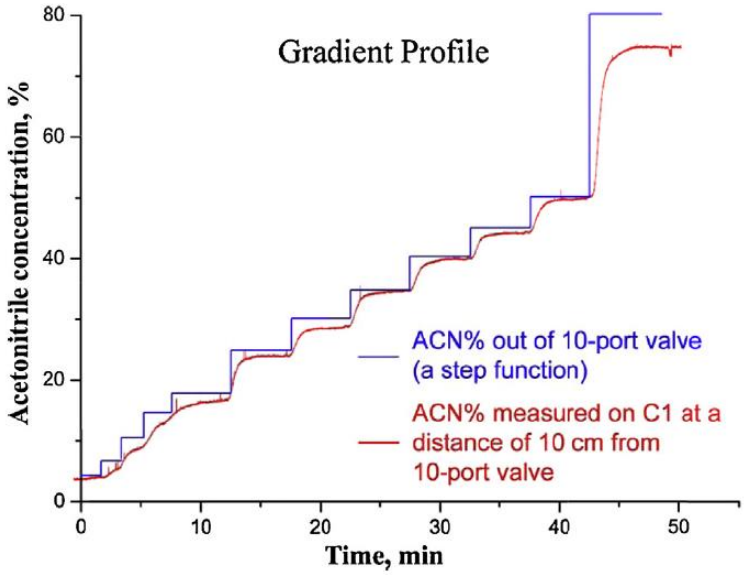

Figure 2-6 Gradient profile generated by nano-HPLC system used for separation of tryptic cytochrome c and BSA (see Figure 2-7).

Gradient steps (blue lines): 2–6–10–14–18–25–30–35–40–45–50–80% ACN; all ACN solutions were prepared in water containing 0.1% TFA. Red traces – experimentally measured gradient profile, which were obtained by setting the UV absorbance at 265 nm. The same series of ACN solutions, after being doped with acetone at (ACN)/(acetone) = 26.7, was used for the profile measurements. The concentration of ACN was calculated based on the corresponding concentration of the acetone, which was observed by its UV absorbance at 265 nm. All other conditions were the same as described in Figure 2-4 and Figure 2-5.

(A)

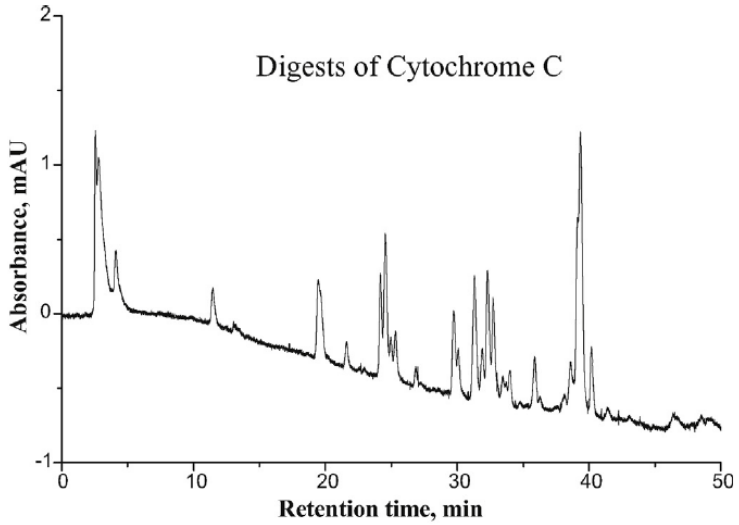

(B)

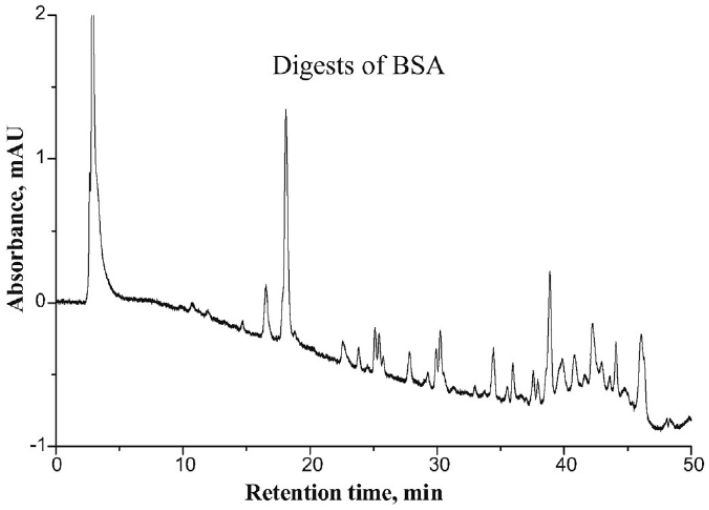

Figure 2-7 Peptide separations using capillary-based nano-HPLC with gradient elution.

Samples – trypsin digests of cytochrome C (10 mg mL) and trypsin digests of BSA (10 mg mL). (A) chromatogram for trypsin digests of cytochrome C; (B) chromatogram for trypsin digests of BSA.

(A)

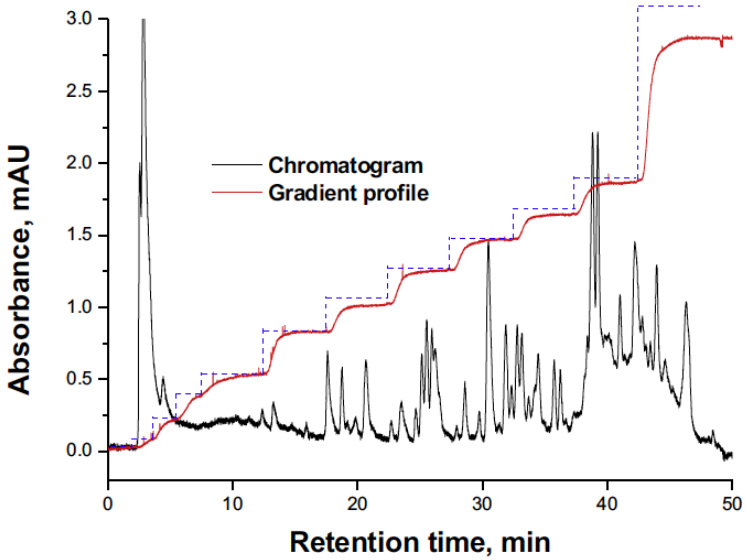

(B)

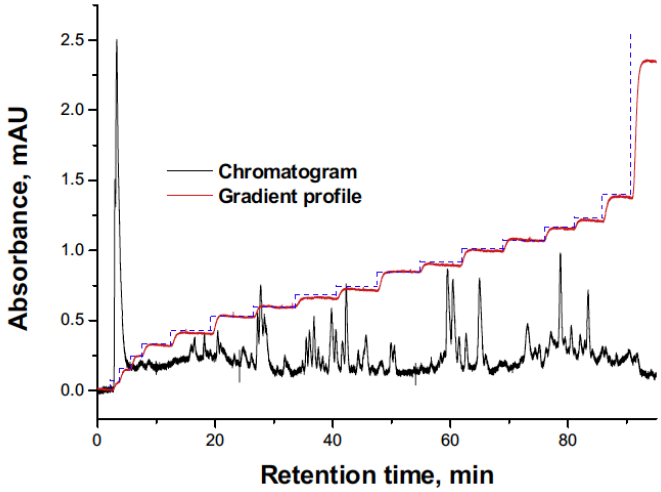

Figure 2-8 Optimizing gradient profile for nano-HPLC separation.

Sample – digests of cytochrome C and BSA (10 mg mL each) mixture, black traces – chromatograms, red traces – experimentally measured gradient profiles, dashed blue lines – gradient steps from the nano-flow gradient generator. Gradient steps for (a): 2–6–10–14–18–25–30–35–40–

45–50–80% ACN, and gradient steps for (b): 2–6–10–14– 18–22–25–27–30–32–35–37–40–42–45–47–50–80% ACN. All other conditions were the same as described in Figure 2-6 and Figure 2-7.

(A)

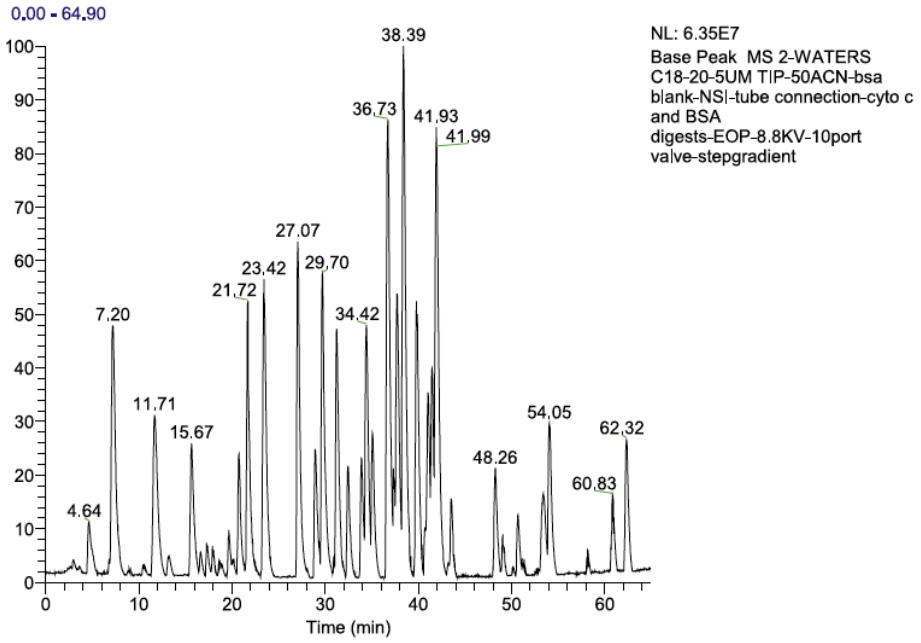
0.00 - 64.90
NL: 6.35E7
Base Peak MS 2-WATERS C18-20-5UM TIP-50ACN-bsa blank-NSI-tube connection-cyto c and BSA digests-EOP-8.8KV-10port valve-stepgradient
38.39
36.73
41.93
41.99
27.07
23.42
29.70
21.72
7.20
34.42
11.71
15.67
54.05
62.32
48.26
60.83
4.64
Time (min)

(B)

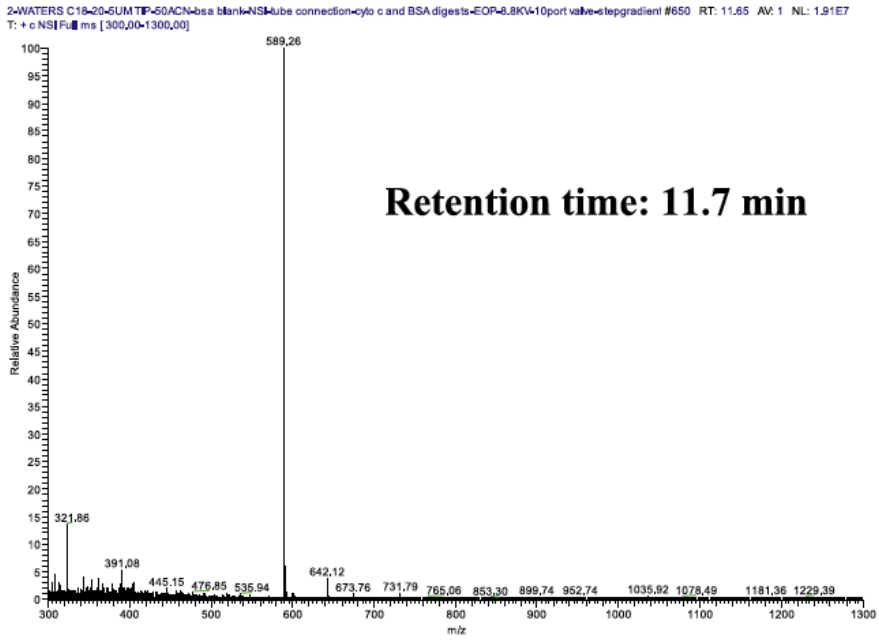
2-WATERS C18-20-5UM TIP-50ACN-bsa blank-NSI-tube connection-cyto c and BSA digests-EOP-8.8KV-10port valve-stepgradient #650 RT: 11.65 AV: 1 NL: 1.91E7
T: + c NSI Full ms [300.00-1300.00]
Retention time: 11.7 min
589.26
321.86
391.08
445.15
476.85
535.94
642.12
673.76
731.79
765.06
853.30
899.74
952.74
1035.92
1078.49
1181.36
1229.39
Relative Abundance
m/z

(C)

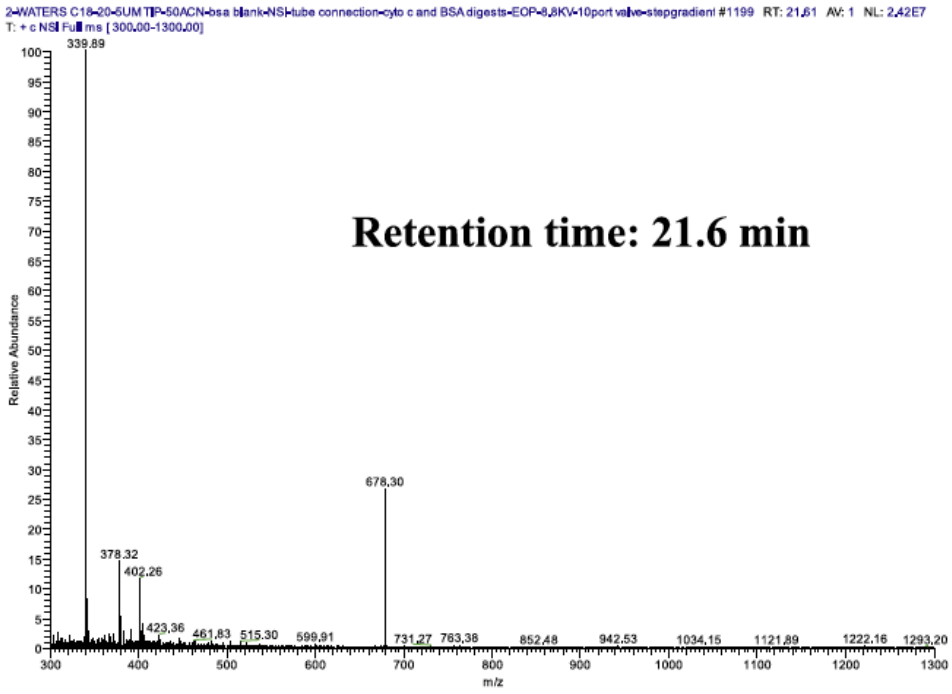

Figure 2-9 Peptide separation using capillary-based nano-HPLC coupled with MS.

A 5-µm-long, 360-µm-o.d., and 20-µm-i.d. fused silica capillary with a 5-µm-i.d. spray tip was used as an ESI emitter. It was set in parallel with the entrance path of the MS, with the tip < 1mm to the MS orifice. ESI voltage was set at 1.82 kV. The MS was operated at a full scan mode with an m/z range of 300–1800. (a)BPI chromatogram; (b) mass spectra of selected chromatogram peak (RT=11.7min); (c) mass spectra of selected chromatogram peak (RT=21.6min). All other conditions were the same as described in Figure 2-8.

2.4.5 Real-world application of nano-HPLC system coupled with mass spectrometry

We used mutant myoglobin samples as real-world samples to further demonstrate the performance of the EOP-driven nano-gradient HPLC system. It is well known that myoglobin down-regulates the cardiac energy status to prevent the heart from injury by reducing nitrite to nitric oxide.[90] Yi et al. has demonstrated that the distal pocket histidine residue (His64) of hh Mb directs the binding of nitrite, and the mutation of histidine to valine (H64V) dramatically decreases the binding rate.[88] Here, we use our system to distinguish the "disease state" from "normal state" of proteins by separating the hh Mb H64V from the mixture of mutant and wt hh Mb. In Figure 2-10A, peak a represents wt hh Mb, while peak c is hh Mb H64V. Peaks a and c have a molecular weight 16,913 Da (Figure 2-11A) and 17,044 Da (Figure 2-11C), respectively, which are consistent with our prediction of molecular weights of hh Mb and hh Mb H64V. Peak b, with the molecular weight 16,913 Da (Figure 2-11B), is hh Mb H64V without the first methionine, since 25% hh Mb expressed in E. coli would lose the N-terminal amino acid.[91] The result shows that we can separate two intact proteins with a single mutation (peaks a and c), as well as a single amino acid difference in length (peaks b and c). The separation efficiency was comparable with that of the Agilent 1200 HPLC (Figure 2-10). This method has potential application in clinical diagnosis.

(A)

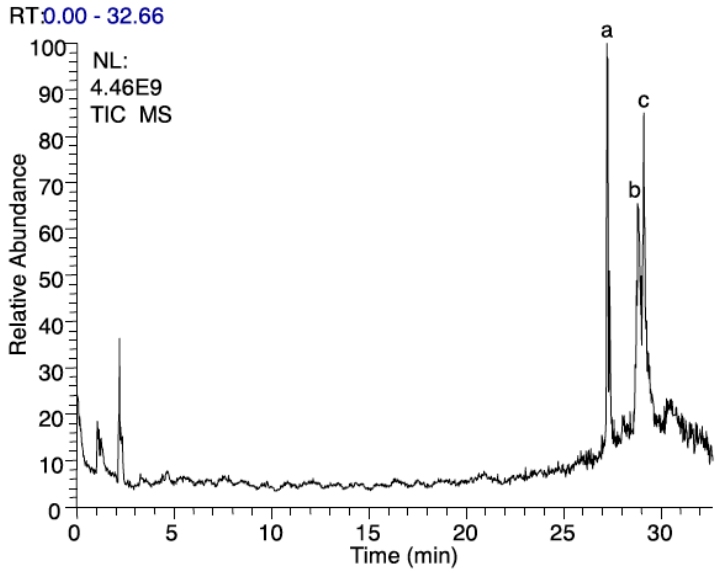

(B)

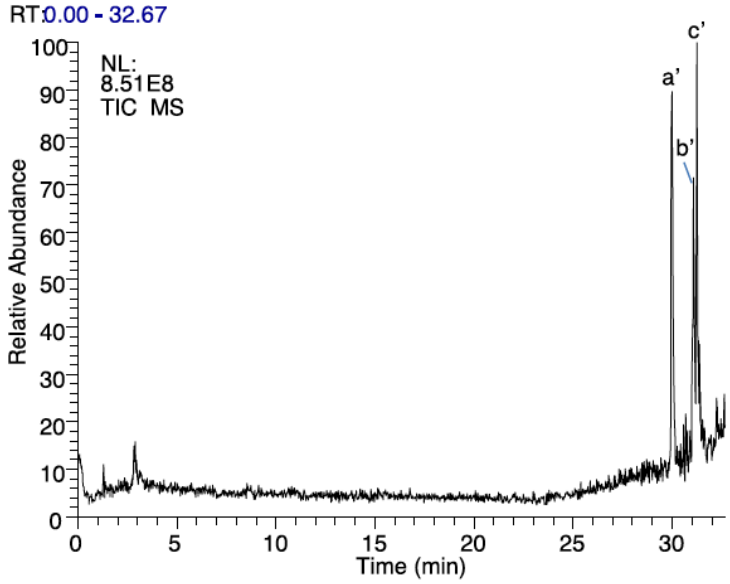

Figure 2-10 Separation of mutant hh Mb (hh Mb H64V) from wt hh Mb.

Sample – normal myoglobin and mutated myoglobin (20 ng/mL each) mixture, separation column – PS-DVB monolithic column, 100 µm i.d. × 25 cm, injection volume – 10 nL, ESI voltage was set at 3.0 kV. The MS was operated at a full scan mode with an m/z range of 700–2000. (A) Separation chromatogram by EOP pump

driven gradient nano-HPLC; gradient: 25–60% ACN%, ACN% increased by 1.25% every 1.06 min; backpressure drop of the separation column was around 1000 psi and the pump rate was around 800 nL/min. (B) Separation chromatogram by Agilent 1200 HPLC system; flow rate was set at 800 nL/min.

(A)

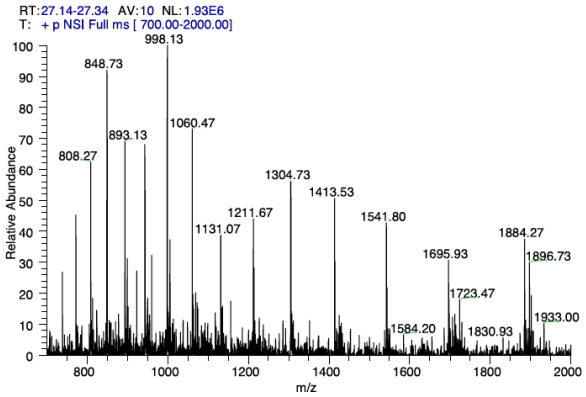

(B)

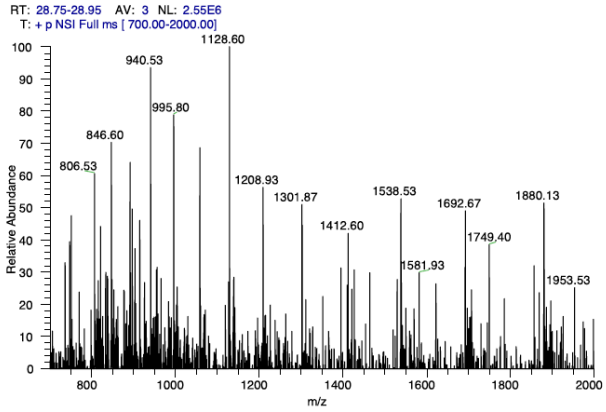

(C)

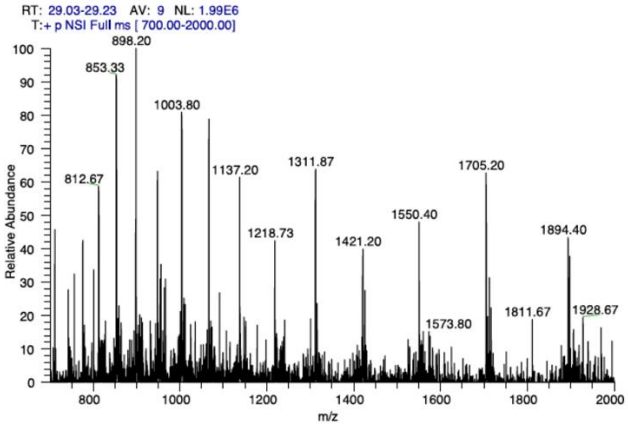

Figure 2-11 Mass spectra of peak a, b, and c in Figure 2-10.

2.5 Concluding remarks

We have developed a capillary-based nano-HPLC system by incorporating a high-pressure EOP with a nanoflow gradient generator, a nanoliter injection valve, and a packed capillary column. We have coupled the nano-HPLC with an ESI–MS for peptide and protein analysis. The EOP could be constructed at relatively a low cost, and it could generate the flow rate and pressure well suited for the rest of the system. In our lab, we can now build the EOP and the column on a chip, and we are developing on-chip valves so that we can integrate all the components on a chip – a microchip HPLC. We expect to construct a miniaturized HPLC module (similar to a cartridge) that can be conveniently coupled with an ESI–MS for proteomic studies, and beyond.

The materials in Chapter 2 are adapted from Chen et al., Analytica Chimica Acta 844 (2014) 90-98. The copyright was obtained from Elsevier and the license number is 4038860972679. For more details, please see Appendix A.

Chapter 3 Combining A Selection Valve And Mixing Chamber For Nanoflow Gradient Generation: Toward Developing A Liquid Chromatography Cartridge Coupled With Mass Spectrometer For Protein And Peptide Analysis

3.1 Abstract

Toward our goal of developing a micro HPLC cartridge, we have recently built a high-pressure electroosmotic pump (EOP). However, we do not recommend people to use this pump to deliver an organic solvent directly, because it often makes the pump rate unstable. We have experimented several approaches to address this issue, but none of them are satisfactory. Here, we develop an innovative approach to address this issue. We first create an abruption (a dead-volume) within a fluid conduit. We then utilize an EOP to withdraw, via a selection valve, a train of eluent solutions having decreasing eluting power into the fluid conduit. When these solutions are further aspirated through the dead-volume, these solutions are partially mixed, smoothing concentration transitions between two adjacent eluent solutions. As these solutions are pushed back, through the dead-volume again, a smooth gradient profile is formed (See Figure 3-1). In this work, we characterize this scheme for gradient formation, and we incorporate this approach with a high pressure EOP, a nanoliter injection valve, and a capillary column, yielding a micro HPLC system. We then couple this micro HPLC with an electrospray ionization mass spectrometer for peptide and protein separations and identifications.

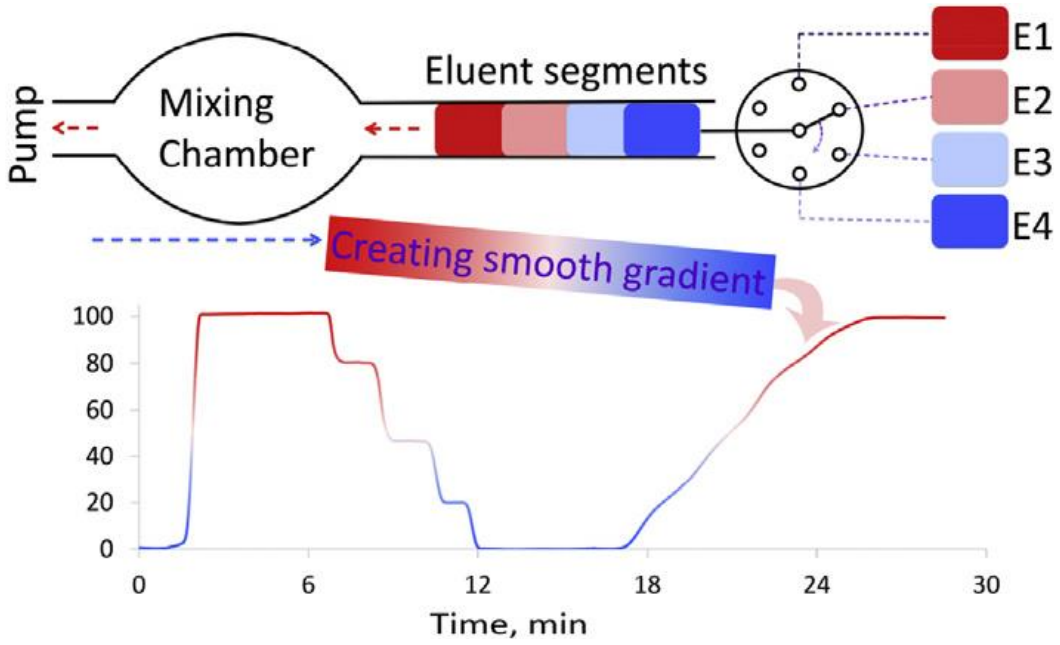

Figure 3-1 Graphical abstract.

3.2 Introduction

The electroosmotic pump (EOP) [92-95] is one of the most promising micropumps that can be used for HPLC due to its compact size, and low fabrication cost. We have recently developed a high-pressure EOP [5,7,96] and incorporated it into a miniaturized HPLC system for protein and peptide separations.[3,5,7,97] Implementing a gradient elution using this EOP has been a challenge, because its pump rate becomes unstable when we use it to pump a high organic-content solvent.[3,97] We have experimented with three approaches for alleviating this issue but none of them were completely satisfactory.[3,5,97] In first approach,[5] we preloaded two eluent segments consecutively into a capillary (with the weaker eluent in front), and this capillary was then connected to the outlet of the EOP. As the EOP drove the eluent segments forward, the two solutions were mixed, forming a gradient eluent at the interfacial region. We then used this gradient to perform peptide separations. Apparently, precisely tuning the gradient profile using this method is difficult.

In the second approach,[3] we utilized a ten-port switching valve connected with two injection loops for gradient delivery. A similar scheme had been described earlier by others.[89] In one position, while a weaker eluent in loop 1 was delivered for analyte elution, a stronger eluent was loaded into loop 2. As the valve was switched to the other position, the eluent in loop 2 was delivered for elution, while loop 1 was loaded with the next stronger eluent. Since these operations could be repeated continuously, a desired gradient could be produced. The downside of this approach is that the gradient created has a step-profile. Its operations are tedious, especially when a close-to-linear gradient is desired.

In the third approach,[97] we constructed a binary EOP for gradient production. The working principle of a binary EOP gradient generator (bi-Egg) was identical to that of a conventional binary gradient pump. Owing to the nature of electroosmotic pumping, a backflow was created whenever there was a head pressure. This backflow complicated the bi-Egg's operation. To address this issue, we developed formulas to tune the voltages on both EOPs to achieve the desired gradient. However, due to the viscosity change with eluent composition, the pressure drop across the column (or the head pressure of the pump) varied, leading to deviations between actual and programmed gradient profiles.

In this work, we develop a novel approach to address this issue. Figure 3-2 presents the basic idea of this approach. We first create an abruption (a dead-volume) within a fluid conduit (see Figure 3-2 A) by inserting a piece of larger inner diameter (i.d.) polyetheretherketone (PEEK) tubing between two pieces of smaller i.d. capillaries (see Figure 3-2 B).We then aspirate a series of eluent solutions having different elution strengths, via a selection valve, into this capillary assembly, and through the PEEK tubing. At a predetermined position (or time), we push these solutions back, through the PEEK tubing again, to a targeted location (e.g., an HPLC column). During the course of these solution movements (back and forth movement inside the capillary assembly and twice through the dead-volume), smooth concentration interfaces are formed between adjacent eluent solutions, creating a smooth gradient profile. Because the number of eluent solutions, the concentrations and volumes of the eluent solutions, the size of the dead-volume, and the pattern (velocity, duration, or movement style) of the solution movement can be conveniently tuned and controlled, any desired gradient profile can be

produced. In this experiment, we characterize this approach for smooth gradient generation. We incorporate such a gradient generator with a high pressure EOP, a nanoliter injection valve, and a capillary column into a compact HPLC platform. We further couple this HPLC with an electro-spray-ionization (ESI) mass spectrometer (MS) for peptide and protein separation and identification.

(A)

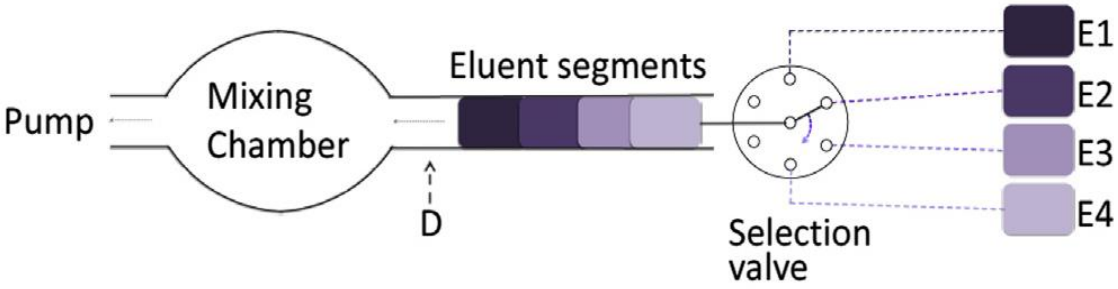

(B)

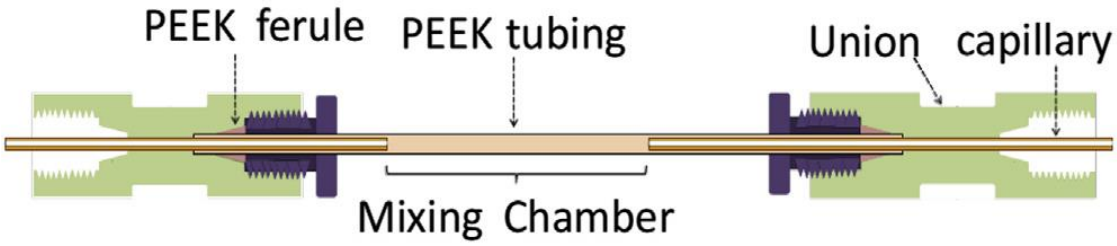

Figure 3-2 Working principle for gradient generation.

(A) Schematic configuration of gradient generator using a dead-volume (mixing chamber) within a fluid conduit. (B) Detailed construction of the mixing chamber. The selection valve in (A) is used to connect the capillary assembly to a specific solution at a given time for a preset duration, while "D" indicates an ultra-violet absorbance detector. The PEEK tubing has an i.d. of 390 mm, while the fused silica capillaries on both sides of the PEEK tubing have an i.d. of 75 mm. The length of the PEEK tubing forming the mixing chamber varies from 0 to 10 mm; the “0 mm” indicates the two pieces of fused silica capillaries are joined together.

3.3 Experimental section

3.3.1 Chemicals and materials

Ethylene glycol dimethacrylate (EDMA, 98% w/w, hereinafter "%" indicates "% w/w" unless otherwise stated) and butyl methacrylate (BMA) were purchased from Alfa Aesar (Ward Hill, MA). 1- propanol and 2,2-azobisiso-butyronitrile (AIBN, 98%) was bought from Aldrich (Steinheim, Germany). Methacryloyloxypropyltrimethoxysilane (***γ***-MAPS, 98%) was obtained from Acros (Fairlawn, NJ). Acrylamide, N,N-Methylene bisacrylamide (bis), N,N,N',N'-Tetramethylethylenediamine (TEMED) and ammonium persulfate (APS) were purchased from Bio-Rad Laboratories (Hercules, CA). 1,4-Butanediol (99%) was purchased from Emerald Bio- Systems (Bainbridge Island, WA). Proteomics grade modified trypsin was obtained from Promega (Madison, WI). LC-MS grade acetonitrile (ACN) was bought from Fisher Scientific (Fair Lawn, NJ). 2-Acrylamido-2-methylpropane sulfonic acid (AMPS, 99%), bovine serum albumin (BSA), sodium hydroxide, ammonium bicarbonate, and sodium acetate were purchased from Sigma-Aldrich (St. Louis, MO). Fused silica capillaries were obtained from Polymicro Technologies (Phoenix, AZ). Hydrochloric acid was obtained from EMD Millipore (Darmstadt, Germany). All solutions were prepared with ultra-pure water purified by a NANO pure infinity ultrapure water system (Barnstead, Newton, WA).

3.3.2 Preparation of EOP monolithic columns

The preparation protocol was similar to what we had described previously, [3] but with some minor modifications. A capillary of 100 × 150 cm (100 μm i.d.× 360 μm

o.d.) was first vinlyized using the following procedure. Briefly, the capillary was first flushed with acetone, and 1.0 M NaOH, each for 10 min. After the capillary was filled with 1.0 M NaOH and its ends were sealed by rubber septa, it was placed in an oven at 100 °C for 2 h. The capillary was then taken out from the oven, and it was flushed with water, 0.1 M HCl, and acetone; each for 20 min. After the capillary was dried with N_2 at 60 psi for 1 h, the capillary was filled with 30% (v/v) γ-MAPS in acetone, and its ends were sealed with septa, and then the capillary was put back in the oven at 50 °C for 14 h. The capillary was vinylized and ready for the monolith preparation after being rinsed with acetone and dried with N_2 at 60 psi for 2 h. The vinylized capillary was then cut into 16 cm long segments. After degassing by purging with helium for ~5 min, a solution containing 10.0 mg AMPS, 230.0 mg BMA, 160.0 mg EDMA, 4.0 mg AIBN, 424.0 mg 1-propanol, 116.0 mg 1,4-butanediol and 60.0 uL water was loaded into a capillary segment. A 500 ~ 600 psi pressure supplied by a nitrogen cylinder was applied to the ends of the capillary, and the capillary was placed in a water bath at 60 °C for polymerization for 20 h. After approximately 2 cm of the capillary ends was trimmed, the monolithic column was flushed first with acetonitrile at 1500 ~ 2000 psi overnight using an HPLC pump to remove unreacted monomers and other chemicals, and then with a 3.0 mM sodium acetate solution (pH 5.0).

3.3.3 Preparation of monolithic polystyrene-divinylbenzene (PS-DVB) columns

The preparation was based on a protocol developed by Premstaller et al.[98] A 90.0 cm long vinlylized fused silica capillary (360 µm o.d., 150 µm i.d.) was filled with a helium-purged solution containing 45.31 mg styrene, 45.70 mg divinylbenzene, 107.77 mg decanol, 17.78 mg tetrahydrofuran (THF), and 2.50 mg of AIBN. After both

ends of the capillary were blocked, the capillary was placed into a water bath at 60 °C for 24 h to allow for the monolith formation. The capillary was then cut into two halves (two columns), and the columns were washed with acetonitrile (ACN) for ~5 h at ~1000 psi to remove the unreacted monomers.

3.3.4 Apparatus

Figure 3-3 presents a schematic configuration of the HPLC system. It consists of two EOPs, a 12-port switching valve (V1, Valco Instruments, Houston, TX), a 7-port stream selector (V2, Valco Instruments), a 60-nL or a 10-nL injection valve (V3, Valco Instruments), a packed capillary column (100 Å, 3 µm, 75 µm × 100 mm, Waters, Atlantis dc18 NanoEase Column) or a home-made PS-DVB monolith column (C), and a Linear UVIS 200 absorbance detector (D, Linear Instruments, Reno, NV). Each EOP was composed of three parallel monolithic columns; these columns were connected in parallel via two micro-crosses (Valco Instruments). The high voltage was applied to the monolithic columns via two micro-tees (Valco Instruments), each being attached with a bubbleless electrode. The protocols for preparing the bubbleless electrode [96] (also see below for details) and assembling the EOP [97] were reported previously. The Linear UVIS 200 absorbance detector was set at 214 nm for peptide and protein separations and 265 nm for gradient profile measurements. An NI multifunctional card DAQ Card (6062E, National Instruments, Austin, TX) was used to acquire the absorbance signal, and the signal was processed by an in-house written LabView program.

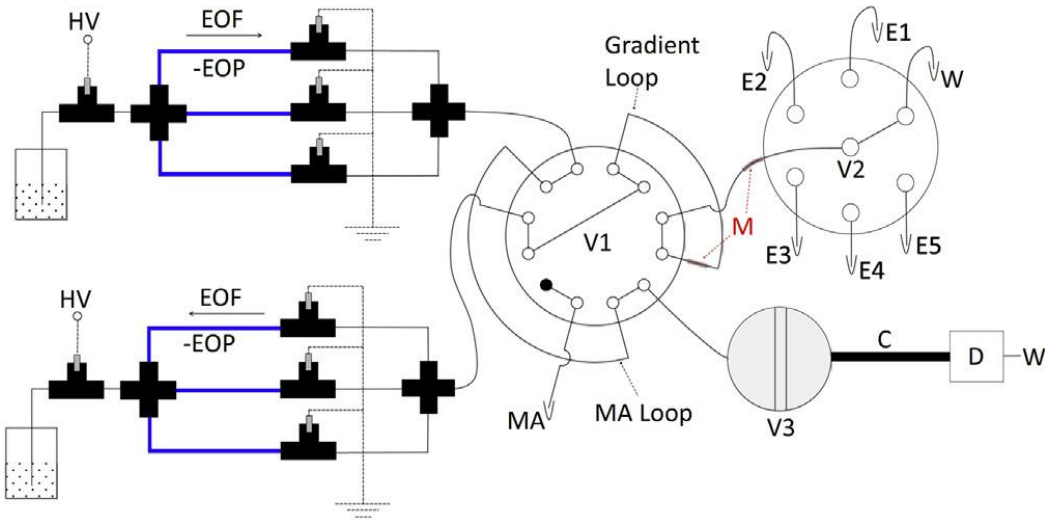

Figure 3-3 Schematic configuration of micro HPLC.

Schematic configuration of micro HPLC. There were two EOPs on the left. HV was a high voltage power supply. Since the EOP monoliths were negatively charged, the electroosmotic flow (EOF) went with the electric field. V1 was a 12-port switching valve; one of the ports (designated by the solid circle) was blocked. M was a mixing chamber (see Figure 3-2A and B). V2 was a selection valve. V3 was a 60-nL injection valve, C was packed capillary column, D was a UV absorbance detector (214 nm for peptide and protein separations or 265 nm for gradient profile measurements). W was designated waste reservoir. The capillaries connecting the EOP to V1 were 100 µm i.d. 360 µm o.d. 15 cm length, the capillary connecting V1 and V2 was 75 µm i.d. 360 µm o.d. 12 cm in length), and the capillary connecting V1 and V3 was 50 µm i.d. 360 µm o.d. 12 cm in length. MA stands for mobile phase A (5% ACN in 0.1% TFA). Gradient Loop and MA-Loop were fused silica capillaries having identical dimensions (100-cm-long 250-µm-i.d. 365- µm-o.d.). E1, E2, E3, E4, and E5 were respectively 45%, 27.5%, 15%, 10%, and 5% ACN in 0.1% TFA.

3.3.5 Preparation of bubbleless electrode

A 20-cm-long and 150-μm-i.d. (360 μm o.d.) capillary was cut, and its inner wall was cleaned by flushing the capillary with 1.0 M NaOH for 45 min, DI water for 15 min, and acetonitrile for 15 min. After the capillary was dried with N_2, the inner wall was reacted with a solution containing 30% (v/v) γ-MAPS in acetone at 50 °C for 14 h. Then, the capillary was flushed with acetonitrile and dried with N_2. A degassed solution containing 9%T (%T stands for the total weight concentration of acrylamide and bis in the solution), 3%C (%C represents bis concentration relative to acrylamide), 0.2% (v/v) TEMED, and 0.1% APS was pressurized into the capillary and remained inside the capillary at 0 °C overnight and then 4 °C for another 24 h. After 1 cm of the capillaries at both ends were trimmed off, 50 mM sodium tetraborate was electrophoretically driven through the polyacrylamide inside the capillary until a stable current was obtained. The above capillary was cut into ~2 cm pieces, and each piece was used as a bubbleless electrode.

3.3.6 Flow rate measurement

The flow rate was determined by connecting an open capillary (i.e., a 360 μm o.d., 200 μm i.d. capillary) to the outlet of the system. After the solution was pumped into the capillary, we monitored the movement of the meniscus (it is preferable to use a microscope here). The overall flow rate was estimated by the equation Qeo (nL min-1) = 314L/t, where L (cm) is the distance the meniscus had moved, and t (min) is the period of the test.

3.3.7 Coupling micro HPLC with ESI-MS

The micro HPLC was coupled with the ESI-MS via a nanospray emitter. The capillary separation column was carefully butt-to-butt connected to a metal-film-coated nanospray ionization (NSI) emitter (a 5-cm-long, 360-μm-o.d., and 20-μm-i.d. fused silica capillary with a 5-μm-i.d. spray tip, New Objective, Woburn, MA) using a zero-dead-volume PTFE coupler (Waters). The voltage was applied directly to the metal film on the spray tip.

3.3.8 Using C^4D to monitor gradient profile

An Agilent 1200 HPLC system was employed to produce linear gradient profiles and execute gradient elutions for performance comparison. To produce low flow rates, a micro-Tee (Upchurch Scientific) was used as flow splitter prior to the separation column. A fused silica capillary (50 μm i.d. × 360 μm o.d. × 50 cm length) was connected to the micro-tee as a restrictor to generate desired backpressures for the separations. The gradient profile after the flow-splitter and before the separation column was measured by a capacitively coupled contactless conductivity detector (C^4D, TraceDec, Innovative Sensor Technologies, Strasshof, Austria). The C^4D measured the impedance variation caused by acetonitrile concentration change of the eluent solution inside the capillary, due to the conductivity change (Figure 3-4). The actual gradient profile was obtained by converting the recorded signal with a calibration curve (Figure 3-5).

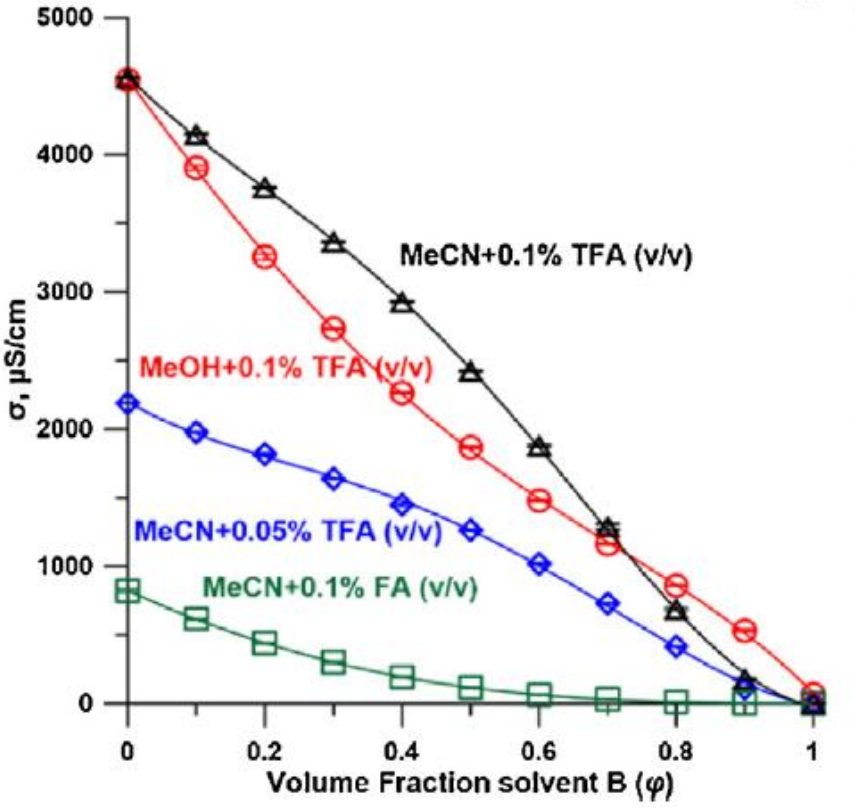

Figure 3-4 Conductivity of MeCN and MeOH with TFA and FA.

Measured by Dionex conductivity detector; cell constant, 4408.7/cm.

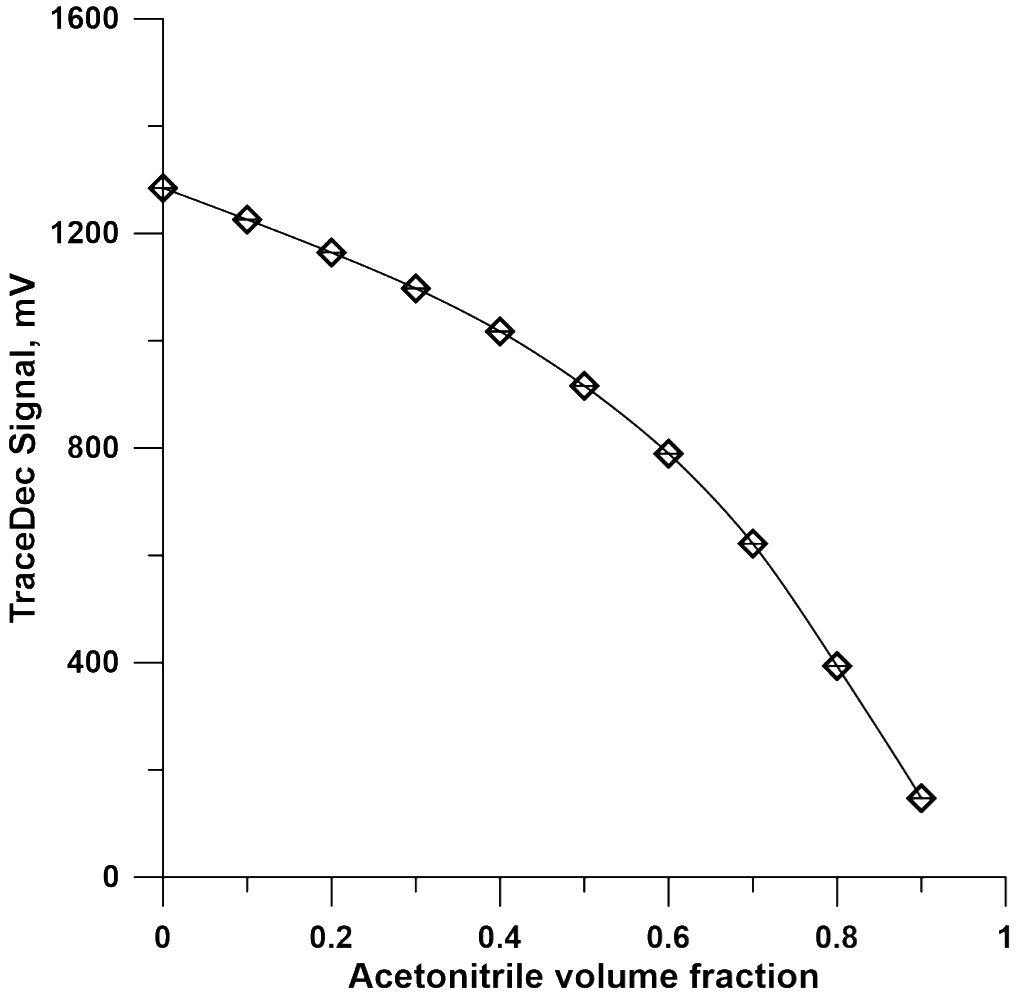

Figure 3-5 TraceDec signal vs the acetonitrile volume fraction.

Solution: 0.1% (v/v) TFA + water + acetonitrile. TraceDec condition: frequency, high; voltage, -18 dB; gain, 50%; offset, 0. Capillary, 75 μm ID X 360 μm OD. Error bar: standard deviation of three measurements.

A serial of pre-mixed water-acetonitrile solutions with 0.1% (v/v) TFA was measured by TraceDec detector. As shown in Figure 3-5, the detector response decreased with increasing acetonitrile volume fraction. A typical measured gradient profile was presented in Figure 3-6.

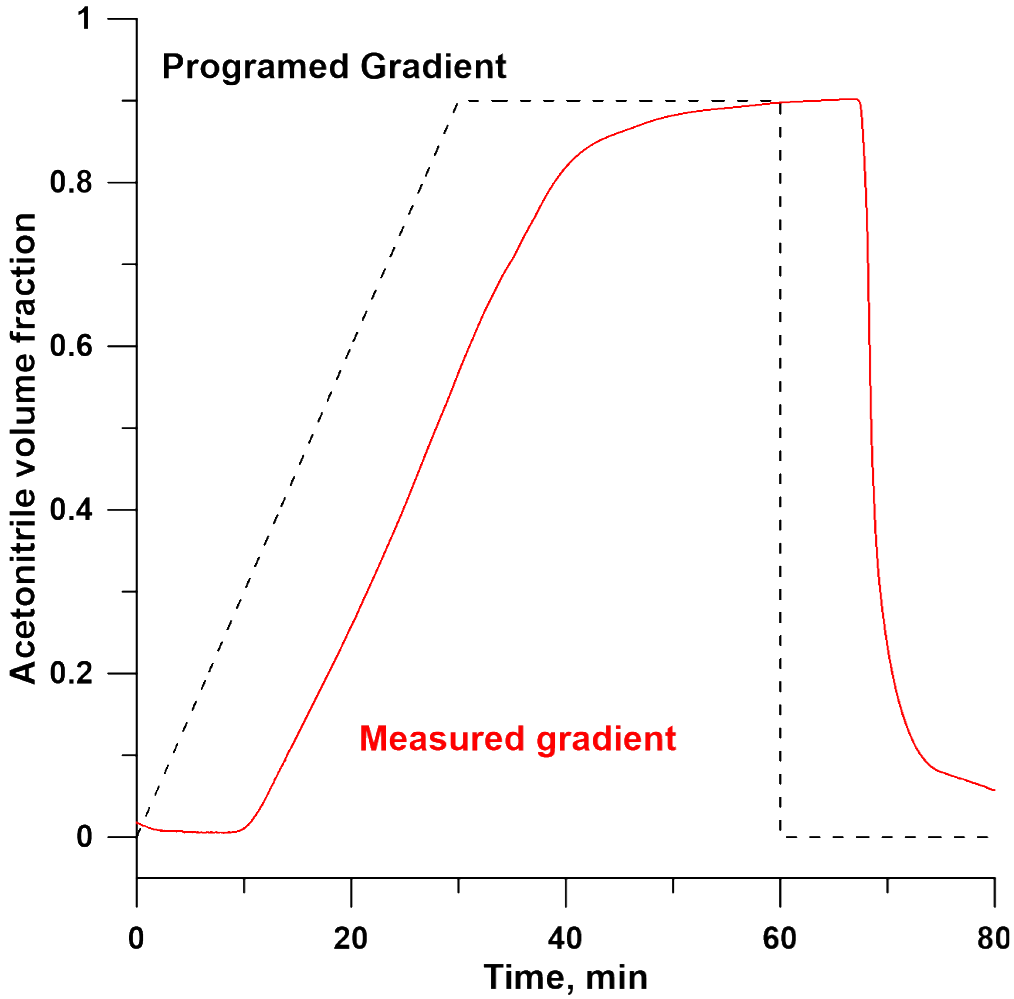

Figure 3-6 Typical gradient profile for Agilent 1200 HPLC. Detector conditions are the same as in Figure 3-5.

3.4 Results and discussion

3.4.1 Performance of nano-flow gradient generator

Referring to Figure 3-3, one of the six ports of V2 was connected to waste (W), and the other five were connected eluents 1 through 5 (E1 through E5). The compositions of E1, E2, E3, E4, and E5 were respectively 45%, 27.5%, 15%, 10%, and 5% ACN in 0.1% TFA. When the top EOP was connected to the column (C) as shown in Figure 3-3, +3.2 kV was applied to the pump (the pump rate at this high voltage was ~150 nL/min). The EOP drove mobile phase A (MP A, composition 5% ACN in 0.1% TFA) to equilibrate C for sample injection. At the same time, +3.6 kV was applied to the bottom EOP for a 10 min to rinse the gradient loop to waste (W). The pump rate under this condition was ~500 nL/min. Higher voltage could be applied to increase flow rate; however, we did not use voltages higher than 10 kV to avoid excessive Joule heating. Then, -3.6 kV was applied to the pump, and V2 was switched to E1, E2, E3, E4, and E5 for 12 min, 9.75 min, 7.8 min, 3.75 min, and 5.5 min, respectively. The pump rate at -3.6 kV was about ~500 nL min. Then, -3.6 kV was turned off, and five eluent solutions were parked inside the gradient loop. A 10-nL injection valve was used to inject 10 nL of a sample, or a 60-nL injection valve and a time-controlled injection scheme (8 s at a flow rate of ~150 nL/min) was used to inject ~20 nL of a sample into the column for separation. After sample injection, V1 was switched to the other position. The top EOP drove the gradient eluent through V3 and C for chromatographic elution. At this time, -3.6 kV was applied to the bottom EOP to aspirate MA for 15-20 min, and

the high voltage was turned off. After the separation was complete, V1 was switched back to initiate a new run.

3.4.2 Nano-flow gradient generation

To test whether an EOP element can form a smooth gradient profile easily, we set up a gradient generator as schematically shown in Figure 3-2A. The PEEK tubing had an i.d. of ~390-µm-i.d., and it was inserted in between two pieces of 75-µm-i.d. capillaries; one had a length of 5 cm, and the other had a length of 15 cm (see Figure 3-2B). The free end of the 5-cm-capillary was then connected to an EOP, while the free end of the 15-cm-capillary was connected to the common port of a selection valve. Five solutions having different acetonitrile concentrations were connected to five ports of the selection valve, and a waste reservoir was connected to the last port of the selection valve. A Linear UVIS 200 absorbance detector was set at 265 nm and affixed to the 15-cm-capillary to monitor the gradient as the solution passed across the detector.

When equal lengths of solutions were aspirated in and pushed out through the capillary assembly, a smoother concentration transition was observed for the last two exiting solutions (normal concentrations ~75% and ~100%), compared to the earlier two exiting solutions (normal concentrations ~25%-~50%). The reason was that the last two exiting solutions were the first two solutions aspirated in and they had traveled a longer distance and mixed more completely than the earlier exiting solutions. There are two ways to compensate the different level of mixing; to aspirate a longer solution segment for an earlier aspirated solution, and/or to reduce the concentration difference between the later aspirated solutions. Figure 3-7 presents the results by reducing the solution segments for the later aspirated solutions; a smooth linear gradient was created.

Increasing the dead-volume can also improve the smoothness of the gradient profile (see Figure 3-8). It is worth pointing out that the mixing chamber volume for a 10-mm long and 390-µm-i.d. capillary was ~1.2 µL.

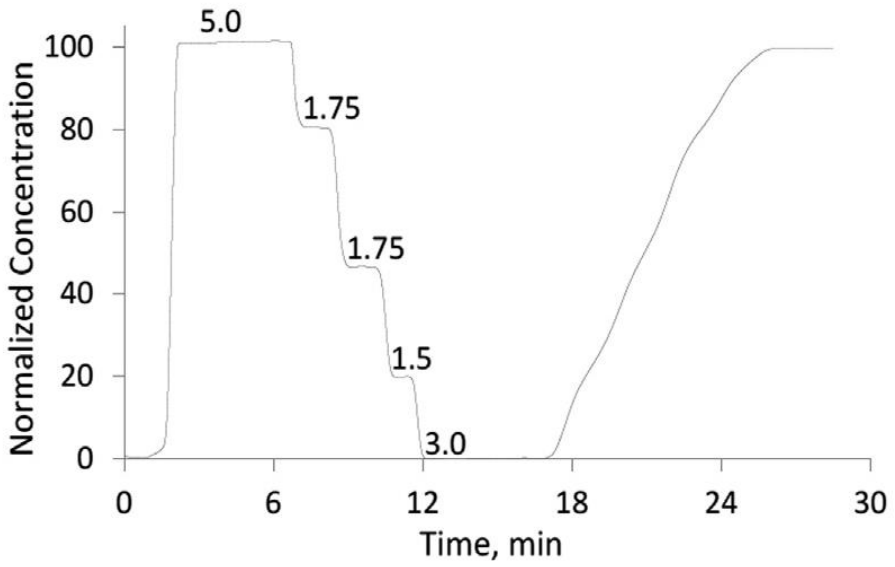

Figure 3-7 An example gradient profile generated by Figure 3-2A.

The PEEK tubing had a length of 10 mm (a dead-volume of ~1.2 mL). E1, E2, E3, and E4 were respectively 75% ACN + 2.5% acetone, 56% ACN + 1.9% acetone, 38% ACN + 1.2% acetone, and 19% ACN + 0.6% acetone in 0.1% TFA aqueous solution. The normalized concentrations were the percentage of the highest signal recorded by D at 265 nm as E1, E2, E3, E4, and water were aspirated into the capillary assembly, and all the solutions were pushed back (at ~14 min). The numbers on the curve indicate the aspiration duration for the specific solutions. The pump aspiration rate was ~300 nL/min, and the forwardpumping rate was ~400 nL/min.

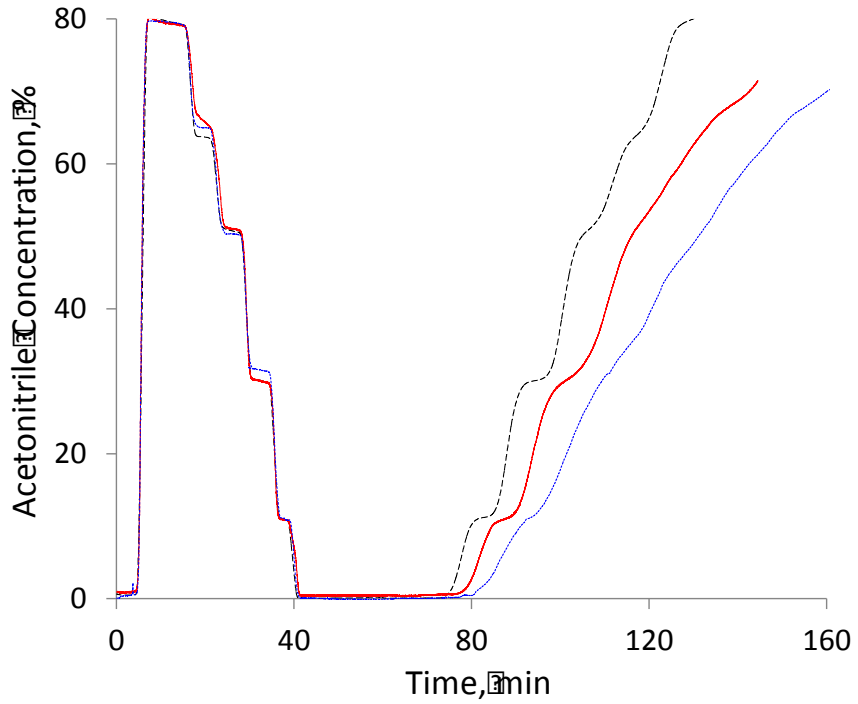

Figure 3-8 Effect of mixing chamber volume on gradient formation.

Five acetonitrile solutions (80%, 64%, 48%, 32%, 16%, and 0% ACN in 0.1% TFA were aspirated in as -1.2 kV was applied on a EOP (flow rate = ~-150 nL/min) for 9.0, 7.0, 6.5, 5.8, 3.1, and 20 min, respectively. Then, the 0% ACN solution was replaced with a waste reservoir, and +1.2 kV was applied to EOP (flow rate = ~150 nL/min) to push the eluent solutions, via the port for the 0% ACN solution to waste. Volumes of mixing chambers were 0 µL (no PEEK tubing) for the black trace, 0.6 µL (5-mm-long PEEK tubing) for the red trace, and 1.2 µL (10-mm-long PEEK tubing) for the blue trace. All other conditions were the same as those described in Figure 3-2.

With the above knowledge, we set up an apparatus as presented in Figure 3-3. A dead-volume was created between V1 and V2 (the thick line M on the connection capillary) or within the Gradient Loop, and an UV absorbance detector was affixed between V1 and V3 to monitor the gradient profile. The smoothness of the gradient profile did improve but not significantly. The reason was that a dead volume of 2-3 µL was present in V1 as the eluents passed through 2 ports from V2 to the Gradient Loop and 2 ports from the Gradient Loop to V3; this dead volume served effectively as a mixing chamber. Therefore, for the rest of this experiment, we did not include any additional dead-volume in the apparatus. However, it is preferable to put a mixing chamber after EOP when a relatively large total volume of eluents (e.g., more than 20 µL) and/or a shallow gradient profile is needed for a long-time separation, such as for proteomics analysis, which often requires the resolution of more than one thousand peaks, since the inherent dead-volume of the valve is not enough to generate a smooth gradient profile, especially when a "zero dead-volume" valve that have been recently developed by Valco Instruments is used.

The very first solution aspirated was usually the strongest eluent, and we often aspirated a large volume of this solution so that we could wash the column thoroughly after the separation. We used another solution with the lowest elution power called mobile phase A (or MA) stored in the other Loop to equilibrate the column for the next separation. The volumes of the Gradient loop and the MA loop should be adequate so that no eluent solutions or MA solution could be aspirated into the EOPs.

3.4.3 Performance of nano-flow gradient generator

To test whether we could produce reproducible gradients, we utilized the apparatus as shown in Figure 3-3, but without V3 and C, to produce gradient profiles repetitively. Figure 3-9 and Figure 3-10 present the results, which show that reproducible gradient profiles were generated. The average standard deviations of the acetonitrile concentration profiles were less than 1%.

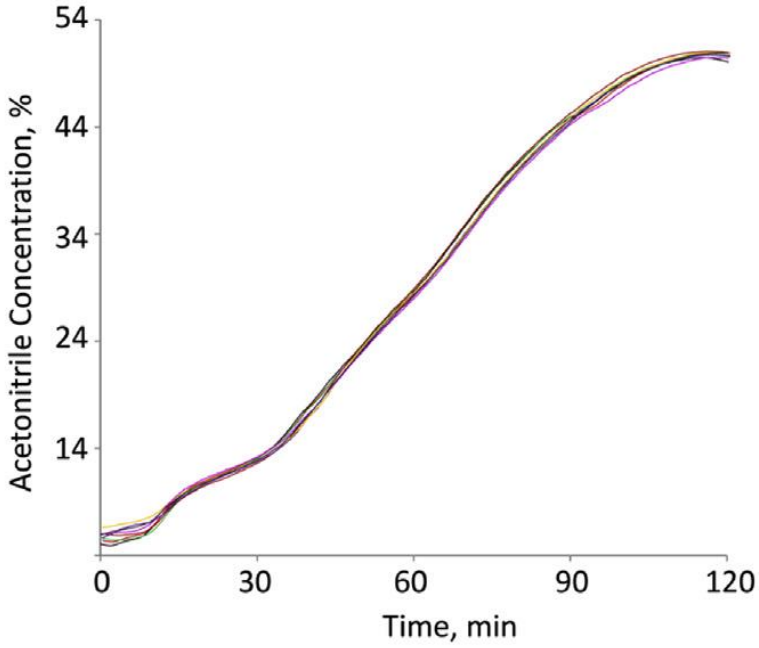

Figure 3-9 Gradient profile formed using the apparatus in Figure 3-3 after removing V3 and C (see Results and Discussions for details).

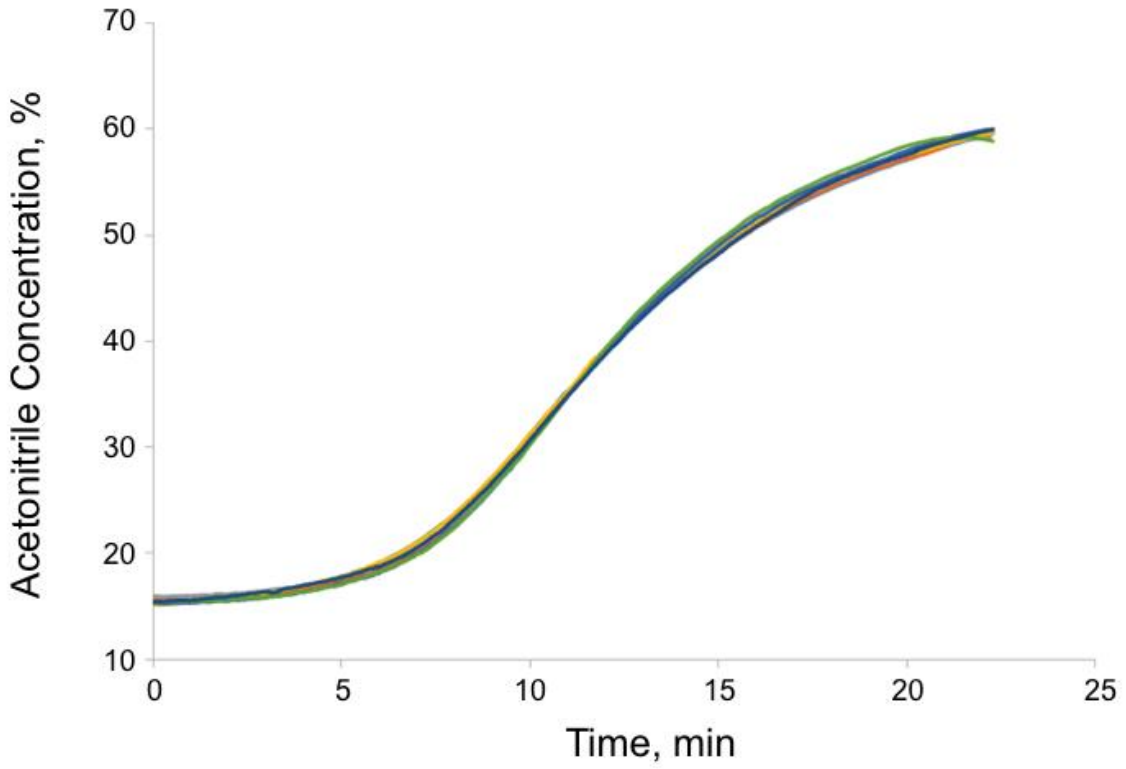

Figure 3-10 Repeatability of gradient profile formed using apparatus shown in Figure 3-3 and Figure 3-9.

E1, E2, E3, E4, and E5 were respectively 60%, 40%, 30%, 20%, and 15% ACN in 0.1% TFA. Seven repeats are shown here. Note that the gradient profiles measured between V1 and V3 using a C^4D detector.

We then incorporated the nanoliter injection valve (V3) and the separation column (C) into a micro HPLC platform. We used this platform for repetitive separations of peptides (trypsin-digested bovine serum albumin); high reproducible chromatograms were produced (see Figure 3-11).

To examine the validity of the above system, we compared its performances with the performance of a commercially available Agilent 1200 HPLC system (Agilent Technologies, Santa Clara, CA). We first used the micro HPLC platform to separate tryptic digests of bovine serum albumin and hh Mb H64V. The same samples were then separated on the Agilent system. These results were presented in Figure 3-12A-D. By visualizing the chromatograms, we can say that comparable efficiencies and resolutions are obtained. The two sets of results did exhibit some differences, however, and these differences could be attributed partially to the gradient profile differences.

It is also important to notice that there was a ~12-min time delay from the programmed gradient profile to the actual gradient profile using the Agilent 1200 HPLC system. Using our micro HPLC system, this time delay was shortened to 3-5 min.

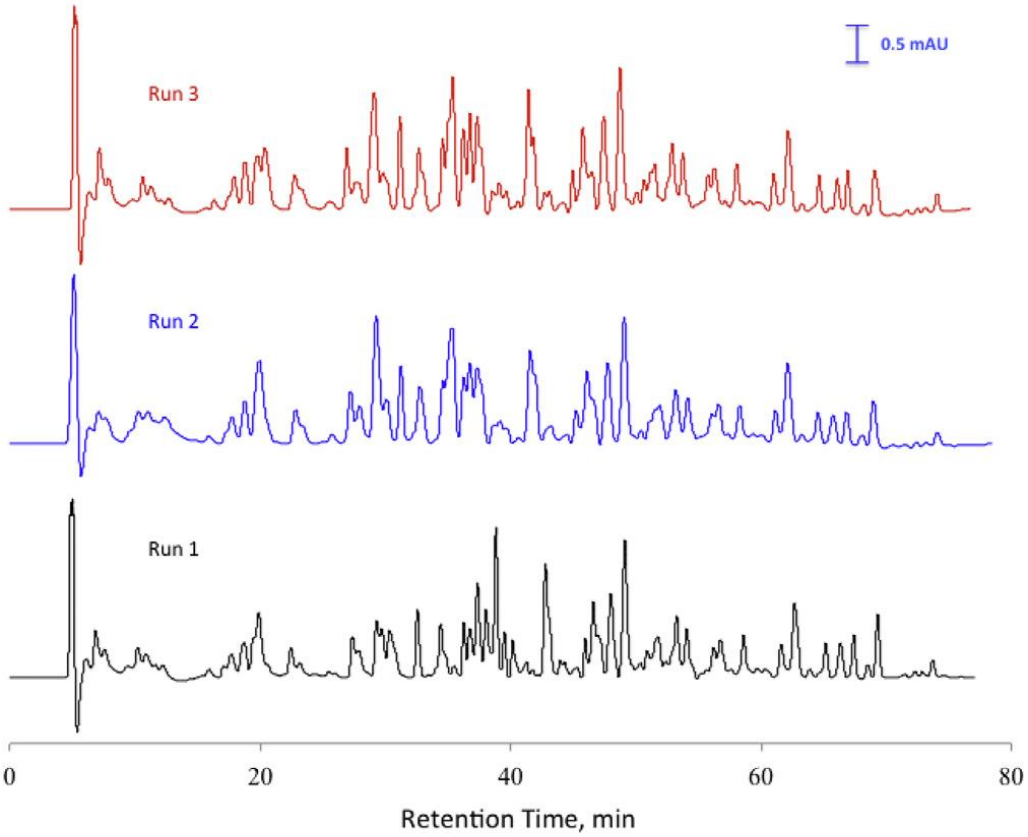

Figure 3-11 Chromatograms for repetitive runs. Sample-trypsin digests of BSA (10 mg/mL).

When a HV of -3.6 kV was applied to the bottom EOP to aspirate five eluent solutions, the aspiration rate was ~500 nL min^{-1}. When +3.2 kV was applied to top EOP for elution or column equilibration, the pump rate was ~150 nL min^{-1}. The 60-nL injection valve (V3) could be set at either a "Load" position or an "Injection" position. Injection of 20 nL sample into C was implemented by switching V3 from "Load" to "Injection" and allowing it stay at "Injection" position for 8 s, and then switching it back to "Load" position. The absorbance signal was monitored at 214 nm.

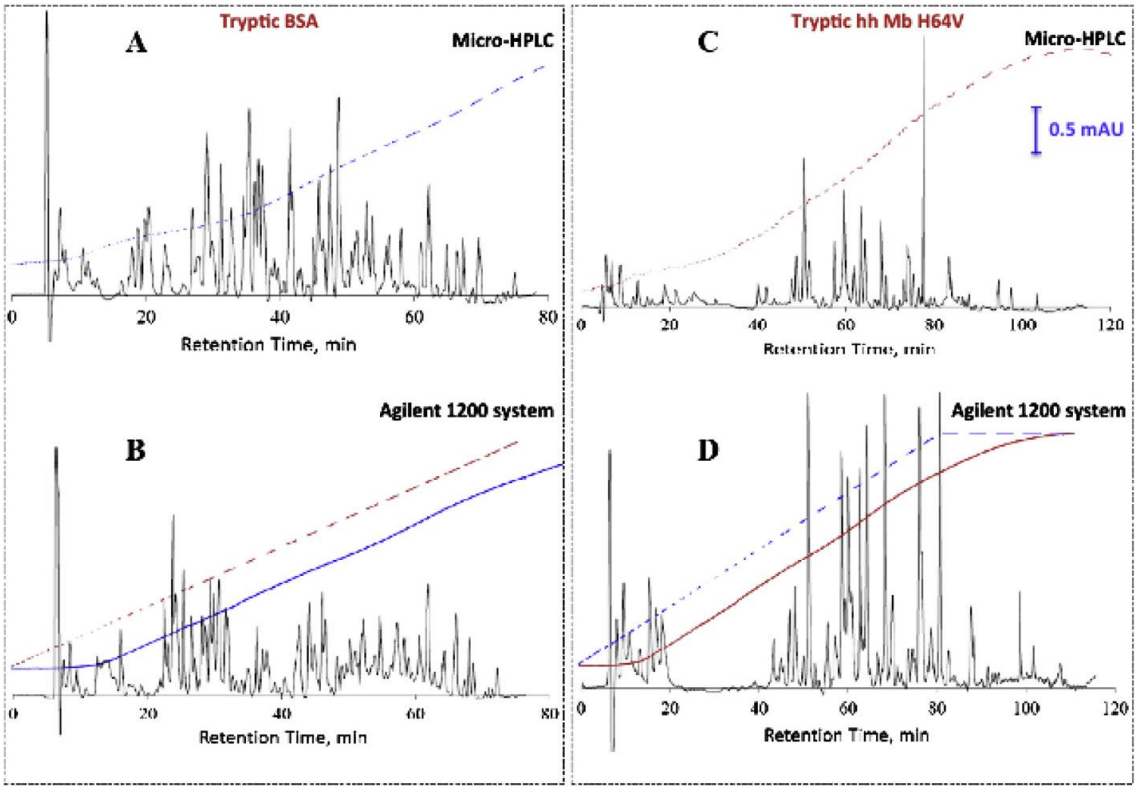

Figure 3-12 Performance comparison between micro HPLC and Agilent 1200 system.

(A) and (C), chromatograms of trypsin digests of BSA (10 mg/mL) and hh Mb H64V (10 mg/mL) obtained from our micro HPLC. (B) and (D), chromatograms of trypsin digests of BSA (10 mg/mL) and hh Mb H64V (10 mg/mL) obtained from Agilent 1200 system. The same Linear UVIS 200 absorbance detector as used in Figure 3-11 was utilized here. The dashed lines in (A) and (C) represent the gradient profiles. The dashed lines in (B) and (D) represent the programmed gradient profiles, while the solid lines represent the gradient profiles measured between V1 and V3 using a C^4D detector.

3.4.4 Coupling a micro HPLC platform with a mass spectrometer for protein separation and identification

Proteins play the most important physiological functions in cells and tissues, and any mutation or mutations in a protein may cause a disease, since a mutated protein can lead to its incorrect three dimensional folding and subsequently cause malfunction of the protein. [99] The development of mass spectrometry allows us to distinguish a single protein from its isoforms and other proteins, lending us an effective tool for characterizing human diseases and ultimately for developing therapies to treat these diseases. [100] Myoglobin is well-known as an oxygen carrier. It also removes nitrite NO_2^- by reducing it to nitric oxide (NO) and lowers the energy status of heart cells, which subsequently prevents heat injury from hypoxic conditions.[90,101] It was reported that a single amino acid mutant of horse heart myoglobin (hh Mb, H64V) dramatically decreased the efficiency of hh Mb as a scavenger to remove NO_2 due to the mutation that changed the H-bonding in the distal pocket of the myoglobin. [88] Here, we coupled our nano- HPLC with a mass spectrometer (LCQ DECA XP plus, Thermo Fisher Scientific Inc., Waltham, MA) for protein separation and identification. Detailed interfacing between micro HPLC and ESI-MS is presented in Figure 3-13.

(A)

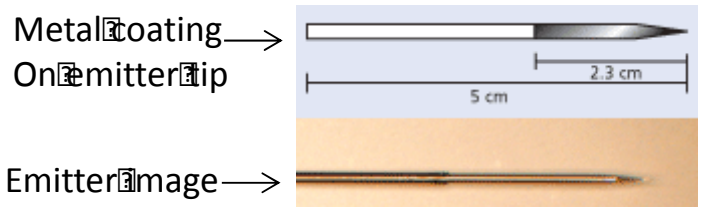

(B)

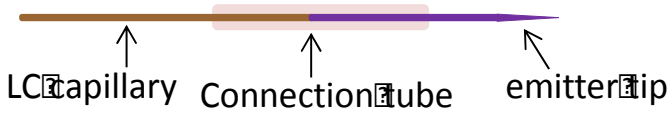

(C)

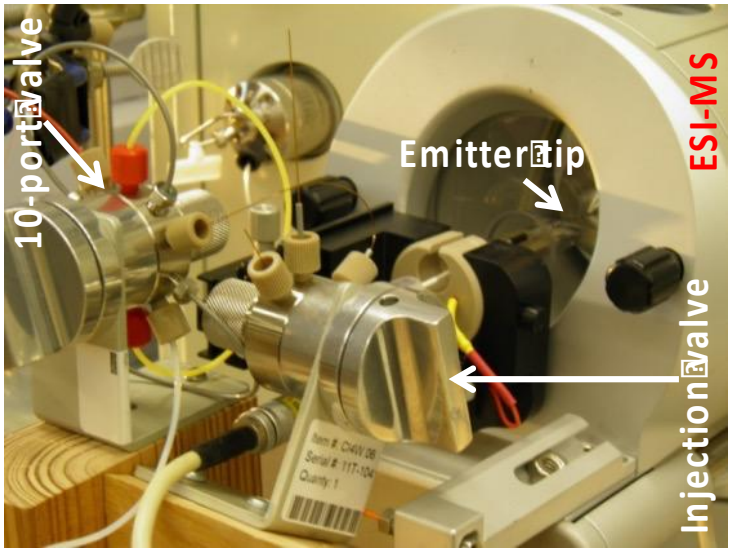

Figure 3-13 Coupling micro HPLC with ESI-MS.

(a) Metal-film-coated nanospray ionization (NSI) emitter, (b) coupling micro HPLC with the emitter, and (c) a picture of the interface between micro HPLC and ESI-MS.

Figure 3-14 presents a chromatogram for a mixture of wild type horse heart myoglobin (wt hh Mb), a mutated hh Mb H64V, and the hh Mb H64V missing the first methionine.[91] Peak a is the wt hh Mb. The mass spectrometer (MS) measured molecular weight is 16,951.76 Da (see inset A), which is consistent with its theoretical value (16951.49 Da [102]). Peak c is the mutated hh Mb H64V, which has one additional methionine at the N-end and its histidine at position 64 is mutated to valine. The MS measured molecular weight is 17,044.81 Da (see inset C), which is consistent with the calculated value (17044.67 Da). Peak b is the mutated hh Mb H64V missing the first methionine [91]. The MS measured molecular weight is 16,913.50 Da (see inset B), which is consistent with calculated value (16913.48 Da). In other words, all proteins could be positively identified with this approach.

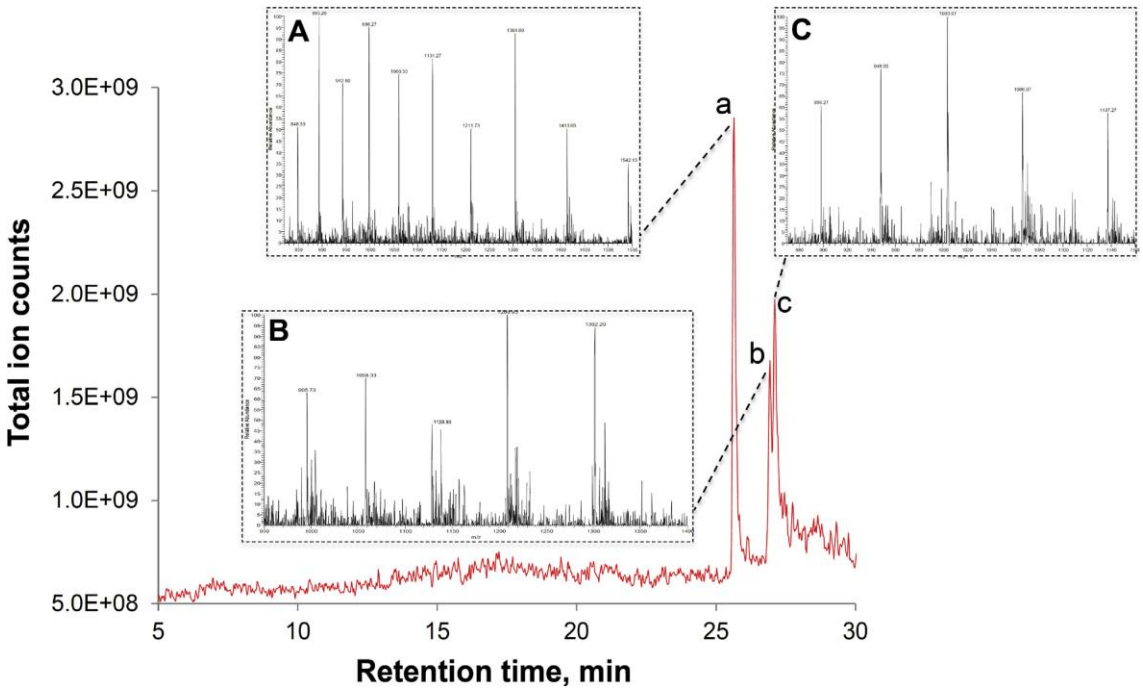

Figure 3-14 Coupling micro HPLC with ESI-MS for real-world sample analysis.

Sample - mutated myoglobin (H64V) and wild type myoglobin (20 ng/mL each) mixture. Separation column - home-made PS-DVB monolithic column 100-µm-i.d. 365-µm-o.d. 25-cm-long. Injection volume - 10 nL. (Note: we used a 10 nL injection valve here.) A HV of -3.6 kV was applied to the bottom EOP to aspirate five eluent solutions (60%, 52.5%, 45%, 37.5%, and 30% ACN in 0.05% TFA respectively for 10, 6, 5.5, 5.0, and 5.5 min. A HV of +4.8 kV was applied to top EOP (pump rate 1/4 ~470 nL/min) for elution. ESI voltage was set at 3.0 kV, and the MS was set as a full scanning mode with m/z range of 700-2000. Insets A, B, and C are mass spectra of peaks a, b, and c, respectively.

3.4.5 Prototype of microHPLC

We have an ongoing project that incorporates the selection valves, EOP, high voltage power supply, and separation column into a small box as the prototype of microHPLC, which is under control of a computer capable of separating proteins and peptides. Figure 3-15 shows the comparison of the prototype of the microHPLC and commercial HPLC. The version 1 prototype of the microHPLC has a smaller dimension and lower mass (total weight is less than 5 lbs and the dimension is about 25 cm × 25 cm × 25 cm) than the commercial one. The size and weight of the microHPLC can be further reduced by optimizing the design and using lighter material to 3D print the box.

Figure 3-15 Comparison of prototype of microHPLC and a commerical HPLC (Aglient 1200).

3.5 Concluding remarks

We have developed an innovative approach for smooth gradient generation. The approach combines an EOP with a selection valve to withdraw a series of solutions having decreasing eluting power into a fluid conduit that comprises of a mixing chamber (in this work the inherent dead-volumes of V1 and V2 were used as the mixing chamber). We have incorporated this approach with a high pressure EOP, a nanoliter injection valve, and a packed capillary column into a micro HPLC system. Theoretically, any type of desired gradient profile can be generated since it is determined by predefined eluents. To automate the process, we are developing an auto-pump controlled by an in-house written system, and the results will be published somewhere else. We have further coupled the micro HPLC with an ESI-MS for peptide and protein analysis. Portability is potentially a highly desirable feature for remote field and point-of-care applications. [103,104] At the time being, the repeatability of our micro HPLC is not as good as the Agilent 1200 system, but it will improve as a more rigid apparatus is developed. Because the micro HPLC could be produced at a cost of $3-4k, compared to a commercial HPLC system that costs $30-40k, the micro HPLC holds great promise in these applications.

The materials in Chapter 3 are adapted from Chen et al., Analytica Chimica Acta 887 (2015) 230-236. The copyright was obtained from Elsevier and the license number is 4038861105398. For more details, please see Appendix B.

One figure in Chapter 3 is adapted from Zhang et al., Journal of Chromatography A.1460: 68-73 (2016). The copyright was obtained from Elsevier and the license number is 4066091195026. For more details, please see Appendix C.

.

Chapter 4 Tunable Electroosmosis-Based Femto-Liter Pipette: A Promising Tool toward Living-Cell Surgery

4.1 Abstract

Single-cell analysis has attracted increasing attention because of cell heterogeneities. Various strategies have been developed for analyzing single cells, but most of these analytical processes kill the cells. Tools that can qualitatively and quantitatively measure the cellular contents without killing the cell are in high demand because they enable us to conduct single-cell time-course studies (e.g., to examine how a cell responds to a therapy before, during and after a treatment). Here we develop a femto-liter (fL) pipette to serve this purpose. To ensure that we can accurately and precisely pipette fL solutions, we fill all conduits with liquid and use an electroosmotic pump (EOP) as the driving force to facilitate withdrawal of cellular contents from single cells. We tentatively term this device an EOP-driven pipette or EDP. We characterize the EDP for accurately and precisely withdrawing solution from ~250 fL to 80 nL; a volume range that covers the applications for most types of cells. To demonstrate the feasibility of utilizing the EDP for a single-cell time-course study, we utilize the EDP to take the cellular contents out at different times during the course of a zebrafish embryo development for cholesterol measurements. More than 50% of the embryos survive after each pipetting and analysis step, and this number will increase considerably as we improve our cell manipulation skills and reduce the pipette-tip diameter. We expect this EDP to become an effective tool for single-cell time-course studies.

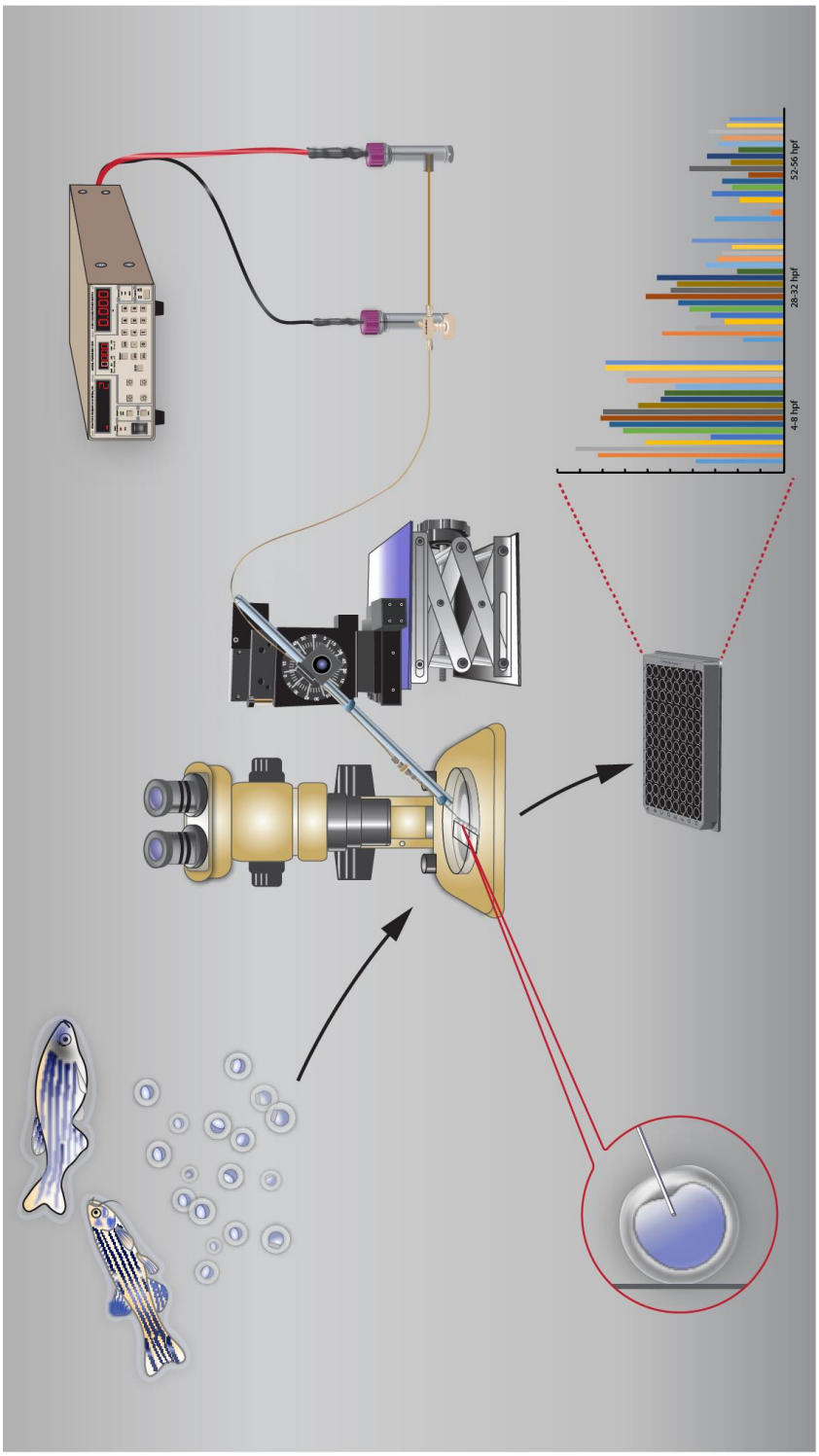

Figure 4-1 Graphical abstract.

4.2 Introduction

Both normal and cancer cells have shown variations and heterogeneity,[14,105] and substantial evidence has indicated that the heterogeneity of individual cells within a genetically identical population can be critical to their chance of survival.[106] Techniques that use average responses from a population can mask the differences between individual cells. To fully understand cell-to-cell variability, analysis of an individual cell from its live state to its cell lysates is essential.

Current single-cell analysis tools usually involve cell isolation and subsequent cell lysis before chemical analysis. Fluorescence-activated cell sorting (FACS)-based techniques and microfluidic devices are commonly employed for high-throughput cell isolation, lysis and analysis.[107-109] Because these methods require the removal of the cell from its original environment, it perturbs the physiological conditions and may cause the loss of contextual information. Lysis of the cell also prevents single-cell time-course studies.

A direct approach is to insert a fine tube into a cell and take cellular contents directly out for analysis.[41,110] The challenges are how to withdraw a small volume of solution accurately and precisely and how not to disturb the cell. Micropipettes have been used to aspirate nanoliters of cytoplasmic samples inside living cells for analyzing their mRNA[111] or metabolite[112] contents, but such a pipette with air between a pipette-tip and a plunger cannot accurately and precisely withdraw small solution volumes. This is because air is compressible and a slight change in solution viscosity will alter the volume of solution withdrawn. Fluidic force microscopy (FluidFM) with a

microfabricated 400-nm sharp tip has recently been used for cellular content withdrawal.[37,39,41,113,114] Because FluidFM is mounted on top of an inverted optical microscope, one can insert the tip into a cell precisely, as well as measure the volume withdrawn accurately. A major issue with this approach is the sophisticated and expensive instrumentation. Other mechanisms such as capillarity force,[115] syringe,[29] electrowetting,[116] and adsorption/absorption,[12,105] etc. have been used for picking up cellular contents, but none of these approaches are satisfactory for single cell analysis.

In this work, we develop a tunable electroosmosis-based femto-liter (fL) pipette for aspirating cellular contents from a single cell for chemical analysis. The driving force of the pipette is an electroosmotic pump (EOP). A key feature of this pipette is that liquid is filled in the entire conduit between the pipette tip and the EOP. Since liquid is incompressible, the volume of solution withdrawn can be accurately and precisely controlled by the EOP; the exact volume withdrawn is a function of the voltage (V) applied on the EOP and pipette-on time (t, the duration of the time the voltage is being applied). Technically, the pipette does not have an upper or a lower volume limit since $V \cdot t$ can change from 0 to infinity. We characterize it primarily from ~250 fL to 80 nL because this volume range covers the applications for most cell types. In addition, we demonstrate the feasibility of utilizing this EOP-driven pipette (EDP) for analyzing cholesterol levels in the yolk of zebrafish embryos during the course of development.

4.3 Experimental section

4.3.1 Reagents and materials

Glass tubes (1.00 mm outer diameter (o.d.) × 0.50 mm inner diameter (i.d.) × 100 mm length, Lot #: 30-0032) were purchased from Harvard Apparatus (Holliston, MA). Bare fused silica capillaries were purchased from Polymicro Technologies Inc. (Phoenix, AZ). Dichlorodimethylsilane, butyl methacrylate (BMA) and ethylene glycol dimethacrylate (EDMA, 98%) were purchased from Alfa Aesar (Ward Hill, MA). Chloroform-D was purchased from Cambridge Isotope Laboratories Inc. (Tewksbury, MA). 2,2'-azobisiso-butyronitrile (AIBN, 98%), 1-propanol, 2-acrylamido-2-methylpropane sulfonic acid (AMPS, 99%), sodium hydroxide, and ammonium acetate were bought from Sigma-Aldrich (St. Louis, MO). γ-Methacryloyloxypropyltrimethoxysilane (γ-MAPS, 98%) was purchased from Acros (Fair Lawn, NJ). Acetonitrile was purchased from Fisher Scientific (Fair Lawn, NJ). 1,4-butannediol (99%) was obtained from Emerald Biosystem (Bainbridge Island, WA). Hydrochloric acid was purchased from EMD Millipore (Darmstadt, Germany). All solutions were made with deionized water from a Barnstead ultrapure water system (Newton, WA).

4.3.2 EOP Preparation

The EOP was prepared following the protocol described previously[2,3] with minor modifications. To prepare a bi-functionalized capillary, the inner wall of a 90-cm-long capillary (100 µm i.d. × 360 µm o.d.) was flushed with acetone for 5 min and then 1.0 M NaOH at 100 °C for 2 h. The capillary was flushed with water, 0.1 M HCl,

acetone, and N_2 successively. After the capillary was filled with 30% (V/V) γ-MAPS in acetone and its ends were sealed with septa, the capillary was put in an oven at 50 °C for 14 h. The capillary was then washed with acetone and dried with N_2.

To prepare a negatively charged monolith, the bi-functionalized capillary was cut into segments, each with 15 cm in length. A solution consisted of 460.0 mg BMA, 20.0 mg AMPS, 320.0 mg EDMA, 850.0 mg 1-propanol, 8.0 mg AIBN, 233.0 mg 1,4-butanediol, and 120.0 µL water was then filled into a capillary segment. After a pressure of 500 psi was applied to both ends of the capillary using a micro-T as described previously,[97] the polymerization reaction was allowed to proceed under 500-psi pressure at 60 °C for 20 h. The capillary was then separated from the micro-T and ~2–3 cm of its ends were trimmed off to gain uniformity. The remaining 10 cm long monolithic capillary was washed with acetonitrile at 1500 psi overnight, and 5.0 mM ammonium acetate for 2 h.

To prepare a polyacrylamide-based bubbleless electrode,[1] a degassed solution containing 10%T (%T is the total weight concentration of acrylamide and Bis in the solution), 2% C (% C represents Bis concentration relative to acrylamide), 0.2% v/v TEMED, and 0.1% APS was pressurized into a 20-cm-long × 250-µm-i.d. × 375-µm-o.d. bi-functionalized capillary. The polymerization reaction was allowed to proceed inside the capillary at 0 ℃ overnight under a pressure of ~300 psi, and then at 4 ℃ for another 24 h. After both ends of the capillary were trimmed off by ~1 cm, cut into 2-cm-long segments and stored in the pump solution (5 mM ammonium acetate) until use. Each segments served as a polyacrylamide-based bubbleless electrode.

To assemble an EOP, a micro-T (VICI Valco Instruments, Houston, TX) was used to join a negatively charged monolith, a bubbleless electrode and an outlet capillary (see the right-hand-side part of Figure 4-2). The free-ends of the monolith and the bubbleless electrode were respectively put into a high voltage (HV) reservoir and a grounding reservoir both containing the pump solution. HV was applied to the monolith via two platinum electrodes dipped into the two reservoirs.

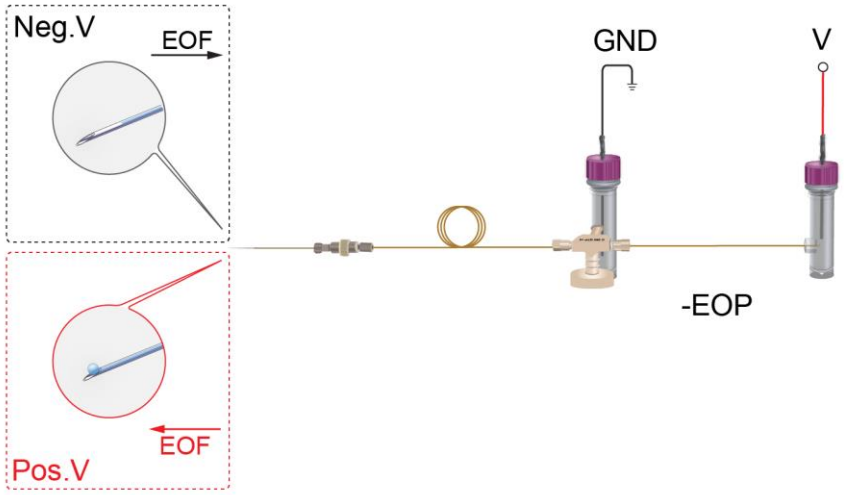

Figure 4-2 Schematic configuration of EDP.

A 50-70 cm in length capillary (50 µm i.d. × 360 µm o.d.) was used to connect the EOP and the pipettor tip via a micro-tee and union, respectively. A bubbleless electrode held by the micro-tee was used to connect EOP to GND. V-voltage, GND-ground, EOF- electroosmotic flow, Neg.V-negative voltage, and Pos.V-positive voltage.

4.3.3 Pipette Tips Preparation

A capillary puller (Model P-2000, Sutter Instrument Company, Novato, CA) was used to pull glass tubes or fused silica capillaries to make tips for a commercial injector (Model PLI-100A, Harvard Apparatus, Holliston, MA) or an EDP. The parameters of the puller for pulling a glass tube were heat (H) = 500, filament (F) = 5, velocity (V) = 65, pull (P) = 17, and delay (D) = 250. For pulling a fused silica capillary, ~1.5–2.0 cm polyimide coating was removed using a razor blade, and the capillary was pulled after setting the puller's parameters to H = 450, F = 5, V = 70, P = 250, and D = 120. The tip was ready to use after being silanized with vapor-dichlorodimethylsilane.

4.3.4 Silanization of Pipettor Tips

Three mL 5% dichlorodimethylsilane in chloroform was put in a 50 mL centrifuge tube (Corning Incoporated, Corning, NY). The other end of a pipettor was inserted into a stopper; then, the centrifuge tube was tighten by the stopper with the pipettor inside. A needle penetrated into the stopper, and the centrifuge tube was vacuumed by a vacuum pump connected to the needle until dichlorodimethylsilane started to boil. The needle was removed and the centrifuge tube was set in a hood until the liquid was gone; usually 24-48 hours.

4.3.5 Calibration of an EDP

An EPD was produced after the pipette tip was joined to the outlet capillary of the EOP, and the pipette was calibrated by measuring the pipetted volumes under an inverted microscope (Eclipse Ti-U, Nikon Instruments Inc., Melville, NY). To prepare for the calibration, the outlet capillary close to the tip was put on the microscope and the

microscope was focused so that one could see the inside of the capillary. Water was initially filled in the outlet capillary, and mineral oil was withdrawn into the outlet capillary until the meniscus (between water and mineral oil) was seen under the microscope. After the pipette tip was then inserted into a target solution, pipetting was started and stopped by switching on and off the HV on the EOP, respectively. Based on the distance, l, the meniscus moved during the pipetting process, the pipetted volume could be computed ($V = \pi r^2 l$, where r is the i.d. of the outlet capillary).

4.3.6 Zebrafish Maintenance and Embryos Production

Adults of zebrafish (*Zebra Danio*) were purchased from a local pet store. The female and male fish were maintained in separate tanks at 28.5 °C with 14-h light/10-h dark light-cycle. Embryos were obtained by spawning adult fish by the following protocol. Briefly, two female and one male fish were introduced in a one-liter breeding tank with a divider at night. The divider was removed the next morning and the fish usually took 20-30 min to mate. The embryos were collected by a sieve net, rinsed with DI water, transferred into a 100 mm petri dish, and maintained at 28.5 °C.

4.3.7 Manipulation of Zebrafish Embryos

For manipulation of 4-8 hpf (hours post fertilization) embryos, the protocol described previously[117-119] was followed with minor modifications. Briefly, after a microscope slide was put in a petri dish, the embryos were loaded in the petri dish and lined up against the microscopic slide. Under a stereo microscope, a pipette tip quickly pierced through the chorion and entered the yolk using a multi motorized-micromanipulator (MPC-325, Sutter Instrument, Novato, CA). A voltage of negative 150 V was applied on the EOP for 50 s to withdraw the cellular contents from the yolk. The pipette tip was pulled out from the yolk and dipped into a 0.2-mL PCR (polymerase chain reaction) tube filled with 10 µL water. The voltage applied on EDP was then switched to positive 2.5 kV for 30 s to deliver the yolk contents into the PCR tube. The samples were stored at -20 °C until analysis.

For the manipulation of 28-32 and 52-56 hpf embryos, the procedure described by Benard et al.[120] was followed with slight modifications. An opening was created on the embryo chorion at a desired location using a pair of dissection tweezers. The embryos were then transferred into a petri dish containing 200 µg/mL 4-aminobenzoic acid (PABA) for 10–20 min for anesthetization. Next, the embryos were transferred onto a flat 3% agarose plate using a regular pipette and the excess water was carefully removed by Kimwipe paper to allow surface tension to stabilize the embryos. The process for pipetting yolk contents was the same as described in the preceding paragraph.

4.3.8 **Quantification of Cholesterol.**

Amplex® Red Cholesterol Assay Kit (Cat #: A12216, Invitrogen) was used to quantitate the cholesterol and the manufacturer recommended protocol was followed. In short, a sample was mixed with 40 µL of 1× Reaction Buffer, vortexed, and centrifuged (to remove bubbles). The mixture was transferred into a well of a 96-well plate. Fifty µL of a working solution of Amplex Red was added into the well. [Note: Duplicate of standard cholesterol solutions were also added into the plate every time.] The 96-well plate was covered by a parafilm tape and incubated at 37 °C for 45 min, and then read by a plate reader (Synergy H1, BioTek Instruments, Inc., Winooski, VT) with excitation and emission wavelengths set at 550 nm and 585 nm respectively. The cholesterol concentration in the sample was evaluated based on a standard calibration curve.

4.4 Results and discussion

4.4.1 EDP Characterization

To characterize the EDP, we measured the pipetted volume as a function of the magnitude of the voltage applied to the EOP and the pipette-on time. Because we specifically wanted to use the EDP for pipetting yolk contents of zebrafish embryos, which has a viscosity of 129 mPa·S,[121] we selected vacuum pump oil (Edwards Inc., Sanborn, NY), which has viscosity of 144 mPa·S, as our model sample. Since the zebrafish yolk volume is ~140 nL, in order to allow the yolk to develop normally we did not want to withdraw more than 5% (~7 nL) of the yolk each time. We characterized the EDP within a specific volume range from 500 pL to 8.0 nL. Figure 4-3 presents the results. Good linear relationships were obtained between pipetted volume and applied voltage (see Figure 4-3A, R^2 = 0.998) as well as between pipetted volume and pipette-on time (see Figure 4-3B, R^2 =0.9993). To demonstrate the feasibility of utilizing the EDP for other applications (e.g., withdrawing cellular contents from a Hela cell which has a diameter of ca. 15–30 μm[122] and a volume up to 4.2 pL[41]), we extended the low-volume limit to ~250 fL; the results are presented in Figure 4-4. Withdrawing larger volume (~ 80 nL) was also tested (as shown in Figure 4-5).

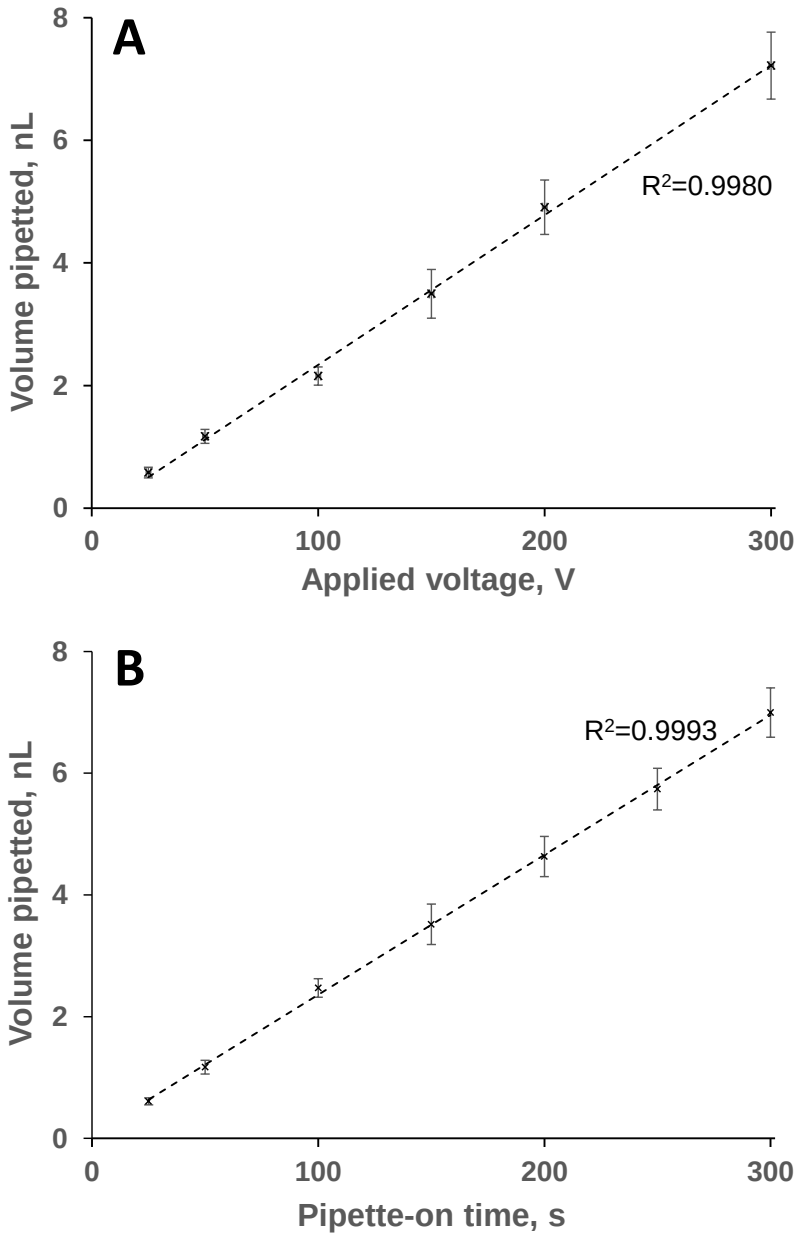

Figure 4-3 Pipetted volume as function of applied voltage and duration of voltage being applied.

The pipette tip was prepared by pulling a 100-µm-i.d. × 360-µm-o.d. capillary. The tip had an i.d. of 9.41 µm and an o.d. of 25.27 µm. The sample withdrawn was vacuum pump oil. The error bars represent standard deviations that were obtained from seven

repetitive measurements. (A) The pipetted volume as function of the applied voltage with a pipette-on time of 50 s. (B) The pipetted volume as function of the pipette-on time with an applied voltage of 50 V.

It is worth pointing out that slopes of the above calibration curves did vary slightly (<5%) when different tips were used, presumably due to the variations of the flow resistances[36] within different tips. This effect was also common for commercial micro-injection systems.[123] These variations can be mitigated by precisely micro-fabricating the tips under identical experimental conditions.[38,40] Nevertheless, it is recommended that a pipette should be calibrated every time a new tip is used.

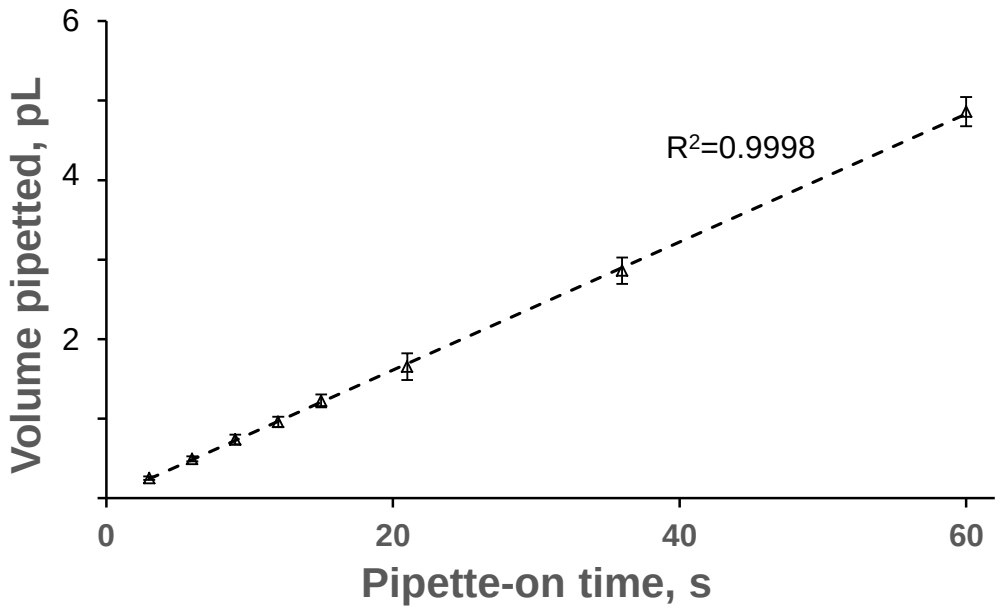

Figure 4-4 Relationship between pipetted volume and pipette-on time.

The voltage applied on EOP was 30 V. The error bars represent standard deviations from six repetitive measurements.

(A)

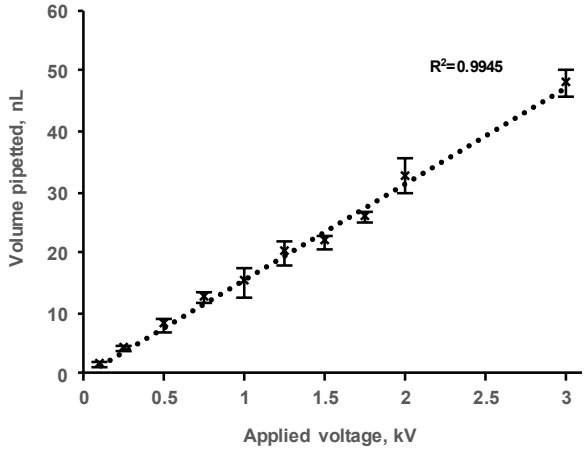

(B)

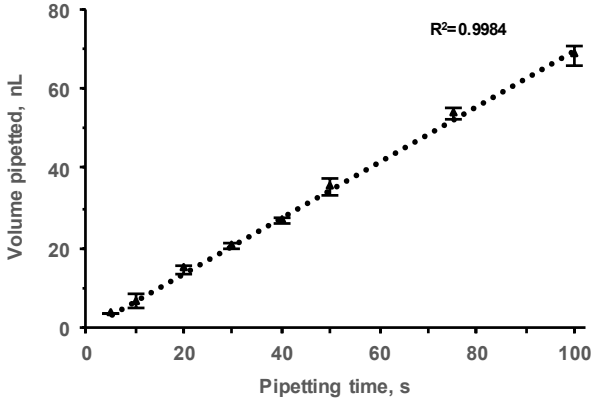

Figure 4-5 Relationship between pipetting volume and (A) applied voltage or (B) Pipetting time.

A pulled capillary (50 µm i.d. × 360 µm o.d., tip outlet 6.11 µm i.d. × 13.76 µm o.d., and taper length= 10.0 mm) was used and (A) the pipetting time was 20 s, or (B) the applied voltage was 1 kV. The error bars represent standard deviation and were obtained from seven repetitive measurements.

4.4.2 EDP Application

To demonstrate the feasibility of using the EDP to withdraw cellular contents from a living cell, we analyzed cholesterol levels in zebrafish embryo yolks at three different development stages (see Figure 4-6). Cholesterol in the human body plays an important role in maintaining cell functions and abnormal cholesterol metabolism may be associated with several diseases.[124] Zebrafish is a model organism that is widely used for development studies, diseases, and drug discovery.[125-127]

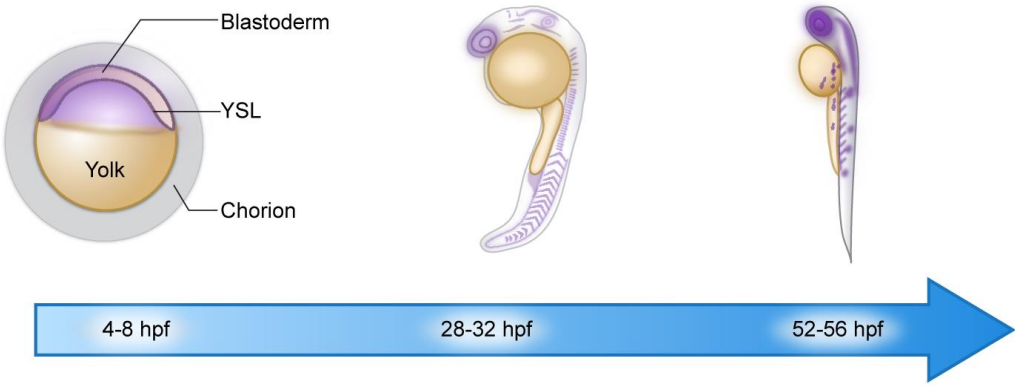

Figure 4-6 Different development stages of a zebrafish embryo.

YSL – yolk syncytial layer. [Note: An embryo has chorion in natural stages of 28-32 hpf and 52-56 hpf, and an opening was created for pipetting yolk contents at 28-32 hpf and 52-56 hpf.]

To determine the yolk cholesterol concentration at 4–8 hpf, we selected 15 zebrafish embryos and pipetted ~3 nL cellular contents from each yolk for cholesterol concentration determination, and duplicated analyses were performed to get statistic data. Before we performed the second analysis at 28–32 hpf, we noticed that 1–3 embryos died from trial to trial. To perform the second analysis, we pipetted ~3 nL of the cellular contents from each yolk for cholesterol measurements. An additional 4–8 embryos died after the second analysis. Lastly, we pipetted ~3 nL cellular contents from each of the remaining yolk for the third analysis at 52–56 hpf, and one day later (76 hpf) only 2–4 baby zebrafish remained alive. Figure 4-7 presents the survival rate results. More than 50% of the embryos survived after each analysis step and 20% survived after the entire process (three analytical steps). We are confident that the survival rate will increase considerably as we became more skillful in performing the embryo manipulation and pipetting.

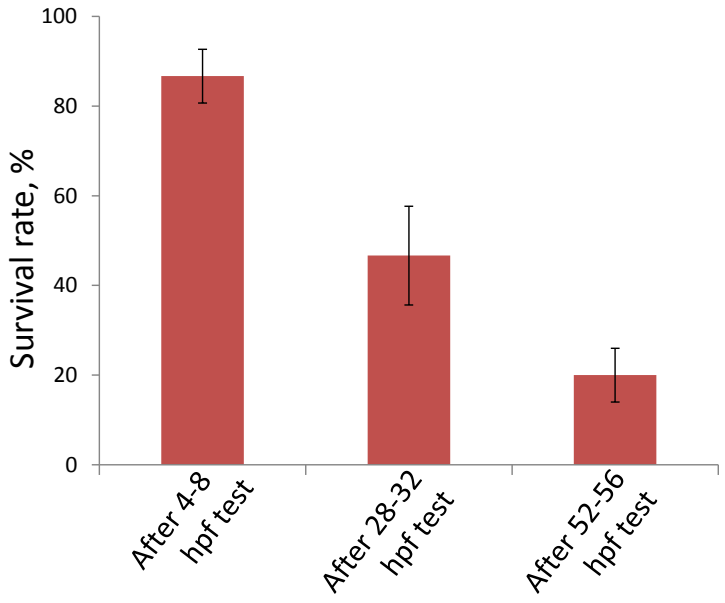

Figure 4-7 Zebrafish embryo survival rate after cholesterol analysis.

The error bars were obtained from four duplicate analyses.

Figure 4-8A presents the change of cholesterol concentration and Figure 4-8B presents the change of total cholesterol quantity in yolk as embryos develop. The total cholesterol quantity in a yolk was estimated by the product of the cholesterol concentration in the yolk and the yolk volume. For a 4-8 hpf embryo, its yolk was approximately a sphere (see Figure 4-6). For a 28-32 or 52-56 hpf embryo, its yolk consists of an ellipsoid and a cone. The volume of the ellipsoid was calculated using equation $V=4\pi abc/3$, where a, b, and c are semi-principal axes and the volume of the cone was calculated using equation $V'=\pi r^2 h/3$, where r is the cone radius and h is the lateral height. All the dimensional parameters of a yolk were measured under an inverted microscope by NIS-Elements software (Nikon Instruments Inc., Melville, NY).

Both concentration and amount of cholesterol varied from yolk to yolk, representing cell heterogeneity. The total amount of cholesterol in yolk decreased with embryo development (see the inset of Figure 4-8B), which is in agreement with the results observed by Fraher et al.[128] Interestingly, the cholesterol amount we measured was only one tenth of those measured by Fraher et al. This is presumably due to the fact that we measured the cholesterol in yolk only, while Fraher et al. measured the average of cholesterol in yolk, yolk membrane and yolk syncytial layer (a syncytial layer forms during the early stages of embryonic development). It has been reported that a large amount of cholesterol is present in both yolk membrane[129] and syncytial layer.[130] Another interesting observation was that we did not see significant cholesterol concentration change in yolk at different development stages (see the inset of Figure 4-8 A); this observation has not been reported before.

To validate the results, we selected 51 zebrafish embryos; 17 of them were used to measure their yolk cholesterol concentrations at 4-8 hpf, 17 other embryos were used to measure cholesterol concentrations at 28-32 hpf, and the remaining 17 embryos were used to measure cholesterol concentrations at 52-56 hpf. The results were presented in Figure 4-9, consistent with the results we obtained in Figure 4-8.

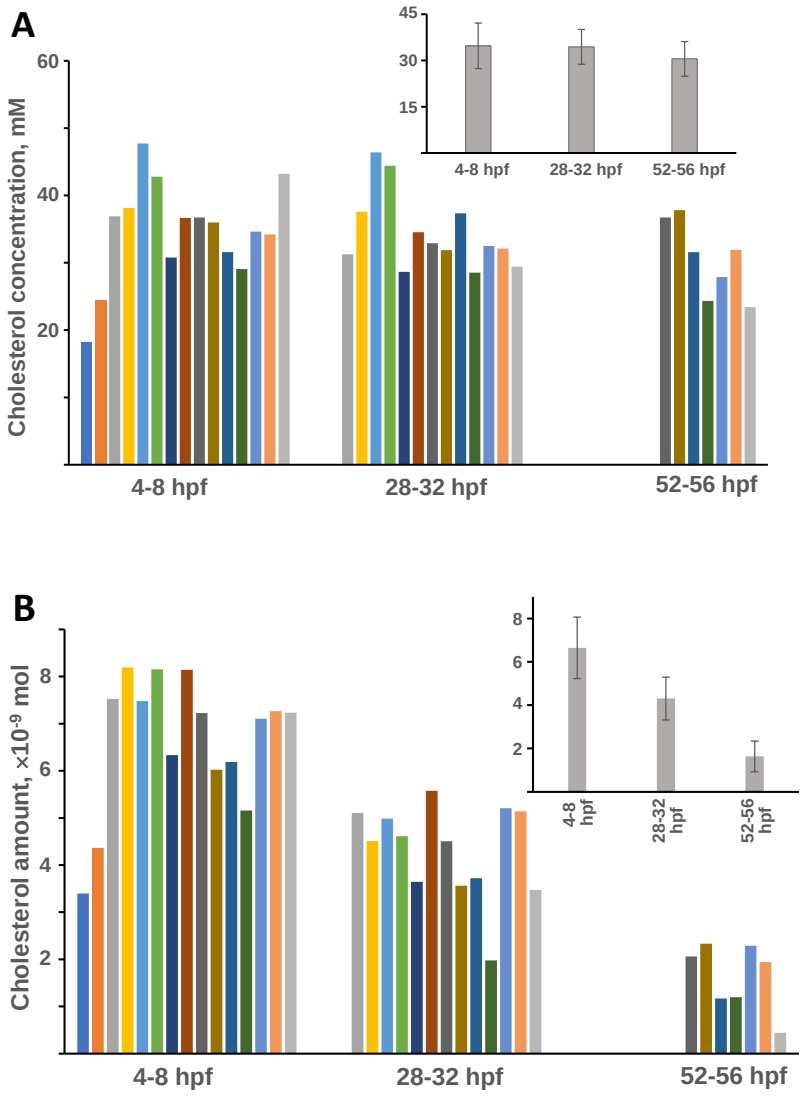

Figure 4-8 Quantitative analysis of cholesterol in the yolk of zebrafish embryos

The abbreviation of hpf stands for hours post fertilization.

Concentration and total amount of cholesterol in the yolk of zebrafish embryos at three developmental stages (4-8 hpf, 28-32 hpf, and 52-56 hpf) are respectively presented in A and B. The insets in (A) and (B) present the average concentration and total amount of yolk cholesterol respectively. Two tails, unpaired t-test (type I) were performed between any two groups and all p-values <<0.01.

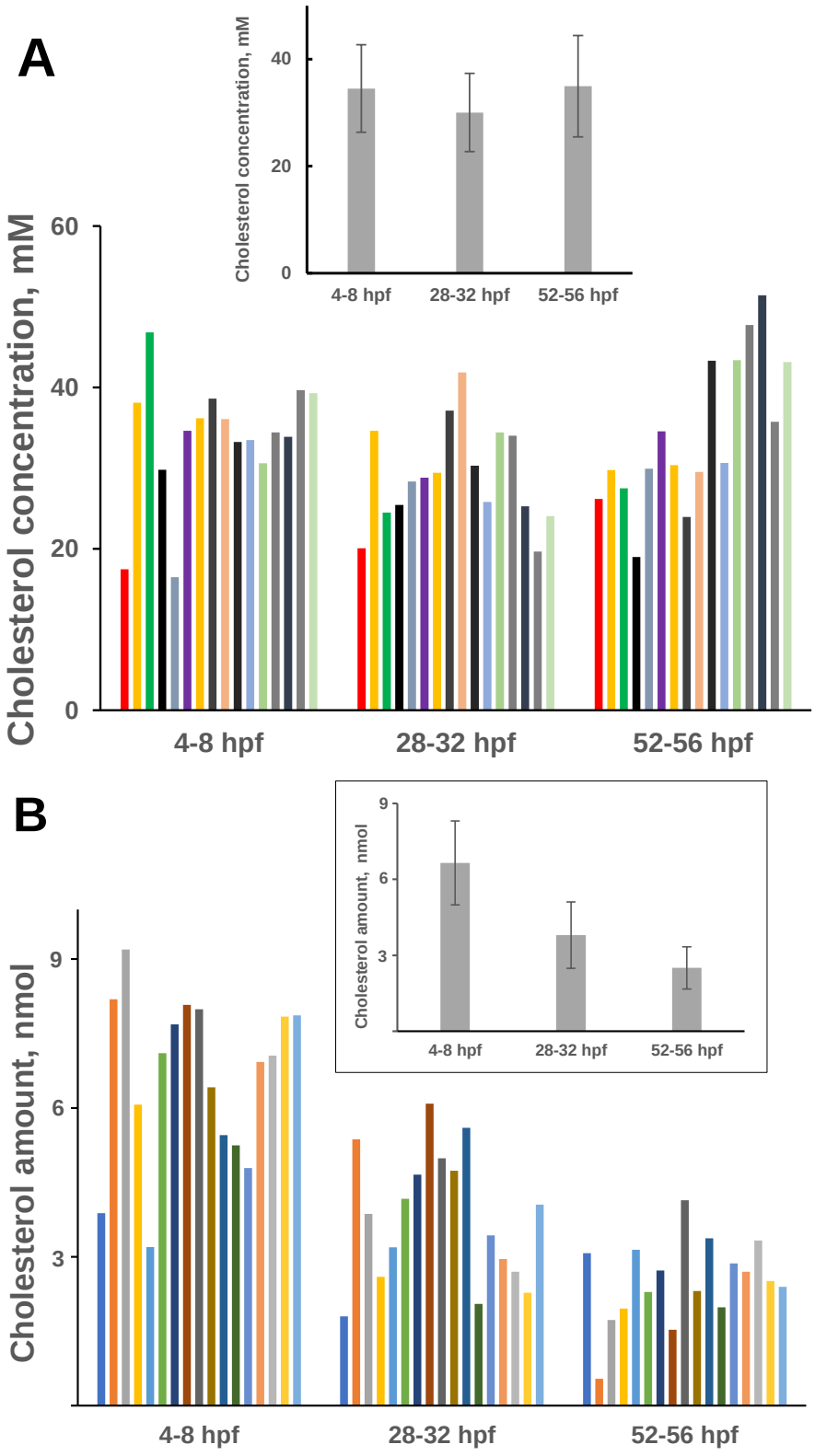

Figure 4-9 Quantitative analysis of cholesterol in the yolk of zebrafish embryos.

The abbreviation “hpf” stands for “hours post fertilization”. Individual zebrafish embryos at three developmental stages (4-8 hpf, 28-32 hpf, and 52-56 hpf) were quantitated. (A) Concentration and (B) total amount of cholesterol in the yolk of zebrafish embryos. The inset in (B) is the average amount of cholesterol. Two tails, unpaired t-test (type II) were performed between any two groups and all p-values $<<0.01$.

4.4.3 EDP for Microinjection

We also tested the EDP for solution injections. We used it to inject a volume of aqueous solution to a mineral oil matrix, measured the radius of the aqueous droplet, and calculated the volume of the droplet. We had a PLI-100A Picoliter Microinjector (Harvard Apparatus, Holliston, MA) in our lab; the manufacturer claimed this system could deliver nL to fL solutions reliably. We utilized it for microinjection using the lowest air pressure (0.1 psi) and compared its performance with that of the EDP. The volume range we examined was from ~300 pL to ~4 nL, and good linear relationships were obtained between injected volume and injection time for both the EDP (R^2=0.991) and the commercial microinjector (R^2=0.976) (see Figure 4-10). Since the parameters we used to operate the commercial microinjector were close to its limit for the lowest-volume injection, relatively large relative-standard-deviations (4~18%) of the injected volumes were yielded. For the EDP, the relative-standard-deviations varied from 4~10%. While we were confident that we could utilize the EDP for injecting fL solution precisely to a targeted location, we did not go lower than ~300 pL because we did not have a suitable machine to measure those droplet volumes accurately.

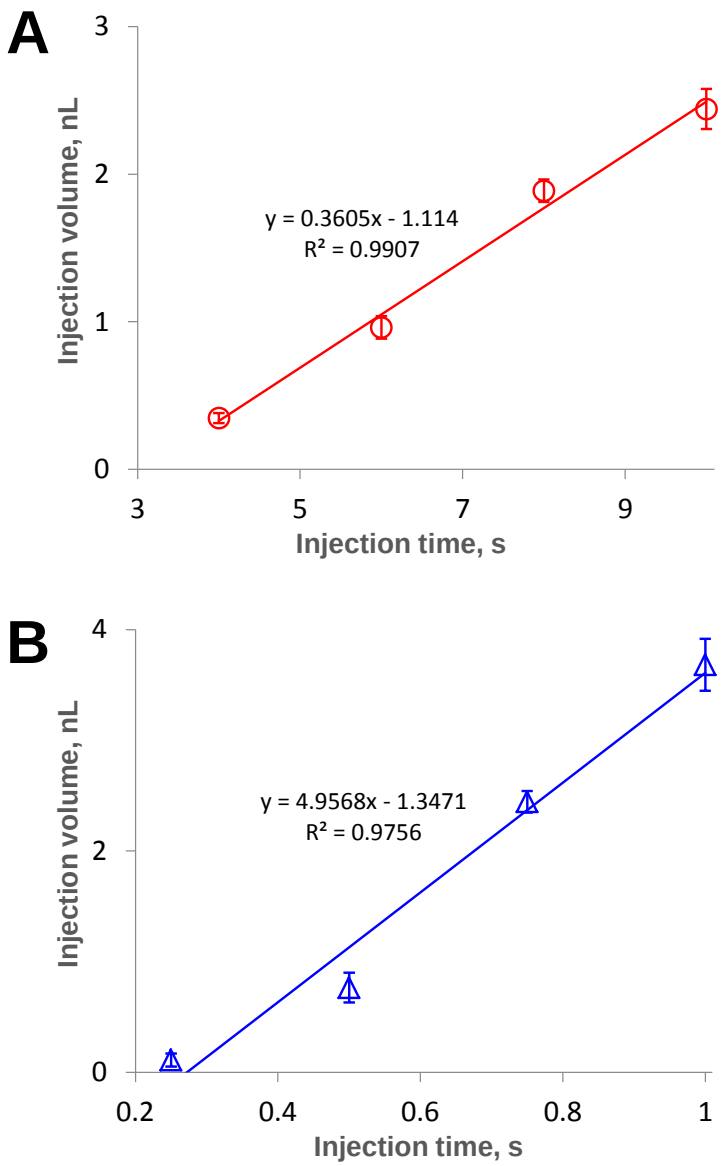

Figure 4-10 Comparison between EDP and commercial micro-injector for solution injection.

For the EDP (A), the injection time was from 2 to 10 s under a voltage of 200 V. For the commercial micro-injector (B), the injection time was from 0.25 to 1 s under a pressure

of 0.1 psi. The error bars represent standard deviation and were obtained from six repetitive measurements.

4.5 Concluding remarks

We have developed an EDP capable of pipetting ~250 fL to 80 nL of cellular contents from single cells. What has enabled us to pipette these small volumes of solutions accurately and precisely is that we have eliminated the use of compressible air and replaced it with an incompressible liquid in all conduits. The volume of solution withdrawn is conveniently controlled by the EOP. Because flow rate of EOP is generally in the range of pL–nL/min, perfectly suited for manipulating solution volumes in the fL–nL regime. We have utilized the EDP for a single-cell time-course study by measuring the yolk cholesterol levels during the development of zebrafish embryos. More than 50% of the embryos survived after each pipetting and analysis step and we believe that this number will increase considerably as we further improve our technique to manipulate the embryos as well as reduce the pipette-tip size. The EDP can also be used for low-volume solution delivery/dispensing; its performances are comparable to or better than that of a commercial microinjector (PLI-100A Picoliter Microinjector, Harvard Apparatus) for delivering low nL to pL solutions.

Chapter 5 Overall Summary And Future Directions

5.1 Overall summary

Part of the work (chapter 2 and 4) in this dissertation was devoted to developing a miniaturized HPLC cartridge. Results from a culmination of previous research in our lab have shown that the EOP can produce up to ~ 1200 bar output pressure, which is sufficient for almost all types of current HPLC. A gradient organic solution (i.e., acetonitrile and methanol) was often used for reverse phase HPLC. However, the EOP cannot directly use organic solutions as the pump solution, since it will make the pump unstable. The work in this thesis is to solve the issue of generating a gradient profile by the EOP.

We originally proposed a method based on incorporating a ten-port valve into the EOP to produce a gradient profile. An eluent in one loop of the valve was delivered to the separation column, while a higher concentration eluent was loaded into another loop of the valve. Once the valve was switched, the second loop was connected to the separation column, while the next gradient eluent was loaded into the first loop. Repeating these steps could form a gradient profile that was close to linear. Since these operations could be repeated continuously, a desired gradient could be produced. In this way, the gradient solution for HPLC separation was separated from the pump solution of the EOP. However, the downside of this approach is that the gradient created has a step-profile and only good for linear gradient profile. Its operations are tedious, especially when a close-to-linear gradient is desired.

We further developed the second method to generate various gradient profiles. In this approach, we incorporated selection valves and a mixing chamber into EOP for nanoflow gradient generation. When a high voltage was applied, the EOP withdrew a series of gradient eluents having different elution strengths via a selection valve. The eluents went through the mixing chamber and towards the EOP. Once an opposite high voltage was applied, the EOP pushed the eluents out, through the mixing chamber again, and towards to the separation column. During the movements of these eluents (i.e., back and forth in the mixing chamber as well as inside of capillary assembly), a smooth gradient profile was formed. Since it is possible to change the size of mixing chamber, the number of eluents, as well as the volume, concentration, and the movement pattern (i.e., duration, velocity, and movement style), desired gradient profile could be generated.

There is increasing interest in single cells analysis, since analyzing a population of cells cannot reveal cell's heterogeneity. Tools are particularly desired to pipette a small portion of contents from a single cell for analysis. Hence, we also developed an EOP-based pipettor for single cell surgery and analysis. In this work, we developed a femtopipettor using a monolith-based EOP, we can use this pipettor to pipette and deliver solutions down to ~250 fL. To demonstrate the feasibility of using femtopipettor to pipette solutions from a single cell, we selected zebrafish embryos as single cell samples and analyzed the cholesterol levels as zebrafish embryos grew. Since we want the embryos to be alive after analysis, we call this process a surgery. We achieved 89.3%-91.7% embryos survival on average after a single surgery. Due to the

compatibility of the pump solution for mass spectrometric analysis, the femtopipettor can be directly coupled with a mass spectrometer for single cell metabolic research.

5.2 Future directions

Making a proto-type of miniaturized HPLC based on the study of this dissertation is a further direction. We have an ongoing project that incorporates all pieces together into a portable HPLC, and the first version of proto-type has been made. The prototype was 20 cm × 20 cm × 17.5 cm (l×w×h respectively) and weighed approximately three kilograms. Since most the weight came from the lexan material used to create the HPLC box, we will change the material and ultilize 3D-printing to make the box for the miniaturized HPLC. The size and weight can be further reduced by optimizing the design and changing the manufacturing materials (i.e., changing valves with lighter materials but keep the resistance for high pressure output). Reproducibility, robustness, and ruggedness of the miniaturized HPLC will be addressed. The final goal of the project is to produce a commercialized portable HPLC with low cost and high stability.

The EOP-based pipettor has shown its potential applications in single cell surgery and analysis. The future work includes several aspects. First, the accuracy and precision of the pipettor tip can be further improved by making the tip with fabrication or carbon nanotubes. The fabricated tip will allow us to deliver and/or pick up smaller volumes with higher repeatability. The carbon nanotube tip will allow us to insert into a single cell more precisely, including reach the sub-cellular organelles, such as the mitochondria and nucleus. Second, since the pump solution of the EOP is compatible

with mass spectrometry, the cellular contents picked up by the pipettor can be directly sent to a mass spectrometer for analysis. Third, the results in Chapters 2 and 3 in this thesis have shown that EOP-based HPLC is reliable for bioanalysis. Therefore, we will combine the pipettor into EOP-based HPLC/MS-MS to carry out online analysis of cellular contents of a living-single-cell.

References

1. Byun, C. K.; Wang, X.; Pu, Q. and Liu, S.(2007). Electroosmosis-Based Nanopipettor. *Anal. Chem.*, 79 (10), 3862-3866.
2. Chen, A.; Lu, J. J.; Gu, C.; Zhang, M.; Lynch, K. B. and Liu, S.(2015). Combining selection valve and mixing chamber for nanoflow gradient generation: Toward developing a liquid chromatography cartridge coupled with mass spectrometer for protein and peptide analysis. *Anal. Chim. Acta*, 887, 230-236.
3. Chen, A.; Lynch, K. B.; Wang, X. C.; Lu, J. J.; Gu, C. Y. and Liu, S. R.(2014). Incorporating high-pressure electroosmotic pump and a nano-flow gradient generator into a miniaturized liquid chromatographic system for peptide analysis. *Anal. Chim. Acta*, 844, 90-98.
4. Dasgupta, P. K. and Liu, S.(1994). Electroosmosis: A Reliable Fluid Propulsion System for Flow Injection Analysis. *Anal. Chem.*, 66 (11), 1792-1798.
5. Gu, C.; Jia, Z.; Zhu, Z.; He, C.; Wang, W.; Morgan, A., et al.(2012). Miniaturized Electroosmotic Pump Capable of Generating Pressures of More than 1200 Bar. *Anal. Chem.*, 84 (21), 9609-9614.
6. He, C.; Lu, J. J.; Jia, Z.; Wang, W.; Wang, X.; Dasgupta, P. K., et al.(2011). Flow Batteries for Microfluidic Networks: Configuring An Electroosmotic Pump for Nonterminal Positions. *Anal. Chem.*, 83 (7), 2430-2433.
7. He, C.; Zhu, Z.; Gu, C.; Lu, J. and Liu, S.(2012). Stacking open-capillary electroosmotic pumps in series to boost the pumping pressure to drive high-

performance liquid chromatographic separations. *J. Chromatogr. A*, 1227 (0), 253-258.

8. Laser, D. J. and Santiago, J. G.(2004). A review of micropumps. *Journal of Micromechanics and Microengineering*, 14 (6), R35-R64.

9. Gawad, C.; Koh, W. and Quake, S. R.(2016). Single-cell genome sequencing: current state of the science. *Nat. Rev. Genet.*, 17 (3), 175-188.

10. Heinemann, M. and Zenobi, R.(2011). Single cell metabolomics. *Curr. Opin. Biotechnol.*, 22 (1), 26-31.

11. Mousoulis, C.; Xu, X.; Reiter, D. A. and Neu, C. P.(2013). Single cell spectroscopy: noninvasive measures of small-scale structure and function. *Methods*, 64 (2), 119-128.

12. Nawarathna, D.; Turan, T. and Wickramasinghe, H. K.(2009). Selective probing of mRNA expression levels within a living cell. *Appl. Phys. Lett.*, 95 (8),

13. Schwartzman, O. and Tanay, A.(2015). Single-cell epigenomics: techniques and emerging applications. *Nat. Rev. Genet.*, 16 (12), 716-726.

14. Van Loo, P. and Voet, T.(2014). Single cell analysis of cancer genomes. *Curr. Opin. Genet. Dev.*, 24, 82-91.

15. Walt, D. R.(2013). Optical Methods for Single Molecule Detection and Analysis. *Anal. Chem.*, 85 (3), 1258-1263.

16. Wang, D. and Bodovitz, S.(2010). Single cell analysis: the new frontier in 'omics'. *Trends Biotechnol.*, 28 (6), 281-290.

17. Willison, K. R. and Klug, D. R.(2013). Quantitative single cell and single molecule proteomics for clinical studies. *Curr. Opin. Biotechnol.*, 24 (4), 745-751.

18. Wu, M. Y. and Singh, A. K.(2012). Single-cell protein analysis. *Curr. Opin. Biotechnol.*, 23 (1), 83-88.

19. Yu, J.; Xiao, J.; Ren, X. J.; Lao, K. Q. and Xie, X. S.(2006). Probing gene expression in live cells, one protein molecule at a time. *Science*, 311 (5767), 1600-1603.

20. Armbrecht, L. and Dittrich, P. S.(2017). Recent Advances in the Analysis of Single Cells. *Anal. Chem.*, 89 (1), 2-21.

21. Zhao, Y. A.; Ashcroft, B.; Zhang, P. M.; Liu, H.; Sen, S. M.; Song, W., et al.(2014). Single-molecule spectroscopy of amino acids and peptides by recognition tunnelling. *Nat. Nanotechnol.*, 9 (6), 466-473.

22. Shen, Y. J.; Nakajima, M.; Ahmad, M. R.; Kojima, S.; Homma, M. and Fukuda, T.(2011). Effect of ambient humidity on the strength of the adhesion force of single yeast cell inside environmental-SEM. *Ultramicroscopy*, 111 (8), 1176-1183.

23. Shen, Y. J.; Ahmad, M. R.; Nakajima, M.; Kojima, S.; Homma, M. and Fukuda, T.(2011). Evaluation of the Single Yeast Cell's Adhesion to ITO Substrates With Various Surface Energies via ESEM Nanorobotic Manipulation System. *IEEE Trans. Nanobioscience*, 10 (4), 217-224.

24. Schrlau, M. G. and Bau, H. H.(2009). Carbon-based nanoprobes for cell biology. *Microfluidics and Nanofluidics*, 7 (4), 439-450.

25. Schrlau, M. G. and Bau, H. H.(2010). Carbon Nanopipettes for Cell Surgery. *Jala*, 15 (2), 145-151.

26. Laffafian, I. and Hallett, M. B.(1998). Lipid-assisted microinjection: Introducing material into the cytosol and membranes of small cells. *Biophys. J.*, 75 (5), 2558-2563.

27. Laffaflan, I. and Hallett, M. B.(2000). Gentle microinjection for myeloid cells using SLAM. *Blood*, 95 (10), 3270-3271.

28. Masujima, T.(2009). Live Single-cell Mass Spectrometry. *Anal. Sci.*, 25 (8), 953-960.

29. Mizuno, H.; Tsuyama, N.; Harada, T. and Masujima, T.(2008). Live single-cell video-mass spectrometry for cellular and subcellular molecular detection and cell classification. *J. Mass Spectrom.*, 43 (12), 1692-1700.

30. Pan, N.; Rao, W.; Kothapalli, N. R.; Liu, R.; Burgett, A. W. and Yang, Z.(2014). The single-probe: a miniaturized multifunctional device for single cell mass spectrometry analysis. *Anal. Chem.*, 86 (19), 9376-9380.

31. Pan, N.; Rao, W.; Standke, S. J. and Yang, Z. B.(2016). Using Dicationic Ion-Pairing Compounds To Enhance the Single Cell Mass Spectrometry Analysis Using the Single-Probe: A Microscale Sampling and Ionization Device. *Anal. Chem.*, 88 (13), 6812-6819.

32. Rao, W.; Pan, N. and Yang, Z.(2016). Applications of the Single-probe: Mass Spectrometry Imaging and Single Cell Analysis under Ambient Conditions. *J. Vis. Exp.*, (112), 53911.

33. Schrlau, M. G.; Falls, E. M.; Ziober, B. L. and Bau, H. H.(2008). Carbon nanopipettes for cell probes and intracellular injection. *Nanotechnology,* 19 (1), 015101.

34. Chen, X.; Kis, A.; Zettl, A. and Bertozzi, C. R.(2007). A cell nanoinjector based on carbon nanotubes. *Proc. Natl. Acad. Sci. U. S. A.*, 104 (20), 8218-8222.

35. Brennan, L. D.; Roland, T.; Morton, D. G.; Fellman, S. M.; Chung, S. Y.; Soltani, M., et al.(2013). Small Molecule Injection into Single-Cell C. elegans Embryos via Carbon-Reinforced Nanopipettes. *PLoS ONE,* 8 (9), e75712.

36. King, R.(2004). Gene delivery to mammalian cells by microinjection. *Methods Mol. Biol.*, 245, 167-174.

37. Meister, A.; Gabi, M.; Behr, P.; Studer, P.; Voros, J.; Niedermann, P., et al.(2009). FluidFM: Combining Atomic Force Microscopy and Nanofluidics in a Universal Liquid Delivery System for Single Cell Applications and Beyond. *Nano Lett.*, 9 (6), 2501-2507.

38. Meister, A.; Polesel-Maris, J.; Niedermann, P.; Przybylska, J.; Studer, P.; Gabi, M., et al.(2009). Nanoscale dispensing in liquid environment of streptavidin on a biotin-functionalized surface using hollow atomic force microscopy probes. *Microelectron. Eng.*, 86 (4-6), 1481-1484.

39. Guillaume-Gentil, O.; Potthoff, E.; Ossola, D.; Franz, C. M.; Zambelli, T. and Vorholt, J. A.(2014). Force-controlled manipulation of single cells: from AFM to FluidFM. *Trends Biotechnol.*, 32 (7), 381-388.

40. Kang, W.; Yavari, F.; Minary-Jolandan, M.; Giraldo-Vela, J. P.; Safi, A.; McNaughton, R. L., et al.(2013). Nanofountain probe electroporation (NFP-E) of single cells. *Nano Lett.*, 13 (6), 2448-2457.

41. Guillaume-Gentil, O.; Grindberg, R. V.; Kooger, R.; Dorwling-Carter, L.; Martinez, V.; Ossola, D., et al.(2016). Tunable Single-Cell Extraction for Molecular Analyses. *Cell*, 166 (2), 506-516.

42. Zhang, S.; Balch, C.; Chan, M. W.; Lai, H. C.; Matei, D.; Schilder, J. M., et al.(2008). Identification and characterization of ovarian cancer-initiating cells from primary human tumors. *Cancer Res.*, 68 (11), 4311-4320.

43. Zhang, Y.(2007). Microinjection technique and protocol to single cells. *Protocol Exchange*, doi:10.1038/nprot.2007.1487.

44. Chen, B. C.; Legant, W. R.; Wang, K.; Shao, L.; Milkie, D. E.; Davidson, M. W., et al.(2014). Lattice light-sheet microscopy: imaging molecules to embryos at high spatiotemporal resolution. *Science*, 346 (6208), 1257998.

45. Bates, M.; Dempsey, G. T.; Chen, K. H. and Zhuang, X.(2012). Multicolor super-resolution fluorescence imaging via multi-parameter fluorophore detection. *ChemPhysChem*, 13 (1), 99-107.

46. Deindl, S. and Zhuang, X.(2012). Monitoring conformational dynamics with single-molecule fluorescence energy transfer: applications in nucleosome remodeling. *Methods Enzymol.*, 513, 59-86.

47. Mukamel, E. A.; Babcock, H. and Zhuang, X.(2012). Statistical deconvolution for superresolution fluorescence microscopy. *Biophys. J.*, 102 (10), 2391-2400.

48. Vaughan, J. C.; Jia, S. and Zhuang, X.(2012). Ultrabright photoactivatable fluorophores created by reductive caging. *Nat. Methods*, 9 (12), 1181-1184.

49. Bates, M.; Jones, S. A. and Zhuang, X.(2013). Stochastic optical reconstruction microscopy (STORM): a method for superresolution fluorescence imaging. *Cold Spring Harb. Protoc.*, 2013 (6), 498-520.

50. Bates, M.; Jones, S. A. and Zhuang, X.(2013). Preparation of photoswitchable labeled antibodies for STORM imaging. *Cold Spring Harb. Protoc.*, 2013 (6), 540-541.

51. Babcock, H.; Sigal, Y. M. and Zhuang, X.(2012). A high-density 3D localization algorithm for stochastic optical reconstruction microscopy. *Opt Nanoscopy*, 1 (6), doi:10.1186/2192-2853-1181-1186.

52. Lakadamyali, M.; Babcock, H.; Bates, M.; Zhuang, X. and Lichtman, J.(2012). 3D multicolor super-resolution imaging offers improved accuracy in neuron tracing. *PLoS ONE*, 7 (1), e30826.

53. Xu, K.; Babcock, H. P. and Zhuang, X.(2012). Dual-objective STORM reveals three-dimensional filament organization in the actin cytoskeleton. *Nat. Methods*, 9 (2), 185-188.

54. Shtengel, G.; Galbraith, J. A.; Galbraith, C. G.; Lippincott-Schwartz, J.; Gillette, J. M.; Manley, S., et al.(2009). Interferometric fluorescent super-resolution microscopy resolves 3D cellular ultrastructure. *Proc. Natl. Acad. Sci. U. S. A.*, 106 (9), 3125-3130.

55. Pastrana, E.(2011). Fast 3D super-resolution fluorescence microscopy. *Nat. Meth.*, 8 (1), 46-46.

56. Huang, B.; Bates, M. and Zhuang, X.(2009). Super-resolution fluorescence microscopy. *Annu. Rev. Biochem.*, 78, 993-1016.

57. Tsien, R. Y.(2003). Imagining imaging's future. *Nat. Rev. Mol. Cell Biol.*, Suppl, SS16-21.

58. Rhee, H. W.; Zou, P.; Udeshi, N. D.; Martell, J. D.; Mootha, V. K.; Carr, S. A., et al.(2013). Proteomic mapping of mitochondria in living cells via spatially restricted enzymatic tagging. *Science*, 339 (6125), 1328-1331.

59. Zhao, Y. M. and Jensen, O. N.(2009). Modification-specific proteomics: Strategies for characterization of post-translational modifications using enrichment techniques. *Proteomics*, 9 (20), 4632-4641.

60. Zenobi, R.(2013). Single-Cell Metabolomics: Analytical and Biological Perspectives. *Science*, 342 (6163), 1201-+.

61. Fujii, T.; Matsuda, S.; Tejedor, M. L.; Esaki, T.; Sakane, I.; Mizuno, H., et al.(2015). Direct metabolomics for plant cells by live single-cell mass spectrometry. *Nat. Protoc.*, 10 (9), 1445-1456.

62. Mizuno, H.; Tsuyama, N. and Masujima, T.(2014). Live Single-cell Mass Spectrometry for Organelle Metabolomics. *Bunseki Kagaku*, 63 (6), 477-484.

63. Tejedor, M. L.; Mizuno, H.; Tsuyama, N.; Harada, T. and Masujima, T.(2012). In Situ Molecular Analysis of Plant Tissues by Live Single-Cell Mass Spectrometry. *Anal. Chem.*, 84 (12), 5221-5228.

64. Rubakhin, S. S.; Romanova, E. V.; Nemes, P. and Sweedler, J. V.(2011). Profiling metabolites and peptides in single cells. *Nat. Meth.*, 8 (4), S20-S29.

65. Tsuyama, N.; Mizuno, H.; Tokunaga, E. and Masujima, T.(2008). Live single-cell molecular analysis by video-mass spectrometry. *Anal. Sci.*, 24 (5), 559-561.

66. Mizuno, H.; Tsuyama, N.; Date, S.; Harada, T. and Masujima, T.(2008). Live Single-cell Metabolomics of Tryptophan and Histidine Metabolites in a Rat Basophil Leukemia Cell. *Anal. Sci.*, 24 (12), 1525-1527.

67. Amantonico, A.; Urban, P. L. and Zenobi, R.(2010). Analytical techniques for single-cell metabolomics: state of the art and trends. *Anal. Bioanal. Chem.*, 398 (6), 2493-2504.

68. Lin, Y. Q.; Trouillon, R.; Safina, G. and Ewing, A. G.(2011). Chemical Analysis of Single Cells. *Anal. Chem.*, 83 (12), 4369-4392.

69. Ghaemmaghami, S.; Huh, W.; Bower, K.; Howson, R. W.; Belle, A.; Dephoure, N., et al.(2003). Global analysis of protein expression in yeast. *Nature*, 425 (6959), 737-741.

70. Huang, B.; Wu, H.; Bhaya, D.; Grossman, A.; Granier, S.; Kobilka, B. K., et al.(2007). Counting low-copy number proteins in a single cell. *Science*, 315 (5808), 81-84.

71. Uchida, M.; Sun, Y.; McDermott, G.; Knoechel, C.; Le Gros, M. A.; Parkinson, D., et al.(2011). Quantitative analysis of yeast internal architecture using soft X-ray tomography. *Yeast*, 28 (3), 227-236.

72. Horvath, C. G.; Preiss, B. A. and Lipsky, S. R.(1967). Fast liquid chromatography: an investigation of operating parameters and the separation of nucleotides on pellicular ion exchangers. *Anal. Chem.*, 39 (12), 1422-1428.

73. Horvath, C. and Lipsky, S. R.(1969). Rapid Analysis of Ribonucleosides and Bases at Picomole Level Using Pellicular Cation Exchange Resin in Narrow Bore Columns. *Anal. Chem.*, 41 (10), 1227-1234.

74. Vissers, J. P. C.; Claessens, H. A. and Cramers, C. A.(1997). Microcolumn liquid chromatography: Instrumentation, detection and applications. *J. Chromatogr. A*, 779 (1-2), 1-28.

75. Vissers, J. P. C.(1999). Recent developments in microcolumn liquid chromatography. *J. Chromatogr. A*, 856 (1-2), 117-143.

76. Scott, R. P. W.(1980). Microbore Columns in Liquid-Chromatography. *J. Chromatogr. Sci.*, 18 (2), 49-54.

77. Cappiello, A.; Famiglini, G.; Florucci, C.; Mangani, F.; Palma, P. and Siviero, A.(2003). Variable-gradient generator for micro- and nano-HPLC. *Anal. Chem.*, 75 (5), 1173-1179.

78. Aebersold, R. and Mann, M.(2003). Mass spectrometry-based proteomics. *Nature*, 422 (6928), 198-207.

79. Mechref, Y. and Novotny, M. V.(2002). Structural investigations of glycoconjugates at high sensitivity. *Chem. Rev.*, 102 (2), 321-369.

80. Hirata, Y. and Novotny, M.(1979). Techniques of Capillary Liquid-Chromatography. *J. Chromatogr.*, 186 (Dec), 521-528.

81. Vanderwal, S. and Yang, F. J.(1983). Gradient Elution System for Capillary and Micro Hplc. *Journal of High Resolution Chromatography & Chromatography Communications*, 6 (4), 216-217.

82. Takeuchi, T.; Niwa, T. and Ishii, D.(1987). Stepwise Gradient Elution Using Switching Valves in Micro High-Performance Liquid-Chromatography. *J. Chromatogr.*, 405, 117-124.

83. Ito, S.; Yoshioka, S.; Ogata, I.; Takeda, A.; Yamashitaa, E. and Deguchi, K.(2004). Nanoflow gradient generator for capillary high-performance liquid chromatography-nanoelectrospray mass spectrometry. *J. Chromatogr. A*, 1051 (1-2), 19-23.

84. Brennen, R. A.; Yin, H. and Killeen, K. P.(2007). Microfluidic gradient formation for nanoflow chip LC. *Anal. Chem.*, 79 (24), 9302-9309.

85. Ishii, D.; Hibi, K.; Asai, K. and Nagaya, M.(1978). Studies of Micro High-Performance Liquid-Chromatography .3. Development of a Micro-Pre-Column Method for Pretreatment of Samples. *J. Chromatogr.*, 152 (2), 341-348.

86. Ishii, D.; Hashimoto, Y.; Asai, H.; Watanabe, K. and Takeuchi, T.(1985). Solvent Gradient Elution in Micro Hplc. *Journal of High Resolution Chromatography & Chromatography Communications*, 8 (9), 543-546.

87. Takeuchi, T. and Ishii, D.(1982). Continuous Gradient Elution in Micro High-Performance Liquid-Chromatography. *J. Chromatogr.*, 253 (1), 41-47.

88. Yi, J.; Heinecke, J.; Tan, H.; Ford, P. C. and Richter-Addo, G. B.(2009). The distal pocket histidine residue in horse heart myoglobin directs the O-binding mode of nitrite to the heme iron. *J. Am. Chem. Soc.*, 131 (50), 18119-18128.

89. Deguchi, K.; Ito, S.; Yoshioka, S.; Ogata, I. and Takeda, A.(2004). Nanoflow gradient generator for capillary high-performance liquid chromatography. *Anal. Chem.*, 76 (5), 1524-1528.

90. Hendgen-Cotta, U. B.; Flogel, U.; Kelm, M. and Rassaf, T.(2010). Unmasking the Janus face of myoglobin in health and disease. *J. Exp. Biol.*, 213 (Pt 16), 2734-2740.

91. Guillemette, J. G.; Matsushimahibiya, Y.; Atkinson, T. and Smith, M.(1991). Expression in Escherichia-Coli of a Synthetic Gene Coding for Horse Heart Myoglobin. *Protein Eng.*, 4 (5), 585-592.

92. Chen, L. X.; Ma, J. P. and Guan, Y. F.(2003). An electroosmotic pump for packed capillary liquid chromatography. *Microchem. J.*, 75 (1), 15-21.

93. Chen, L. X.; Ma, J. P. and Guan, Y. F.(2004). Study of an electroosmotic pump for liquid delivery and its application in capillary column liquid chromatography. *J. Chromatogr. A*, 1028 (2), 219-226.

94. Tripp, J. A.; Svec, F.; Frechet, J. M. J.; Zeng, S. L.; Mikkelsen, J. C. and Santiago, J. G.(2004). High-pressure electroosmotic pumps based on porous polymer monoliths. *Sensors and Actuators B-Chemical*, 99 (1), 66-73.

95. Nie, F. Q.; Macka, M.; Barron, L.; Connolly, D.; Kent, N. and Paull, B.(2007). Robust monolithic silica-based on-chip electro-osmotic micro-pump. *Analyst*, 132 (5), 417-424.

96. Wang, W.; Gu, C. Y.; Lynch, K. B.; Lu, J. J.; Zhang, Z. Y.; Pu, Q. S., et al.(2014). High-Pressure Open-Channel On-Chip Electroosmotic Pump for Nanoflow High Performance Liquid Chromatography. *Anal. Chem.*, 86 (4), 1958-1964.

97. Zhou, L.; Lu, J. J.; Gu, C. and Liu, S.(2014). Binary electroosmotic-pump nanoflow gradient generator for miniaturized high-performance liquid chromatography. *Anal. Chem.*, 86 (24), 12214-12219.

98. Premstaller, A.; Oberacher, H. and Huber, C. G.(2000). High-performance liquid chromatography-electrospray ionization mass spectrometry of single- and double-stranded nucleic acids using monolithic capillary columns. *Anal. Chem.*, 72 (18), 4386-4393.

99. Valastyan, J. S. and Lindquist, S.(2014). Mechanisms of protein-folding diseases at a glance. *Dis. Model. Mech.*, 7 (1), 9-14.

100. Tipton, J. D.; Tran, J. C.; Catherman, A. D.; Ahlf, D. R.; Durbin, K. R. and Kelleher, N. L.(2011). Analysis of intact protein isoforms by mass spectrometry. *J. Biol. Chem.*, 286 (29), 25451-25458.

101. Shiva, S.(2013). Nitrite: A Physiological Store of Nitric Oxide and Modulator of Mitochondrial Function. *Redox Biol*, 1 (1), 40-44.

102. Zaia, J.; Annan, R. S. and Biemann, K.(1992). The correct molecular weight of myoglobin, a common calibrant for mass spectrometry. *Rapid Commun. Mass Spectrom.*, 6 (1), 32-36.

103. Asensio-Ramos, M.; Hernandez-Borges, J.; Rocco, A. and Fanali, S.(2009). Food analysis: a continuous challenge for miniaturized separation techniques. *J. Sep. Sci.*, 32 (21), 3764-3800.

104. Kutter, J. P.(2012). Liquid phase chromatography on microchips. *J. Chromatogr. A*, 1221, 72-82.

105. O'Huallachain, M.; Karczewski, K. J.; Weissman, S. M.; Urban, A. E. and Snyder, M. P.(2012). Extensive genetic variation in somatic human tissues. *Proc. Natl. Acad. Sci. U. S. A.*, 109 (44), 18018-18023.

106. Yin, H. and Marshall, D.(2012). Microfluidics for single cell analysis. *Curr. Opin. Biotechnol.*, 23 (1), 110-119.

107. Kovarik, M. L. and Allbritton, N. L.(2011). Measuring enzyme activity in single cells. *Trends Biotechnol.*, 29 (5), 222-230.

108. Lo, S. J. and Yao, D. J.(2015). Get to Understand More from Single-Cells: Current Studies of Microfluidic-Based Techniques for Single-Cell Analysis. *Int. J. Mol. Sci.*, 16 (8), 16763-16777.

109. Wu, M. and Singh, A. K.(2012). Single-cell protein analysis. *Curr. Opin. Biotechnol.*, 23 (1), 83-88.

110. Phelps, M. S.; Sturtevant, D.; Chapman, K. D. and Verbeck, G. F.(2016). Nanomanipulation-Coupled Matrix-Assisted Laser Desorption/ Ionization-Direct Organelle Mass Spectrometry: A Technique for the Detailed Analysis of Single Organelles. *J. Am. Soc. Mass Spectrom.*, 27 (2), 187-193.

111. Vangelder, R. N.; Vonzastrow, M. E.; Yool, A.; Dement, W. C.; Barchas, J. D. and Eberwine, J. H.(1990). Amplified Rna Synthesized from Limited Quantities of Heterogeneous Cdna. *Proc. Natl. Acad. Sci. U. S. A.*, 87 (5), 1663-1667.

112. Saha-Shah, A.; Weber, A. E.; Karty, J. A.; Ray, S. J.; Hieftje, G. M. and Baker, L. A.(2015). Nanopipettes: probes for local sample analysis. *Chemical Science*, 6 (6), 3334-3341.

113. Guillaume-Gentil, O.; Potthoff, E.; Ossola, D.; Dorig, P.; Zambelli, T. and Vorholt, J. A.(2013). Force-Controlled Fluidic Injection into Single Cell Nuclei. *Small*, 9 (11), 1904-1907.

114. Guillaume-Gentil, O.; Rey, T.; Kiefer, P.; Ibanez, A. J.; Steinhoff, R.; Bronnimann, R., et al.(2017). Single-Cell Mass Spectrometry of Metabolites Extracted from Live Cells by Fluidic Force Microscopy. *Anal. Chem.*, 89 (9), 5017-5023.

115. Prager, D. J.; Bowman, R. L. and Vurek, G. G.(1965). Constant Volume, Self-Filling Nanoliter Pipette: Construction and Calibration. *Science*, 147 (3658), 606-608.

116. Actis, P.; Maalouf, M. M.; Kim, H. J.; Lohith, A.; Vilozny, B.; Seger, R. A., et al.(2014). Compartmental genomics in living cells revealed by single-cell nanobiopsy. *ACS Nano*, 8 (1), 546-553.

117. Rosen, J. N.; Sweeney, M. F. and Mably, J. D.(2009). Microinjection of zebrafish embryos to analyze gene function. *J. Vis. Exp.*, (25), 1115.

118. Huang, Y. and Linsen, S. E.(2015). Partial depletion of yolk during zebrafish embryogenesis changes the dynamics of methionine cycle and metabolic genes. *BMC Genomics*, 16, 427.

119. Jardine, D. and Litvak, M. K.(2003). Direct yolk sac volume manipulation of zebrafish embryos and the relationship between offspring size and yolk sac volume. *J. Fish Biol.*, 63 (2), 388-397.

120. Benard, E. L.; van der Sar, A. M.; Ellett, F.; Lieschke, G. J.; Spaink, H. P. and Meijer, A. H.(2012). Infection of zebrafish embryos with intracellular bacterial pathogens. *J. Vis. Exp.*, (61), 3781.

121. Hernandez-Vega, A.; Marsal, M.; Pouille, P. A.; Tosi, S.; Colombelli, J.; Luque, T., et al.(2016). Polarized cortical tension drives zebrafish epiboly movements. *EMBO J.*, 36, 25-41.

122. Moran, U.; Phillips, R. and Milo, R.(2010). SnapShot: Key Numbers in Biology. *Cell*, 141 (7), 1262-1262.

123. Minaschek, G.; Bereiterhahn, J. and Bertholdt, G.(1989). Quantitation of the Volume of Liquid Injected into Cells by Means of Pressure. *Exp. Cell Res.*, 183 (2), 434-442.

124. Maxfield, F. R. and Tabas, I.(2005). Role of cholesterol and lipid organization in disease. *Nature*, 438 (7068), 612-621.

125. Zon, L. I. and Peterson, R. T.(2005). In vivo drug discovery in the zebrafish. *Nat. Rev. Drug Discov.*, 4 (1), 35-44.

126. Seth, A.; Stemple, D. L. and Barroso, I.(2013). The emerging use of zebrafish to model metabolic disease. *Dis. Model. Mech.*, 6 (5), 1080-1088.

127. Grunwald, D. J. and Eisen, J. S.(2002). Headwaters of the zebrafish -- emergence of a new model vertebrate. *Nat. Rev. Genet.*, 3 (9), 717-724.

128. Fraher, D.; Sanigorski, A.; Mellett, N. A.; Meikle, P. J.; Sinclair, A. J. and Gibert, Y.(2016). Zebrafish Embryonic Lipidomic Analysis Reveals that the Yolk Cell Is Metabolically Active in Processing Lipid. *Cell Rep*, 14 (6), 1317-1329.

129. van Meer, G.; Voelker, D. R. and Feigenson, G. W.(2008). Membrane lipids: where they are and how they behave. *Nat. Rev. Mol. Cell Biol.*, 9 (2), 112-124.

130. Carvalho, L. and Heisenberg, C. P.(2010). The yolk syncytial layer in early zebrafish development. *Trends Cell Biol.*, 20 (10), 586-592.

Appendix A

Thank you for your order!

Dear Dr. Apeng Chen,

Thank you for placing your order through Copyright Clearance Center's RightsLink® service.

Order Summary

Order Date:	Jan 30, 2017
Order Number:	4038861105398
Publication:	Analytica Chimica Acta
Title:	Combining selection valve and mixing chamber for nanoflow gradient generation: Toward developing a liquid chromatography cartridge coupled with mass spectrometer for protein and peptide analysis
Type of Use:	reuse in a thesis/dissertation
Order Total:	0.00 USD

View or print complete details of your order and the publisher's terms and conditions.

Please note: You will be invoiced within 24 hours.

Sincerely,

Copyright Clearance Center

How was your experience? Fill out this survey to let us know.

Tel: +1-855-239-3415 / +1-978-646-2777
customercare@copyright.com
https://myaccount.copyright.com

Copyright Clearance Center RightsLink®

Appendix B

Thank you for your order!

Dear Dr. Apeng Chen,

Thank you for placing your order through Copyright Clearance Center's RightsLink® service.

Order Summary

Order Date:	Jan 30, 2017
Order Number:	4038861105398
Publication:	Analytica Chimica Acta
Title:	Combining selection valve and mixing chamber for nanoflow gradient generation: Toward developing a liquid chromatography cartridge coupled with mass spectrometer for protein and peptide analysis
Type of Use:	reuse in a thesis/dissertation
Order Total:	0.00 USD

View or print complete details of your order and the publisher's terms and conditions.

Please note: You will be invoiced within 24 hours.

Sincerely,

Copyright Clearance Center

How was your experience? Fill out this survey to let us know.

Tel: +1-855-239-3415 / +1-978-646-2777
customercare@copyright.com
https://myaccount.copyright.com

Copyright Clearance Center RightsLink®

Appendix C

Thank you for your order!

Dear Dr. Apeng Chen,

Thank you for placing your order through Copyright Clearance Center's RightsLink® service.

Order Summary

Order Date:	Mar 11, 2017
Order Number:	4066091195026
Publication:	Journal of Chromatography A
Title:	Monitoring gradient profile on-line in micro- and nano-high performance liquid chromatography using conductivity detection
Type of Use:	reuse in a thesis/dissertation
Order Total:	0.00 USD

View or print complete details of your order and the publisher's terms and conditions.

Sincerely,

Copyright Clearance Center

How was your experience? Fill out this survey to let us know.

Tel: +1-855-239-3415 / +1-978-646-2777
customercare@copyright.com
https://myaccount.copyright.com